DISSERTATION

ENHANCEMENT OF COUPLED SURFACE / SUBSURFACE FLOW MODELS IN WATERSHEDS: ANALYSIS, MODEL DEVELOPMENT, OPTIMIZATION, AND USER ACCESSIBILITY

Submitted by

Seonggyu Park

Department of Civil and Environmental Engineering

In partial fulfillment of the requirements

For the Degree of Doctor of Philosophy

Colorado State University

Fort Collins, Colorado

Fall 2018

Doctoral Committee:

Advisor: Ryan T. Bailey

Neil S. Grigg
Michael J. Ronayne
Thomas Sale

ABSTRACT

ENHANCEMENT OF COUPLED SURFACE / SUBSURFACE FLOW MODELS IN WATERSHEDS: ANALYSIS, MODEL DEVELOPMENT, OPTIMIZATION, AND USER ACCESSIBILITY

The shortage of freshwater supply has been recognized as one of the most critical and global issues. Population growth, land use, and climate change are exacerbating current and future stresses on freshwater scarcity. Many techniques and methods have been developed and used to quantify water resources at the regional scale, including large-scale watershed models.

However, the majority of large-scale watershed models are lumped hydrologic models that ignore or treat simplistically the flow of groundwater and its interaction with surface water features. Integrated surface water – groundwater models are being used more frequently, but no systematic approach of model construction, sensitivity analysis, parameter estimation, and uncertainty analysis has been provided. In addition, there is a need to develop tools for constructing these models, for ease of implementation in watersheds worldwide.

This dissertation establishes a general framework for implementing and applying integrated surface water-groundwater models to address water management questions in watersheds and river basins. These methods include model construction, sensitivity and uncertainty analysis, parameter estimation for coupled groundwater/surface water models, using the integrated surface water-groundwater model SWAT-MODFLOW as an example modeling tool, thereby providing a general framework for implementation and use of integrated hydrologic models. All project objectives are illustrated through a model application to the Middle Bosque River watershed

(471 km^2) in central Texas, a region that relies on groundwater and surface water to satisfy water demand.

Model construction is facilitated through the development of a graphical user interface (GUI) tool, QSWATMOD. The GUI is developed as a plug-in tool for QGIS, an open-source, free graphical information system. QSWATMOD was applied to the Middle Bosque River Watershed in Texas to demonstrate the linkage between existing SWAT and MODFLOW. The visualization of the results from the SWAT-MODFLOW simulation is beneficial in displaying model output and comparing with observed streamflow and groundwater data. QSWATMOD can be a valuable tool in assisting users to create and manage SWAT-MODFLOW projects, allowing coupled surface water/groundwater models to become more accessible to a broader hydrologic modelling community.

Parameter estimation and uncertainty analysis is performed using the PEST software, with new pre-processing and post-processing algorithms developed to modify and assess jointly land surface and hydrogeological parameters. The monthly NSE values of streamflow discharge for calibration and validation were calculated to be 0.45 and 0.66, respectively, and for whole simulation was 0.55, which are considered acceptable for monthly stream discharge ($\geq$ 0.5). The PBIAS value for calibration reveals a small percent under-prediction (2.62), but a large percent over-prediction (-16.79) for validation probably due to an overestimation of baseflow between storm events. The patterns of the hydrographs of simulated hydraulic heads for both locations are similar to their observed data, the daily R^2 values for two observation wells are considered low because the simulated hydraulic heads show less fluctuation, or a small percent under-prediction compared to their observed values.

The water resources from surface and sub-surface domains were assessed simultaneously. For the hydrologic fluxes, results demonstrate a high spatial-temporal variability in simulated hydraulic head, recharge rates and surface-subsurface water interaction rates, which can have a profound impact on watershed management. For example, the spatio-temporal variation of recharge and groundwater discharge maps can help identify potential areas of nutrient loading from the aquifer to the stream network or of pollution infiltration from surface to the aquifer. In addition, this area could be used to support decisions about alternative management strategies in the areas of landuse change, climate change, water allocation, and pollution control.

Sensitivity analysis is performed to determine the controlling land surface and hydrogeologic factors on hydrologic responses of the watershed (streamflow, water table elevation). The results from the composite sensitivity (CSP) show in general the significance of the land surface parameters in controlling streamflow and groundwater level The normalized sensitivity coefficient (NSC) of the land surface parameters also is higher than for the hydrogeological properties; however, the aquifer properties (K, S_y) do exhibit a moderate influence particularly for alluvium and terrace deposits, which are near-surface geologic units and thus have a control and land surface processes and associated surface runoff and streamflow in the MBRW system.

Analysis of the simulation uncertainties of hydrologic responses (streamflow, water table elevation, watershed water balance) is performed with the impact of short-term climatic events and future development scenario. For the impact of short-term climatic events, results show climate events such as drought, multi-year drought, and extreme flooding events have a significant impact on surface water storage, groundwater storage, and watershed fluxes (recharge, groundwater-surface water interaction, lateral flow, surface runoff). Besides, the results show that even the same intensity and length of a stress or even its pre-conditions on different

hydrologic response variables can result in their response time, scales and durations in a very different way. Results from groundwater development scenario (aquifer-storage-recovery) show injecting water results in higher changes in water table than extracting water from the aquifer (similar to scale change of hydrological responses and water balance). The results suggest that their response time, scales and durations not only vary but also are influenced by pre-conditions (i.e. soil moisture, water table), their distances to pumping wells.

The proposed modelling framework for model construction, parameter estimation, sensitivity and uncertainty analysis can assist in implementing and applying integrated surface water-groundwater models for estimating watershed water resource and analysing the effect of changes in land use, population, and climate. Keys to the framework are the ability to jointly estimate land surface and hydrogeological parameters and quantify their impact on hydrologic responses (streamflow, water table elevation, GW-SW interactions). This framework, particularly if used with SWAT-MODFLOW, can facilitate the use of integrated models worldwide to assist with finding technical solutions to water issues.

ACKNOWLEDGEMENTS

I wonder whether my advisor (Dr. Ryan Bailey) has ever been frustrated with my slow progress on the dissertation. But, even if he did, he always told me “You will do great!”. He never let me doubt myself and always fully supported me. For that, I am truly thankful.

I would also like to thank my defense committee members, Prof. Neil S. Grigg , Dr. Michael J. Ronayne and Dr. Thomas Sale. All of them were incredibly tolerant to my (literally) last minute submissions. I am so grateful for their encouragement and insightful comments.

Of course, it would be almost impossible for me to complete my Ph.D., without never ending joyful talks to my colleagues and research comments from them. I would especially never forget “Thursday food meeting”.

DEDICATION

To the most beautiful woman in the universe,

my amazing wife, Yun,

whose unconditional love and sacrificial care for me and our children

made it possible for me to complete my Ph.D.,

and to our children,

Elliot and Eliana,

who are indeed a gift from the Lord.

TABLE OF CONTENTS

LIST OF TABLES

LIST OF FIGURES

CHAPTER 1 LITERATURE REVIEW AND RESEARCH OVERVIEW

1.1. Objective and expected significance

The overall aim of this dissertation is to develop a framework for implementing and applying integrated surface water-groundwater models to address water management questions in watersheds and river basins. These methods include model construction, sensitivity and uncertainty analysis, parameter estimation for coupled groundwater/surface water models, using the integrated surface water-groundwater model SWAT-MODFLOW as an example modeling tool, thereby providing a general framework for implementation and use of integrated hydrologic models. This overall aim will be accomplished by through the following specific objectives:

(1) Develop an easy-to-use workflow for users preparing input data, configuring simulation settings, and visualizing and interpreting results. The GUI is developed as a plug-in tool for QGIS, an open-source, free graphical information system. The development of a QGIS-based graphical user interface for the SWAT-MODFLOW model will allow coupled surface water/groundwater models to become more accessible to the broad hydrologic modeling community.

(2) Quantify surface water resources, groundwater resources, and water flux rates between storage components as impacted by multi-decadal climate patterns and extreme climate events (major drought, storms) in a semi-arid regional-scale watershed.

(3) Develop a methodology to optimize a SWAT-MODFLOW model automatically. Parameter estimation and composite sensitivity analysis are performed using the PEST software, with new pre-processing and post-processing algorithms developed to modify and assess jointly land surface and hydrogeological parameters.

(4) Perform local sensitivity analysis (LSA) with one-at-time (OAT) approach to evaluate the individual controlling land surface and hydrogeologic factors on hydrologic responses of the watershed (streamflow, water table elevation).

(5) Perform an analysis of the simulation uncertainties of hydrologic responses (streamflow, water table elevation, watershed water balance) with the impact of short-term climatic events and future development scenario.

1.2. Background

A variety of methods have been used to quantify water resources for watersheds, river basins, or other geographical areas. These techniques include lumped water balance hydrologic models over large geographical regions and global scales (Alcamo et al., 1997; Döll et al., 2003; Alcamo et al., 2003; Wada et al., 2010), the use of satellite observations such as with GRACE (Gravity Recovery and Climate Experiment) (Rodell et al., 2007; Longuevergne et al., 2010; Famiglietti et al., 2011; Feng et al., 2013; Voss et al., 2013), and physically-based spatially-distributed hydrologic models. Whereas large-scale lumped models neglect groundwater storage, GRACE results often are limited to estimating changes in groundwater storage, become uncertain at small spatial scales (less than a few hundred km), and are dependent on the accuracy in accounting for soil moisture change. In addition, changes in surface water storage are difficult to estimate.

Physically-based, spatially-distributed coupled land surface/subsurface hydrologic models such as SWAT (Arnold et al., 1998); CATHY (Camporese et al., 2009), ParFlow (Kollet and Maxwell, 2006), GSFLOW (Markstrom et al., 2008), and SWAT-MODFLOW (Bailey et al., 2016) can be used to estimate components of groundwater and surface water storage. Model applications range from global scale (de Graaf et al., 2015; de Graaf et al., 2017), to continental scale (Schuol et al., 2008; Abbaspour et al., 2015; Maxwell et al., 2015), to river basins and

catchments (Gauthier et al, 2009; Perrin et al., 2012; Morway et al., 2013; Tanvir Hassan et al., 2014; Tian et al., 2015; Bailey et al., 2016). Whereas the global-scale and continental-scale models provide global trends in groundwater supply, results are neither accurate enough nor resolved enough to assist in conjunctively managing groundwater and surface water resources at the regional scale. Smaller-scale studies often focus on fluxes (Perrin et al., 2012; Tanvir Hassan et al., 2014; Bailey et al., 2016) and hydrologic responses to management practices (Morway et al., 2013; Tian et al., 2015), rather than an assessment of stored volumes of groundwater and surface water through decadal periods, which are required to assist with water management.

These coupled flow models, however, include substantial uncertainties with respect to input data, forcing data, initial and boundary conditions, model structure, and parameter non-uniqueness due to a lack of data and poor knowledge of hydrological response mechanisms (Ye et al., 2008; Doherty and Welter, 2010; Shi and Zhou, 2010; Zhang et al., 2011; Gupta et al., 2012; Foglia et al., 2013). These uncertainties have negative effects on the model accuracy, thereby inducing uncertainties in the simulated results. Therefore, if hydrologic models are to be used to as decision-making aids, the uncertainty associated with model calibration and model predictions must be assessed (Gallagher and Doherty, 2007). In addition, these coupled flow models often are not used extensively due to the level of complexity of preparing input data, configuring model options, executing models, and interpreting results (Barthel and Banzhaf, 2016; Nielsen et al., 2017). In particular, preparing input data for coupled hydrological models is often a slow, tedious, and error-prone process. To save time and avoid errors, Bailey et al. (2017) developed SWATMOD-Prep, a stand-alone graphical user interface (GUI) that facilitates preparing linkage files for a SWAT-MODFLOW model simulation (Bailey et al., 2016). The

GUI, however, does not provide geographical context and does not allow linkage between an already existing SWAT model with an existing MODFLOW model.

Overall, no systematic approach of model construction and use has been provided for the coupled surface-subsurface flow models, limiting their wide application. There is a need for a generalized approach to perform UA, quantify the influence of the vast array of model parameters and factors on watershed response (e.g. stream discharge, groundwater head) through SA, develop a systematic approach to parameter estimation for both land surface and hydrogeological parameters, thereby providing modelling results that assess both groundwater and surface water resources accurately in a watershed setting while relaying the degree of uncertainty to decision makers.

1.3. Significance of research

This dissertation presents a framework for implementing and applying integrated surface water-groundwater models to address water management questions in watersheds and river basins. Model construction is facilitated through the development of a graphical user interface (GUI) tool, QSWATMOD capable of generating required input files, configuring simulation settings, and visualizing and interpreting results. A methodology to optimize a SWAT-MODFLOW model is presented with automatic calibration process and sensitivity analysis using PEST software through the development of new pre-processing and post-processing algorithms to modify and assess jointly land surface and hydrogeological parameters. In addition, the local sensitivity analysis (LSA) with one-at-time (OAT) approach is presented to evaluate the individual controlling land surface and hydrogeologic factors on hydrologic responses of the watershed (streamflow, water table elevation). Under climatic events and future development scenario, an analysis of the simulation uncertainties of hydrologic responses is performed.

The proposed modelling framework and a QGIS-based graphical user interface for the SWAT-MODFLOW model can facilitate the use of integrated models worldwide to assist with finding technical solutions to water issues. Results can help enhance understanding regarding the spatio-temporal patterns of hydraulic head elevation, recharge, surface-subsurface water interaction and the water resource availability and the hydrological responses under climatic and future development scenarios.

1.4. Organization of the dissertation

The dissertation is organized in four chapters. The second chapter presents a paper under revision by a journal, presenting a graphical user interface for SWAT-MODFLOW models; the third chapter is a paper currently under review by a journal, quantifies effect of decadal and extreme climate events on watershed water resources and fluxes using SWAT-MODFLW; the fourth chapter demonstrates a framework for quantifying uncertainty, sensitivity, and estimating parameters for integrated surface water - groundwater models; and the fifth chapter provides conclusions and recommendations for future research.

REFERENCES

Abbaspour, K.C., Rouholahnejad, E., Vaghefi, S., Srinivasan, R., Yang, H. and Klove, B. (2015) 'A continental-scale hydrology and water quality model for Europe: Calibration and uncertainty of a high-resolution large-scale SWAT model', Journal of Hydrology, 524, 733-752, available: http://dx.doi.org/10.1016/j.jhydrol.2015.03.027.

Alcamo, J., Doll, P., Henrichs, T., Kaspar, F., Lehner, B., Rosch, T. and Siebert, S. (2003) 'Development and testing of the WaterGAP 2 global model of water use and availability', Hydrological Sciences Journal-Journal Des Sciences Hydrologiques, 48(3), 317-337, available: http://dx.doi.org/10.1623/hysj.48.3.317.45290.

Bailey, R., Rathjens, H., Bieger, K., Chaubey, I. and Arnold, J. (2017) 'SWATMOD-PREP: GRAPHICAL USER INTERFACE FOR PREPARING COUPLED SWAT-MODFLOW SIMULATIONS', Journal of the American Water Resources Association, 53(2), 400-410, available: http://dx.doi.org/10.1111/1752-1688.12502.

Bailey, R.T., Wible, T.C., Arabi, M., Records, R.M. and Ditty, J. (2016) 'Assessing regional-scale spatio-temporal patterns of groundwater-surface water interactions using a coupled SWAT-MODFLOW model', Hydrological Processes, 30(23), 4420-4433, available: http://dx.doi.org/10.1002/hyp.10933.

Barthel, R. and Banzhaf, S. (2016) 'Groundwater and Surface Water Interaction at the Regional-scale - A Review with Focus on Regional Integrated Models', Water Resources Management, 30(1), 1-32, available: http://dx.doi.org/10.1007/s11269-015-1163-z.

Camporese, M., Paniconi, C., Putti, M. and Salandin, P. (2009) 'Ensemble Kalman filter data assimilation for a process-based catchment scale model of surface and subsurface flow', Water Resources Research, 45, available: http://dx.doi.org/10.1029/2008wr007031.

de Graaf, G., Bartley, D., Jorgensen, J. and Marmulla, G. (2015) 'The scale of inland fisheries, can we do better? Alternative approaches for assessment', Fisheries Management and Ecology, 22(1), 64-70, available: http://dx.doi.org/10.1111/j.1365-2400.2011.00844.x.

de Graaf, I.E.M., van Beek, R., Gleeson, T., Moosdorf, N., Schmitz, O., Sutanudjaja, E.H. and Bierkens, M.F.P. (2017) 'A global-scale two-layer transient groundwater model: Development and application to groundwater depletion', Advances in Water Resources, 102, 53-67, available: http://dx.doi.org/10.1016/j.advwatres.2017.01.011.

Doll, P., Kaspar, F. and Lehner, B. (2003) 'A global hydrological model for deriving water availability indicators: model tuning and validation', Journal of Hydrology, 270(1-2), 105-134, available: http://dx.doi.org/10.1016/s0022-1694(02)00283-4.

Famiglietti, J.S., Lo, M., Ho, S.L., Bethune, J., Anderson, K.J., Syed, T.H., Swenson, S.C., de Linage, C.R. and Rodell, M. (2011) 'Satellites measure recent rates of groundwater depletion in California's Central Valley', Geophysical Research Letters, 38, available: http://dx.doi.org/10.1029/2010gl046442.

Feng, W., Zhong, M., Lemoine, J.M., Biancale, R., Hsu, H.T. and Xia, J. (2013) 'Evaluation of groundwater depletion in North China using the Gravity Recovery and Climate Experiment (GRACE) data and ground-based measurements', Water Resources Research, 49(4), 2110-2118, available: http://dx.doi.org/10.1002/wrcr.20192.

Gallagher, M. and Doherty, J. (2007) 'Parameter estimation and uncertainty analysis for a watershed model', Environmental Modelling & Software, 22(7), 1000-1020, available: http://dx.doi.org/10.1016/j.envsoft.2006.06.007.

Gauthier, M.J., Camporese, M., Rivard, C., Paniconi, C. and Larocque, M. (2009) 'A modeling study of heterogeneity and surface water-groundwater interactions in the Thomas Brook

catchment, Annapolis Valley (Nova Scotia, Canada)', Hydrology and Earth System Sciences, 13(9), 1583-1596, available: http://dx.doi.org/10.5194/hess-13-1583-2009.

Hassan, S.M.T., Lubczynski, M.W., Niswonger, R.G. and Su, Z. (2014) 'Surface-groundwater interactions in hard rocks in Sardon Catchment of western Spain: An integrated modeling approach', Journal of Hydrology, 517, 390-410, available: http://dx.doi.org/10.1016/j.jhydrol.2014.05.026.

Kollet, S.J. and Maxwell, R.M. (2006) 'Integrated surface-groundwater flow modeling: A free-surface overland flow boundary condition in a parallel groundwater flow model', Advances in Water Resources, 29(7), 945-958, available: http://dx.doi.org/10.1016/j.advwatres.2005.08.006.

Longuevergne, L., Scanlon, B.R. and Wilson, C.R. (2010) 'GRACE Hydrological estimates for small basins: Evaluating processing approaches on the High Plains Aquifer, USA', Water Resources Research, 46, available: http://dx.doi.org/10.1029/2009wr008564.

Maxwell, S. (2005) '2005 update on water industry consolidation trends', Journal American Water Works Association, 97(10), 34-36.

Nielsen, A., Bolding, K., Hu, F.J. and Trolle, D. (2017) 'An open source QGIS-based workflow for model application and experimentation with aquatic ecosystems', Environmental Modelling & Software, 95, 358-364, available: http://dx.doi.org/10.1016/j.envsoft.2017.06.032.

Perrin, J., Ferrant, S., Massuel, S., Dewandel, B., Marechal, J.C., Aulong, S. and Ahmed, S. (2012) 'Assessing water availability in a semi-arid watershed of southern India using a semi-distributed model', Journal of Hydrology, 460, 143-155, available: http://dx.doi.org/10.1016/j.jhydrol.2012.07.002.

Schuol, J., Abbaspour, K.C., Srinivasan, R. and Yang, H. (2008) 'Estimation of freshwater availability in the West African sub-continent using the SWAT hydrologic model', Journal of Hydrology, 352(1-2), 30-49, available: http://dx.doi.org/10.1016/j.jhydrol.2007.12.025.

Tian, Y., Zheng, Y., Wu, B., Wu, X., Liu, J. and Zheng, C. (2015) 'Modeling surface water-groundwater interaction in arid and semi-arid regions with intensive agriculture', Environmental Modelling & Software, 63, 170-184, available: http://dx.doi.org/10.1016/j.envsoft.2014.10.011.

Voss, K.A., Famiglietti, J.S., Lo, M.H., de Linage, C., Rodell, M. and Swenson, S.C. (2013) 'Groundwater depletion in the Middle East from GRACE with implications for transboundary water management in the Tigris-Euphrates-Western Iran region', Water Resources Research, 49(2), 904-914, available: http://dx.doi.org/10.1002/wrcr.20078.

Wada, Y., van Beek, L.P.H., van Kempen, C.M., Reckman, J., Vasak, S. and Bierkens, M.F.P. (2010) 'Global depletion of groundwater resources', Geophysical Research Letters, 37, available: http://dx.doi.org/10.1029/2010gl044571.

CHAPTER 2

A QGIS-BASED GRAPHICAL USER INTERFACE FOR APPLICATION AND EVALUATION OF SWAT-MODFLOW MODELS

Highlights

This article presents QSWATMOD, a QGIS-based graphical user interface for application and evaluation of SWAT-MODFLOW models. QSWATMOD includes: (i) pre-processing modules to prepare input data for model execution, (ii) configuration modules for SWAT-MODFLOW options, and (iii) post-processing modules to view and interpret model results. QSWATMOD, written in Python, creates linkage files between SWAT and MODFLOW models, runs a simulation, and displays results (e.g. streamflow, groundwater head), within the open source Quantum Geographic Information System (QGIS) environment. QSWATMOD is equipped with functionalities that assist in storing and retrieving user and default configuration settings and parameter values, performing the linkage and simulation processes, and uses various geo-processing functionalities (e.g., selection, intersection, union, geometry) of QGIS. The use of QSWATMOD is demonstrated through an application to the 471 km2 Middle Bosque River Watershed in central Texas. As the number of SWAT-MODFLOW users grows worldwide, QSWATMOD can be a valuable tool to assist in creating and managing SWAT-MODFLOW projects.

2.1. Introduction

Many techniques and methods have been developed to quantify water resources at the regional scale, including large-scale watershed models. While many models focus principally on surface water (Postel et al., 1996; Vorosmarty et al., 2000; Alcamo et al., 2002; Oki et al., 2006)

and therefore ignore the availability of groundwater and its important interaction with surface water (Winter et al., 1998; Sophocleous et al., 2002; Karl et al., 2009), a new generation of models employ a more sophisticated approach in coupling land surface and subsurface hydrologic processes (e.g. ParFlow, Kollet and Maxwell, 2006; GSFLOW, Markstrom et al., 2008; SWAT-MODFLOW, Kim et al., 2008; HydroGeoSphere, Therrien et al., 2010; CATHY, Camporese et al., 2010; FEFLOW, Diersch, 2013). These coupled flow models, however, often are not used extensively due to the level of complexity of preparing input data, configuring model options, executing models, and interpreting results (Barthel and Banzhaf, 2016; Nielsen et al., 2017). In particular, preparing input data for coupled hydrological models is often a slow, tedious, and error-prone process. To save time and avoid errors, Bailey et al. (2017) developed SWATMOD-Prep, a stand-alone graphical user interface (GUI) that facilitates preparing linkage files for a SWAT-MODFLOW model simulation (Bailey et al., 2016). The GUI, however, does not provide geographical context and does not allow linkage between an already existing SWAT model with an existing MODFLOW model.

This article presents QSWATMOD, a QGIS-based GUI plugin that allows an existing SWAT model and a MODFLOW model to be linked within a geographical information system (GIS) setting, thus facilitating model preparation and model results viewing. The linkage is based on the SWAT-MODFLOW modeling code of Bailey et al. (2016), in which MODFLOW-NWT (Niswonger et al., 2011) is imbedded within the SWAT 2012 modeling code (Revision 591) to simulate groundwater flow and groundwater-surface water interactions. This new GUI handles a variety of scenarios for connecting MODFLOW river cells with SWAT subbasin channels for groundwater-surface water flow interactions. The availability of QSWATMOD can allow coupled surface water/groundwater models to become more accessible to a broad hydrologic

modeling community, particularly since the tool is based on the free and open-source QGIS platform. The features and capabilities of QSWATMOD are demonstrated through an application to the Middle Bosque River Watershed (471 km^2) in the Texas-Gulf region of central Texas (Figure 2.1). The Middle Bosque River Watershed is predominantly comprised of either pasture (65.4 % of area) or farms (20.3 %), with minor land covers of forests (8.5 %) and residential areas (3.2%) (USGS, 2007). The Middle Bosque River dissects the Edwards Limestone and has therefore produced major groundwater discharge and stream seepage areas (Cannata, 1988). Several tributaries feed the Middle Bosque River, with a streamflow gage measuring at the outlet. Subsurface geology consists of mainly sedimentary (limestone) rocks (Cannate, 1988; Pearson, 2007), with two observation wells located near the river. The climate of the study area is characterized by semi-arid conditions, with long hot summers and brief mild winters. The annual precipitation between 1985 and 2012 ranges from about 340 to 950 mm/year. Individual, basic SWAT and MODFLOW models of the watershed were constructed for the purpose of demonstration (see Table 2.1 for details). Preliminary results of an uncalibrated model are compared with observation data (streamflow and groundwater head) to demonstrate the result viewing features of QSWATMOD.

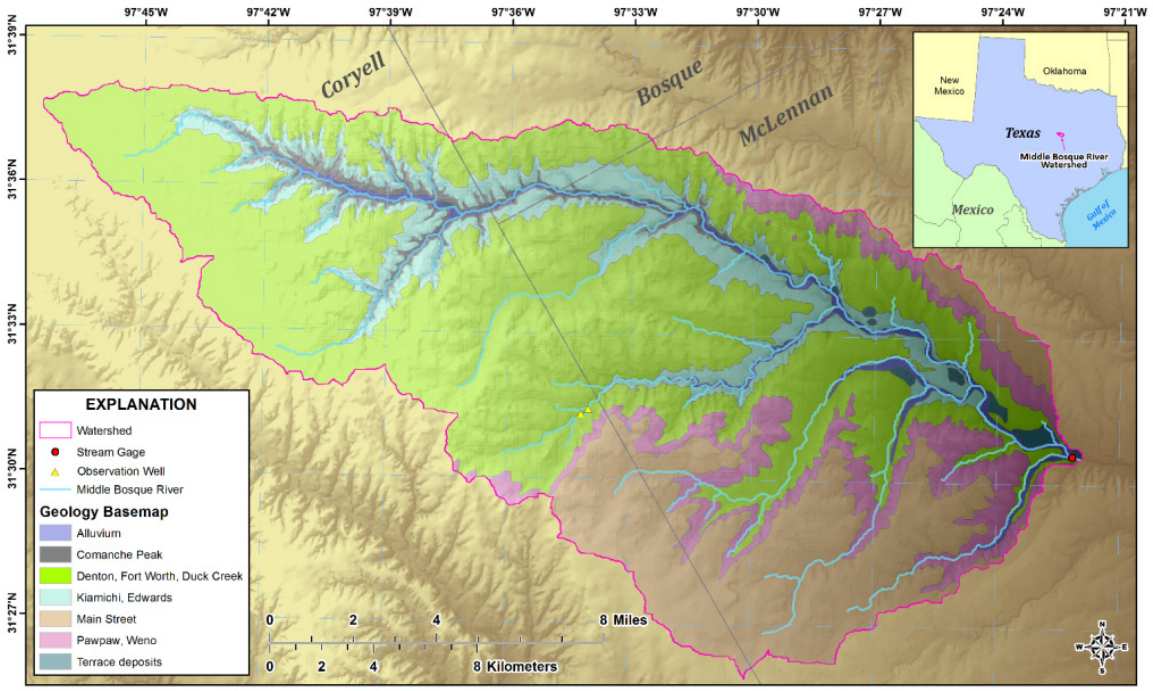

Figure 2.1. Map showing the location of the Middle Bosque River Watershed within McLennan, Bosque, and Coryell Counties, Texas. The outline of the watershed is the extent of the SWAT and MODFLOW models.

Table 2.1. Summary Characteristics of the SWAT and MODFLOW models.

Model Characteristics	Value	Unit
Watershed area	471	[km^2]
Number of SWAT HRUs	6,416	-
Number of SWAT Sub-basins	69	-
Number of MODFLOW cells	19,176	-
Number of MODFLOW layers	5	-
MODFLOW grid cell size (m)	150	[m]
Number of MODFLOW River cells	1,468	-
Range of Hydraulic Conductivity values	$1e^{-4}$ – 300	[m day^{-1}]
Range of Specific Yield	0.01– 0.25	-

2.2. Development and Application of QSWATMOD

2.2.1. QSWATMOD Overview and Development

QSWATMOD (Figure 2.2) is cross-platform compatible and implemented in the open source QGIS platform. Documentation and a QSWATMOD installer are available through http://swat.tamu.edu/software/swat-modflow. The QGIS software must be installed on the

system prior to the installation of QSWATMOD. We recommend installing the latest "long term release (LTR)" version of QGIS through OSgeo4W, a binary distribution of open source geospatial software (https://trac.osgeo.org/osgeo4w). QSWATMOD has been tested in the latest version of QGIS (Las Palmas 2.18.21). QSWATMOD has dependencies to third-party Python packages including FloPy3 (Bakker et al., 2016), Pandas (McKinney et al., 2010), OpenCV (Bradski et al., 2000), and pyshp. These packages will be installed automatically in the designated Python environment after QSWATMOD is activated in QGIS. QSWATMOD has the option of creating a new project or opening a saved existing project from a previous session (Figure 2.3). A project consists of a QGIS file (*.qgs), which stores the information of QGIS status, loaded layers, user settings, and a project directory, which holds all project inputs and outputs. Default user inputs and simulation settings are stored in a designated SQLite (Hipp et al., 2015) project database. QSWATMOD includes its own built-in plotting functions based on Matplotlib (Hunter et al., 2007). The tabs of QSWATMOD (Figure 2.2) are "Pre-Processing", "Simulation", and "Post-Processing", which will be summarized in the next sections. All data processing is based on the pre-processing, configuration, and post-processing modules as outlined in Figure 2.3.

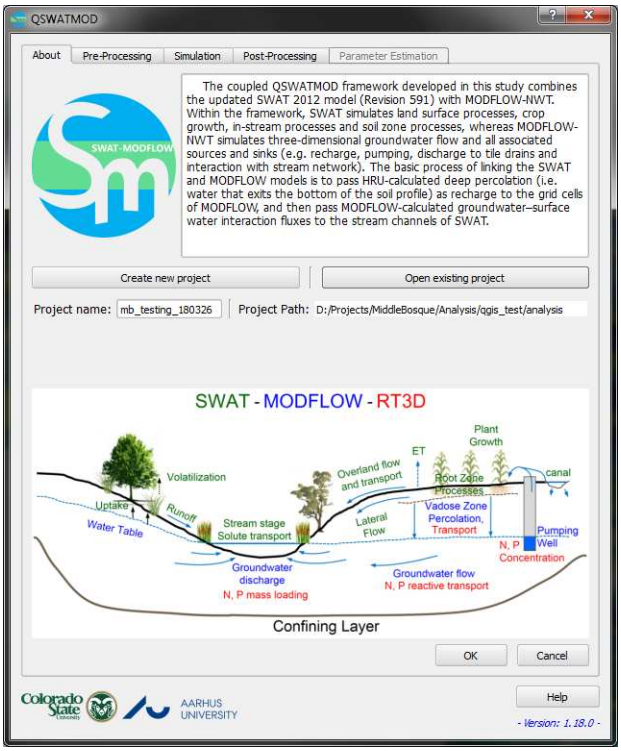

Figure 2.2**.** Main QSWATMOD GUI platform.

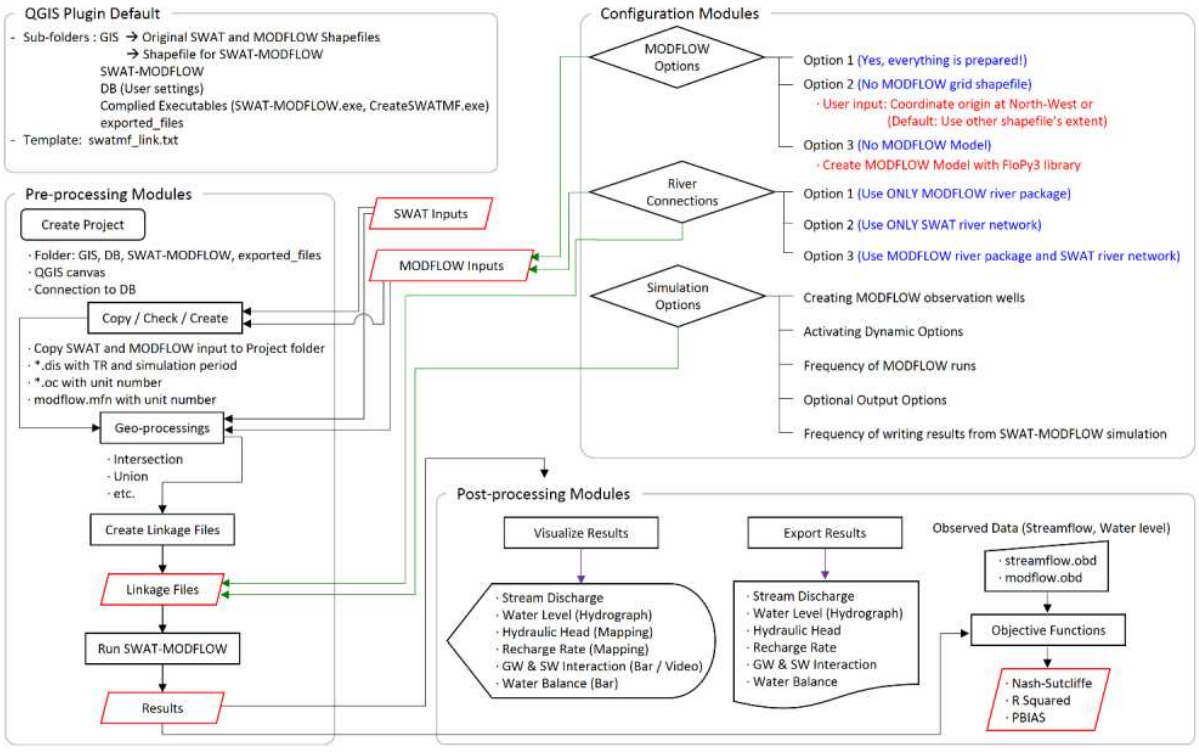

Figure 2.3. Schematic showing the Pre-processing, Configuration, and Post-processing modules of QSWATMOD to prepare inputs and visualize results for a SWAT-MODFLOW simulation.

2.2.2. Pre-Processing Tab

The main role of the Pre-Processing tab is to guide users to specify paths to the folders containing input files, prepare MODFLOW data, and perform geo-processing routines to link the two models. Shapefiles for the river network, subbasins, and HRUs from an existing SWAT model are required (Figure 2.4).

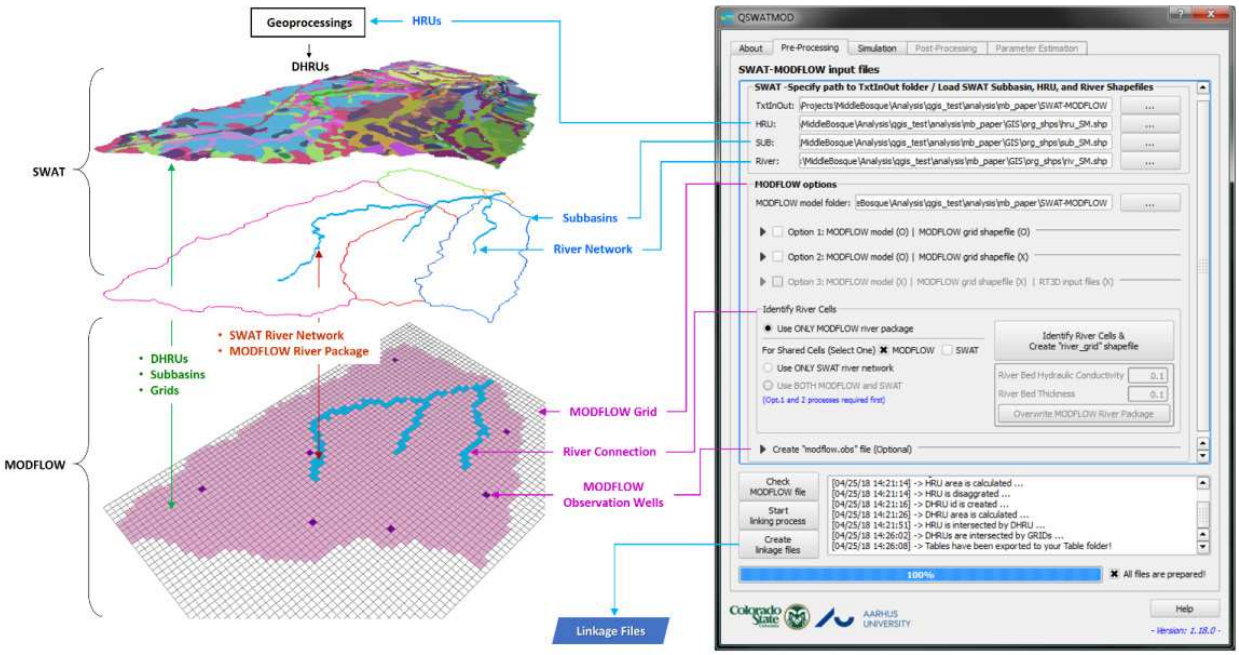

Figure 2.4. QSWATMOD interface for the Pre-processing tab, using shapefiles from the Middle Bosque River Watershed.

2.2.2.1. SWAT Inputs

QSWATMOD creates copies of all SWAT model input files and associated GIS files (rasters, vectors) in the project folder once users specify the path to an existing SWAT model. The copied HRU, sub-basin, and river network shapefiles are then imported to the QGIS canvas. These shapefiles are available with the original SWAT model created using either ArcSWAT (Olivera et al., 2006) or QSWAT (Dile et al., 2016). HRU shapefiles should be created with no thresholds so that the entire land surface area is covered by Disaggregated HRUs (DHRUs), single polygons

that will be intersected with MODFLOW grid cells for passing SWAT HRU data to the MODFLOW grid (Bailey et al., 2016).

2.2.2.2. MODFLOW Options

QSWATMOD provides the user with three options for MODFLOW (Figure 2.4):

1) MODFLOW model files and grid shapefile are available;
2) MODFLOW model files are available but there is no grid shapefile; and
3) MODFLOW model has not yet been constructed.

The first option guides users to specify the path to an existing MODFLOW model and MODFLOW grid shapefile, with the latter requiring the same projection as the SWAT shapefiles. For the second option, the user specifies the coordinate of the North-West corner of the MODFLOW boundary or, as default, the MODFLOW grid area is based on the extent of the SWAT subbasin shapefile, with both reading cell information (width, depth, top elevation) from the MODFLOW discretization file (*.dis). The MODFLOW grid shapefile (mf_grid.shp) is then created and the cell information is added to the attribute table of the MODFLOW grid shapefile (see Figure 2A.1 in Appendix A).

Through the third option, a simple MODFLOW model, powered by the FloPy3 (Bakker et al., 2016) package, is developed (Figure 2.5). First, a folder to store MODFLOW input files is created. A model name is then created by the user and DEM and boundaries of the watershed are uploaded (Figure 2.5). The MODFLOW grid is established using specified width (X) and depth (Y) of grid cells, and the cells are intersected with the SWAT river network to establish River cells. River bed properties are specified by the user to estimate conductance values for each river cell, and aquifer properties can be specified by a single value or a raster. The ratio of horizontal K to vertical K (horizontal anisotropy) and layer type are also specified. Finally, the “Write MODFLOW Information” button is selected to write input files to the model folder. Locations

for comparing model results (groundwater head) with observation data can be established by either an observation well shapefile or through the user selecting cells on the generated MODFLOW grid shapefile on the QGIS canvas (see Figure 2A.2 in Appendix A).

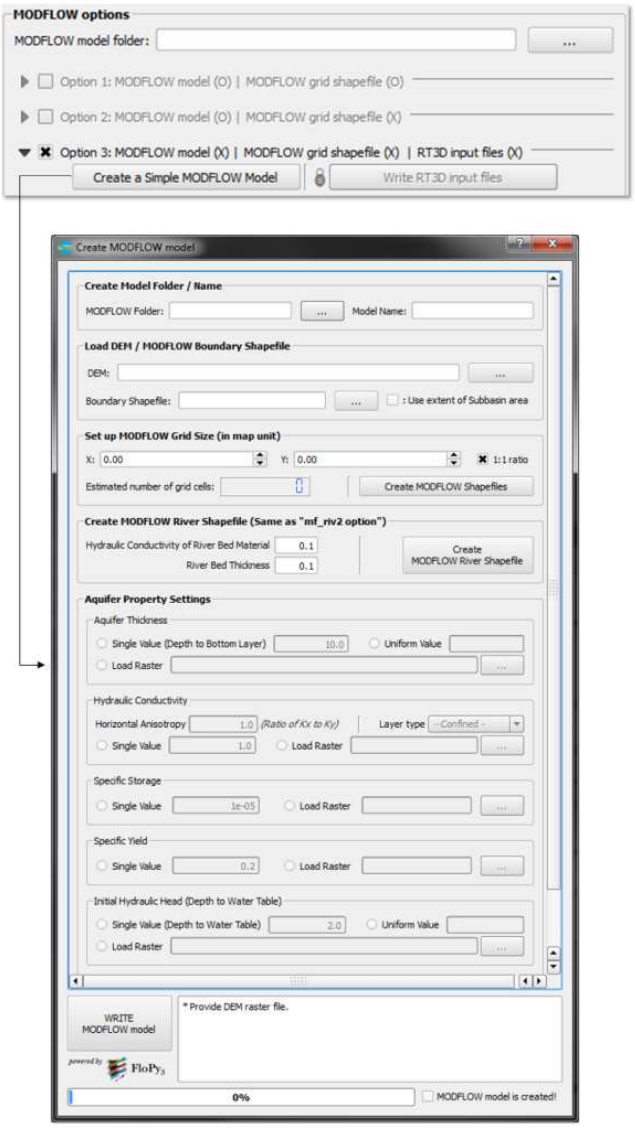

Figure 2.5. MODFLOW tab within the Pre-Processing tab, which loads information to create a single-layer MODFLOW model.

2.2.2.3. River Connections

Linking the cells in the MODFLOW River package with the SWAT river network is required to simulate groundwater-surface water interactions. QSWATMOD provides three options: 1)

Use Only MODFLOW river package, 2) Use Only SWAT river network, and 3) Use Both MODFLOW and SWAT (Figure 6d). For the first option, QSWATMOD extracts river cell values (river stage, river bed conductance, river bottom elevation) from the MODFLOW River package file (*.riv), and then writes these values into the attribute table of a new "mf_riv1.shp" shapefile. For the second option, QSWATMOD creates the "mf_riv2.shp" by intersecting the MODFLOW grid with the SWAT river network shapefile and then calculates the river cell parameters for each river cell based on information provided by the SWAT river network (DEM, stream length and width) and user inputs (thickness and hydraulic conductivity of river bed material). For the third option, the existing MODFLOW river cells are compared to the SWAT river network (Figure 2.6e) to determine if river cells should be added. The user then decides which information will be used for the new cells.

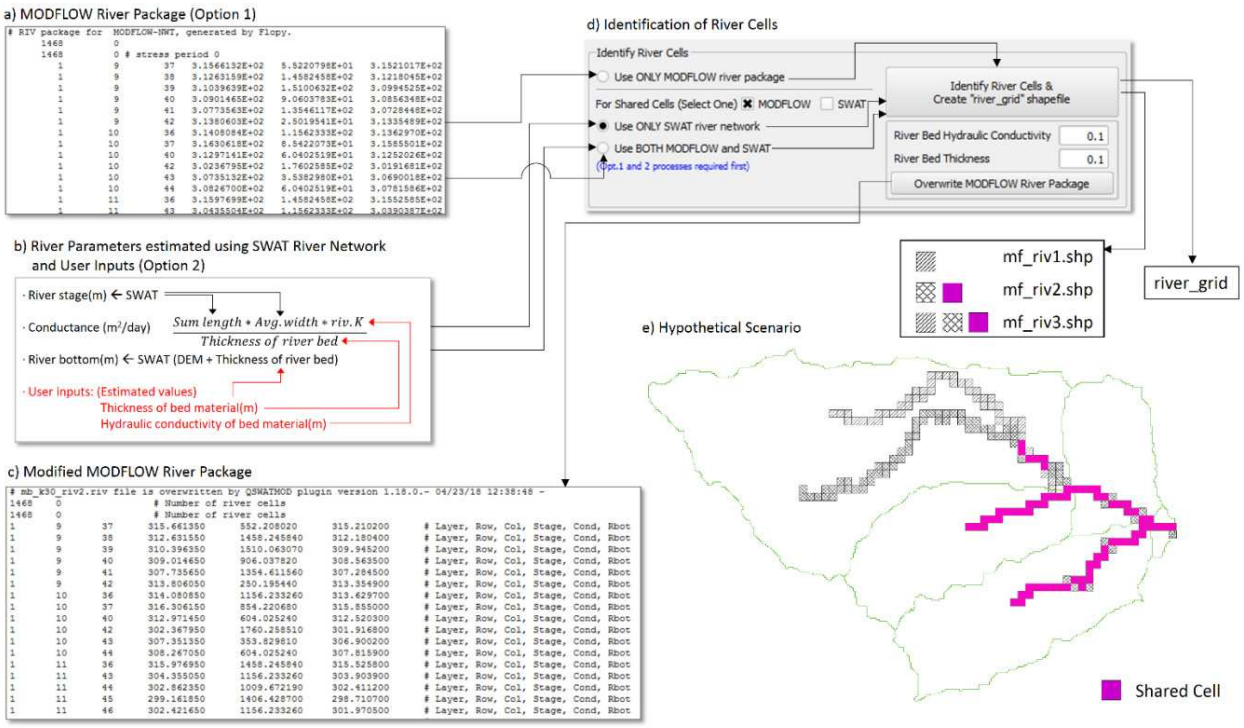

Figure 2.6. River connections a) Option1: MODFLOW River Package; b) Option 2: River Parameters estimated using SWAT River Network and User Inputs; c) Modified MODFLOW River Package; and d) Interface for Identification of River Cells.

2.2.2.4. Linking Process

Through the linking process (Figure 2.4), the HRUs are disaggregated to create DHRUs, which are then intersected with MODFLOW grid cells. MODFLOW river cells are identified using the SWAT stream network or other river connection options (see Section 2.2.2.3), and the set of river cells within each subbasin are identified for mapping groundwater-surface water exchange rates from river cells to SWAT subbasin channels. These generated shapefiles are used to create the four required SWAT-MODFLOW linkage files ("swatmf_dhru2hru.txt", "swatmf_dhru2grid.txt", "swatmf_grid2dhru.txt", and "swatmf_river2grid.txt"; see Bailey et al., 2016), which are stored in the project folder.

For the Middle Bosque model, the second option for the MODFLOW model was used with reading the origin coordinates of the subbasin shapefile. To identify the river cells, the "Use ONLY MODFLOW river package" option was chosen. The time required by QSWATMOD to create the DHRUs, the MODFLOW grid cells, identify the river cells and create the "river_grid" shapefile, create the "hru_dhru" and "dhru_grid" shapefiles, and write the linkage files was 5.5 s, 6.2 s, 0.5 s, 297.7 s, and 4.8 s, respectively. A total of 12,366 DHRUs were created and 1,468 river cells were identified to link with the SWAT river network. In addition, the first development option for the MODFLOW grid, and the second and third options of "Identify River Cells" were tested (Table 2.2).

Table 2.2. Process time for QSWATMOD functions for the Middle Bosque River Watershed.

Process	Processing Time [Second]
Creating MODFLOW grid cells	
- Import a grid shapefile and write MODFLOW info.	4.5
- Create a grid shapefile and write MODFLOW info.	5.5
Identifying River cells and create river_grid	
- Use ONLY MODFLOW river package	6.2
- Use ONLY SWAT river network (additional	8.6

time)	5.5
- Use Both MODFLOW and SWAT (additional time)	
Checking MODFLOW inputs	0.5
Linking	297.7
Writing linkage files	4.8

2.2.3. Simulation Tab

In the "Simulation" tab (Figure 2.7), starting date, ending date, warm-up period, and time step of the simulation are provided based on information in the SWAT input file "file.cio" and used for synchronizing the MODFLOW model time and writing simulation results. In the configuration settings, users can activate SWAT-MODFLOW simulation options and change the frequency of SWAT calls to MODFLOW. The optional model output (HRU deep percolation, MODFLOW cell-by-cell recharge, subbasins channel depth, MODFLOW river cell stage, groundwater/surface water exchange rates for each SWAT sub-basin, groundwater/surface water exchange rates for each MODFLOW river cell) is also specified. Due to the potentially large output files (> 1 GB), the current version of SWAT-MODFLOW adds two functionalities: writing monthly and annual average SWAT-MODFLOW results, and setting the frequency of writing SWAT-MODFLOW results. Finally, the "Create 'swatmf_link.txt' file" button is selected to export the configuration settings to the project folder and the "Run Simulation" button is selected to call the SWAT-MODFLOW executable and run the simulation. For the Middle Bosque model, the frequency of MODFLOW runs was set to 1, signifying daily interaction between the two models. The "Read in observation cells from 'modflow.obs'" was checked to compare simulated and observed hydraulic head values.

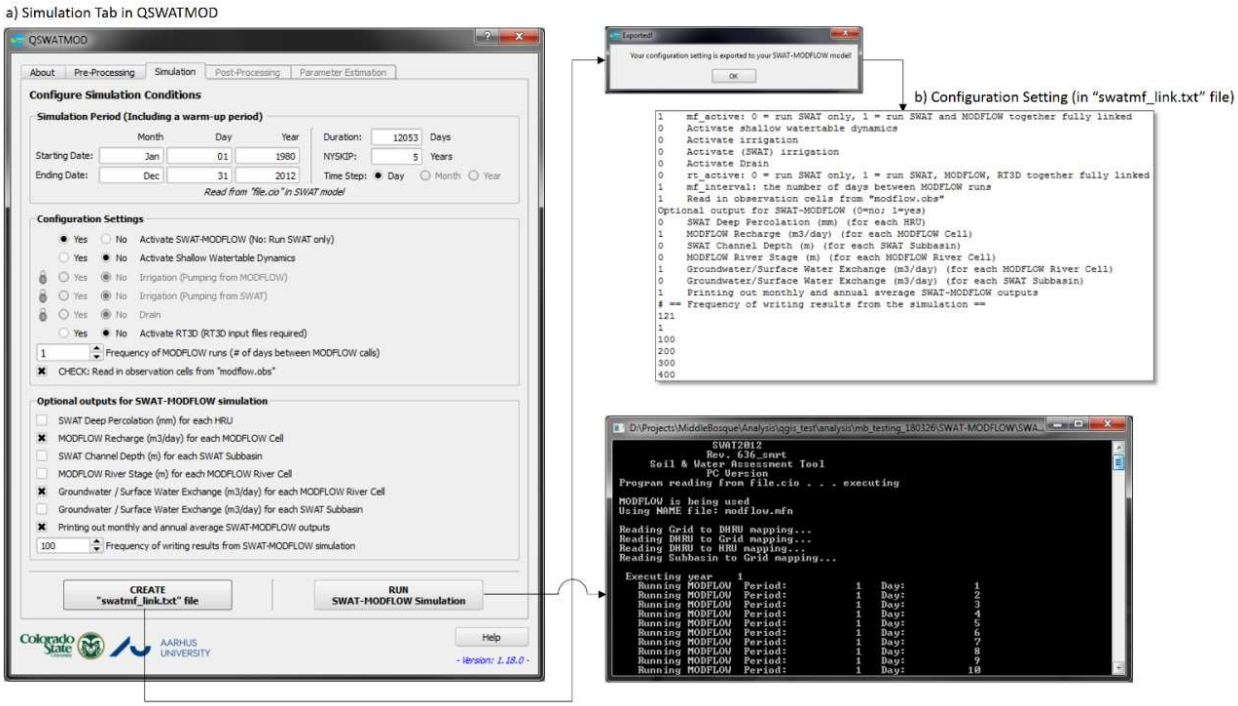

Figure 2.7. QSWATMOD interface for a) Simulation Tab; b) Configuration Settings (in "swatmf_link.txt" file).

2.2.4. Post-Processing Tab

The Post-Processing tab and results for the Middle Bosque SWAT-MODFLOW model are shown in Figure 2.8. The main purpose of this tab is to help disclose issues of interest to the user (Dile et al., 2016), facilitate mapping of results within QGIS, and display SWAT-MODFLOW results dynamically during the simulation run. QSWATMOD has three types of post-processing modules: plotting, mapping, and exporting results. The plot function shows hydrographs for streamflow and groundwater head and is intended mainly for comparisons between simulated and observed results for each sub-basin or observation well location. Once the observation data from streamflow and hydraulic head are provided in the formats "streamflow.obd" (see Figure 2A.3a in Appendix A) and "modflow.obd" (see Figure 2A.3b in Appendix A), objective function summary values such as Nash-Sutcliffe Efficiency (NSE), Percent bias (PBIAS), and R-squared (R^2) will be displayed on the figures (Figure 2.8a and 2.8b). The mapping function is designed to

show maps of recharge (Figure 2.8c) and groundwater head (Figure 2.8d) on the QGIS canvas. After users specify the period of visualization, the data are exported to a shapefile and stored in its attribute table.

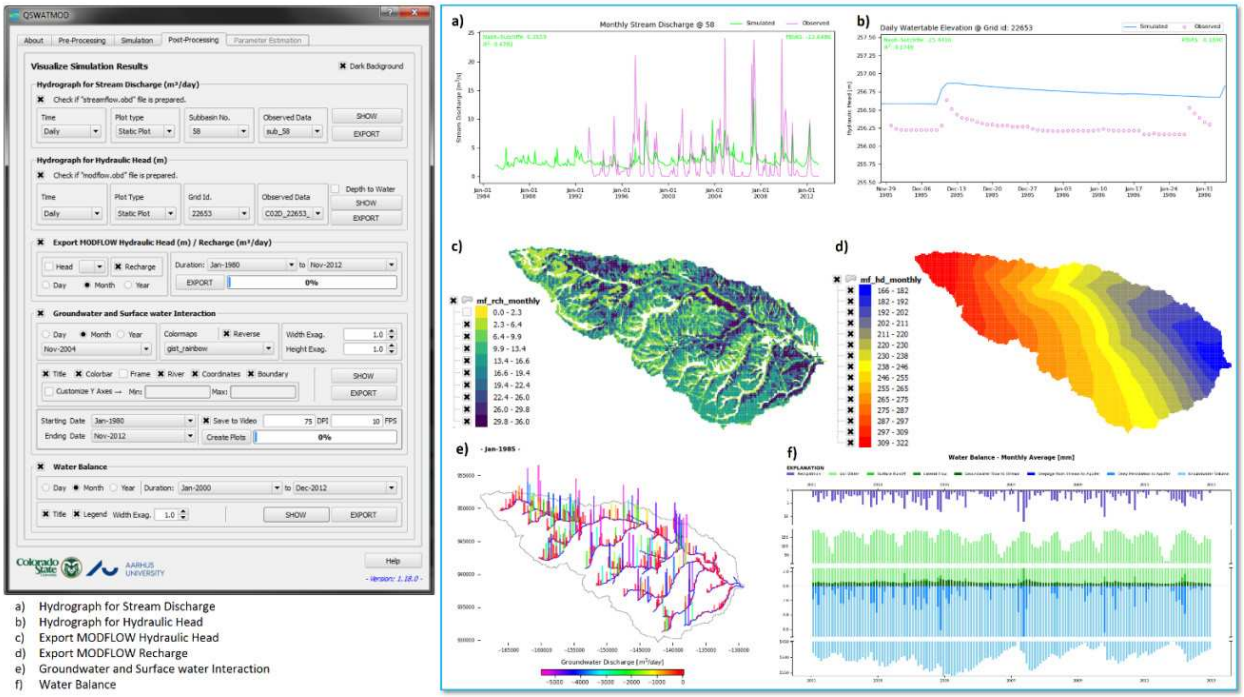

Figure 2.8. QSWATMOD interface for Post-processing tab, showing results from the Middle Bosque SWAT-MODFLOW simulation.

Visualizing the spatially distributed patterns of surface and groundwater interactions, watershed boundaries, and river networks for watersheds are performed using the "pyshp" package (Figure 2.8e). Once users create the figures for the period of visualization, the figures can be converted to a single video clip by selecting the "Save to Video" icon, according to the "DPI" and "FPS" settings (see Video 2A.4 in Appendix A). The water balance option reads the SWAT "output.std" file and uses precipitation, surface runoff, lateral flow, groundwater flow to streams, deep percolation to groundwater, soil water, seepage from streams to the aquifer, and groundwater volume to display a time series of water balance components (Figure 2.8f). Except for spatially distributed groundwater head and recharge values, users can export all results to

text-formatted files, including simulated observed data and objective functions (see Figure 2A.5 in Appendix A).

2.3. Conclusion

QSWATMOD, a QGIS-based graphical user interface for SWAT-MODFLOW models, was developed to provide an easy-to-use workflow for users preparing input data, configuring simulation settings, and visualizing and interpreting results. QSWATMOD includes options for using an existing MODFLOW or creating a new one, with a variety of options for linking MODFLOW river cells with SWAT subbasins for groundwater-surface water interactions. QSWATMOD was applied to the Middle Bosque River Watershed in Texas to demonstrate the linkage between existing SWAT and MODFLOW. The visualization of the results from the SWAT-MODFLOW simulation is beneficial in displaying model output and comparing with observed streamflow and groundwater data. QSWATMOD can be a valuable tool in assisting users to create and manage SWAT-MODFLOW projects, allowing coupled surface water/groundwater models to become more accessible to a broader hydrologic modelling community.

REFERENCES

Bailey, R., Rathjens, H., Bieger, K., Chaubey, I. and Arnold, J. (2017) 'SWATMOD-Prep: graphical user interface for preparing coupled SWAT-MODFLOW simulations', *Journal of the American Water Resources Association*, 53(2), 400-410, available: http://dx.doi.org/10.1111/1752-1688.12502.

Bailey, R.T., Wible, T.C., Arabi, M., Records, R.M. and Ditty, J. (2016) 'Assessing regional-scale spatio-temporal patterns of groundwater-surface water interactions using a coupled SWAT-MODFLOW model', *Hydrological Processes*, 30(23), 4420-4433, available: http://dx.doi.org/10.1002/hyp.10933.

Bakker, M., Post, V., Langevin, C.D., Hughes, J.D., White, J.T., Starn, J.J., and Fienen, M.N., 2016, FloPy v3.2.6: U.S. Geological Survey Software Release, 19 March 2017, http://dx.doi.org/10.5066/F7BK19FH

Barthel, R. and Banzhaf, S., 2016. Groundwater and surface water interaction at the regional-scale–A review with focus on regional integrated models. Water Resources Management, 30(1), pp.1-32, available: https://doi.org/10.1007/s11269-015-1163-z

Camporese, M., Paniconi, C., Putti, M. and Orlandini, S., 2010. Surface-subsurface flow modeling with path-based runoff routing, boundary condition-based coupling, and assimilation of multisource observation data. Water Resources Research, 46(2), available: https://doi.org/10.1029/2008WR007536.

Cannata, S.L., 1988. Hydrogeology of a portion of the Washita Prairie Edwards aquifer: central Texas (Doctoral dissertation, Baylor University).

Diersch, H.J.G., 2013. FEFLOW: finite element modeling of flow, mass and heat transport in porous and fractured media. Springer Science & Business Media, available: https://doi.org/10.1007/978-3-642-38739-5.

Dile, Y.T., Daggupati, P., George, C., Srinivasan, R. and Arnold, J., 2016. Introducing a new open source GIS user interface for the SWAT model. Environmental modelling & software, 85, pp.129-138, available: https://doi.org/10.1016/j.envsoft.2016.08.004.

Hipp, D. R., Kennedy, D., Mistachkin, J., (2015) SQLite (Version 3.8.10.2) [Computer software]. SQLite Development Team. Retrieved 2015-06-15. Available from <https://www.sqlite.org/src/info/2ef4f3a5b1d1d0c4>

Hunter, J.D. (2007) 'Matplotlib: A 2D graphics environment', *Computing in Science & Engineering*, 9(3), 90-95, available: http://dx.doi.org/10.1109/mcse.2007.55.

Kim, N.W., Chung, I.M., Won, Y.S. and Arnold, J.G., 2008. Development and application of the integrated SWAT–MODFLOW model. Journal of hydrology, 356(1), pp.1-16, available: https://doi.org/10.1016/j.jhydrol.2008.02.024.

Markstrom, S.L., Niswonger, R.G., Regan, R.S., Prudic, D.E. and Barlow, P.M., 2008. GSFLOW-Coupled Ground-water and Surface-water FLOW model based on the integration of the Precipitation-Runoff Modeling System (PRMS) and the Modular Ground-Water Flow Model (MODFLOW-2005) (No. 6-D1). Geological Survey (US).

McKinney, W., 2010, June. Data structures for statistical computing in python. In *Proceedings of the 9th Python in Science Conference* (Vol. 445, pp. 51-56). Austin, TX: SciPy.

Neitsch, S. L., Arnold, J. G., Kiniry, J. R., & Williams, J. R. (2011). Soil and water assessment tool theoretical documentation version 2009. Texas Water Resources Institute, available: http://hdl.handle.net/1969.1/128050.

Nielsen, A., Bolding, K., Hu, F. and Trolle, D., 2017. An open source QGIS-based workflow for model application and experimentation with aquatic ecosystems. Environmental Modelling & Software, 95, pp.358-364, available: https://doi.org/10.1016/j.envsoft.2017.06.032.

Oki, T. and Kanae, S. (2006) 'Global hydrological cycles and world water resources', *Science*, 313(5790), 1068-1072, available: http://dx.doi.org/10.1126/science.1128845.

Park, C., Lee, J., Koo, M., 2013. Development of a fully-distributed daily hydrologic feedback model addressing vegetation, land cover, and soil water dynamics (VELAS). J. Hydrol. 493, 43–56. http://dx.doi.org/10.1016/j.jhydrol.2013.04.027.

Pearson, D.K., 2013. Geologic database of Texas: Project summary, Database contents, and user's guide: Document prepared by the US Geological Survey for the Texas Water Development Board, Austin, 22 p.

Poeter, E.P. and Hill, M.C., 1998. Documentation of UCODE, a computer code for universal inverse modeling. DIANE Publishing, available: https://doi.org/10.1016/s0098-3004(98)00149-6.

Sophocleous, M., 2002. Interactions between groundwater and surface water: the state of the science. Hydrogeology journal, 10(1), pp.52-67, available: https://doi.org/10.1007/s10040-001-0170-8.

Karl, T.R. ed., 2009. Global climate change impacts in the United States. Cambridge University Press.

Therrien, R., McLaren, R.G., Sudicky, E.A. and Panday, S.M., 2010. HydroGeoSphere: a three-dimensional numerical model describing fully-integrated subsurface and surface flow and solute transport. Groundwater Simulations Group, University of Waterloo, Waterloo, ON.

Vorosmarty, C.J., Green, P., Salisbury, J. and Lammers, R.B. (2000) 'Global water resources: Vulnerability from climate change and population growth', *Science*, 289(5477), 284-288, available: http://dx.doi.org/10.1126/science.289.5477.284.

Winter, T.C., 1998. Ground water and surface water: a single resource (Vol. 1139). DIANE Publishing Inc.

CHAPTER 3

QUANTIFYING EFFECT OF DECADAL AND EXTREME CLIMATE EVENTS ON WATERSHED WATER RESOURCES AND FLUXES USING SWAT-MODFLOW

Highlights

Combined use of groundwater resources and surface water resources is essential to provide reliable water supply in the coming decades. This study provides the methodology whereby available surface water and groundwater resources and the impact of climate events on these resources can be quantified in semi-arid regions using the coupled SWAT-MODFLOW modelling code. Methodology is demonstrated for the Middle Bosque watershed (471 km^2) in the Texas-Gulf region of central Texas, which is subject to both major drought and flooding conditions. Model results are tested against both streamflow and groundwater levels. Results show strong spatio-temporal variability of groundwater head, recharge to the water table, surface-subsurface exchange flow rates, and other watershed water balance components. Recharge rates are highest along the river corridor, with rates up to 221 mm/year, and water table levels can fluctuate up to 7 m. Results from interactions between groundwater and surface water show that the majority of surface - subsurface interactions is groundwater discharge to the stream, with a few locations where stream water seeps to the aquifer. Extreme drought conditions result in approximately a 50% decrease in streamflow, but only a 0.05% decrease in groundwater levels near streams. Lateral flow and soil water decrease by over 50%, but groundwater flow to streams only decreases by 2%. For intense storms (20 inches), streamflow increases by 2,000%, but groundwater levels only by 0.4%, although the change persists much longer (years) than the change in streamflow. Surface runoff and soil deep percolation are affected the most, followed

stream seepage, lateral flow, and groundwater flow to streams. Pre-conditions (e.g. soil water content) has a significant impact on the duration of drought/storm impact on water balance components. Results enhance understanding regarding the spatio-temporal patterns of system-response variables and water balance components in watersheds, which can aid decisions about alternative management strategies in the areas of landuse change, climate change, water allocation, pollution control and groundwater development scenarios.

3.1. Introduction

The shortage of freshwater supply is one of the most critical and global issues facing society currently and within the coming decades. As groundwater becomes a more significant resource for drinking water and irrigation water in many regions worldwide and also affects important ecological functions (Dams et al., 2012), conjunctive management of surface water and groundwater within a watershed system becomes important (Wrachien and Fasso, 2002; Cosgrove and Johnson, 2005; Liu et al., 2013; Singh et al., 2015), particularly during periods of water scarcity. In addition to quantifying the time-dependent volumes of both surface water and groundwater, estimating the water fluxes between storage components (e.g. stream channels, soils, aquifer) of the watershed is also important for understanding trends in storage change. The impact of changes in climate patterns, climate events, population growth, and land use on watershed water resources may also be significant (Postel et al., 1996; Cosgrove and Rijsberman, 2000; Vorosmarty et al., 2000; Döll et al., 2003; Oki and Kanae, 2006; Murray et al, 2012), and thus should also be assessed to assist with future water management.

A variety of methods have been used to quantify water resources for watersheds, river basins, or other geographical areas. These techniques include lumped water balance hydrologic models

over large geographical regions and global scales (Alcamo et al., 1997; Döll et al., 2003; Alcamo et al., 2003; Wada et al., 2010), the use of satellite observations such as with GRACE (Gravity Recovery and Climate Experiment) (Rodell and Famiglietti, 2003; Rodell et al., 2007; Longuevergne et al., 2010; Famiglietti et al., 2011; Feng et al., 2013; Voss et al., 2013), and physically-based spatially-distributed hydrologic models. Whereas large-scale lumped models neglect groundwater storage, GRACE results often are limited to estimating changes in groundwater storage, become uncertain at small spatial scales (less than a few hundred km), and are dependent on the accuracy in accounting for soil moisture change. In addition, changes in surface water storage are difficult to estimate.

Physically-based, spatially-distributed coupled land surface/subsurface hydrologic models such as SWAT (Arnold et al., 1998); CATHY (Camporese et al., 2009), ParFlow (Kollet and Maxwell, 2006), GSFLOW (Markstrom et al., 2008), and SWAT-MODFLOW (Bailey et al., 2016) can be used to estimate components of groundwater and surface water storage. Model applications range from global scale (de Graaf et al., 2015; de Graaf et al., 2017), to continental scale (Schuol et al., 2008; Abbaspour et al., 2015; Maxwell et al., 2015), to river basins and catchments (Gauthier et al, 2009; Perrin et al., 2012; Morway et al., 2013; Tanvir Hassan et al., 2014; Tian et al., 2015; Bailey et al., 2016). Whereas the global-scale and continental-scale models provide global trends in groundwater supply, results are neither accurate enough nor resolved enough to assist in conjunctively managing groundwater and surface water resources at the regional scale. Smaller-scale studies often focus on fluxes (Perrin et al., 2012; Tanvir Hassan et al., 2014; Bailey et al., 2016) and hydrologic responses to management practices (Morway et al., 2013; Tian et al., 2015), rather than an assessment of stored volumes of groundwater and surface water through decadal periods, which are required to assist with water management.

The effect of climate on water storage and water fluxes within a watershed setting should also be estimated for regional-scale water management of both groundwater and surface water. Numerous studies have used groundwater models, land surface models, and coupled land surface/subsurface models to assess the impact of climate on water storage, with an emphasis placed on future climate scenarios. As examples, Scibek and Allen (2006) and Scibek et al., (2007) used Global Circulation Model (GCM) forcing to estimate recharge, groundwater levels, and groundwater surface-water interactions through the year 2099 in British Columbia, Canada, using MODFLOW. Woldeamlak and de Smedt (2007) used MODFLOW to estimate impact of future (2050-2099) wet and dry climate scenarios on a 575 km^2 groundwater system in Belgium. Goderniaux et al. (2009), also for Belgium, applied HydroGeoSphere to determine the impact of climate on groundwater reserves and surface water flow through 2080 under six climate model scenarios. Ali et al. (2012) assess climate scenario impact on groundwater levels in Australia for the year 2030, and Meixner et al. (2016) quantified the effect of climate change on groundwater recharge in the western United States. The SWAT model has been used extensively to estimate the impact of future climate on patterns of land surface fluxes (water yield, surface flow, groundwater recharge, lateral flow) for Ontario (Jyrkama and Sykes, 2007), California (Ficklin et al., 2009), Iran (Vaghefi et al., 2013), Africa (Faramarzi et al., 2013), Australia (Tweed et al., 2009; Brown et al., 2015), and globally (Haddeland et al., 2010). Surfleet and Tullos (2014) used GSFLOW to investigate future climate change impact on surface runoff, streamflow, and overland flow for a 4700 km^2 area in Oregon.

These studies, however, focus on long-term climate impact rather than near-term or current climate events that often pose more immediate stress on regional water supply or region infrastructure. Such severe climate events include drought, multi-year drought, and extreme

flooding events. The impact of these climate events on surface water storage, groundwater storage, and watershed fluxes (recharge, groundwater-surface water interaction, lateral flow, surface runoff) should be quantified under a variety of event magnitudes. This will assist in understanding short-term and long-term hydrologic response of a watershed system to these events, and also assist regional water managers in forecasting water supply.

In this study, the recently developed SWAT-MODFLOW modelling code of Bailey et al. (2016) is used to quantify surface water resources, groundwater resources, and water flux rates between storage components as impacted by multi-decadal climate patterns and extreme climate events (major drought, storms) in a semi-arid regional-scale watershed. The Middle Bosque watershed (area of 471 km^2) in the Texas-Gulf region of central Texas, prone to both severe drought and intense storms, is used as an example. Spatio-temporal patterns of groundwater hydraulic head, recharge as calculated deep percolation, groundwater–surface water interaction and water resources availability (global water balance) are explored throughout the watershed during the (1980-2012) period using the SWAT-MODFLOW model. Using the tested model, the impact of severe drought, experienced during 1999, on hydrologic responses and watershed water storage, will be quantified. The impact of high-rainfall storm events also will be assessed, using hypothetical storm events based on the largest recorded thunderstorm events in central Texas. Results will aid in understanding hydrological responses to decadal and short-term climatic events and thereby assist with water management for the region in conjunctively using groundwater and surface water.

3.2. Methodology

3.2.1. Study area

The Middle Bosque River Watershed (MBRW) includes portions of McLennan, Bosque, and Coryell counties (Figure 3.1). There are sedimentary rocks from the Washita and Fredericksburg Groups of early Cretaceous, and Comanchean age. The formation of the Washita Group is the Georgetown Limestone including Main Street, Pawpaw, Weno, Denton, Fort Worth, Duck Creek, and Kiamichi members (Cannata, 1988; Pearson, 2007). The two formations of the Fredericksburg Group, the Edwards Limestone and Comanche Peak Limestone, are used in the study area. The altitude of the study region varies from 367 m at the highest point on the northwestern edge to 161 m on the eastern edge. The MBRW is predominantly comprised of either pasture (65.4 % of area) or farms (20.3 % of area), with minor land covers of forests (8.5 % of area), and residential areas (3.2% of area) (USGS, 2007). The Middle Bosque River dissects the Edwards Limestone and has therefore produced major groundwater discharge and stream seepage areas (Cannata, 1988).

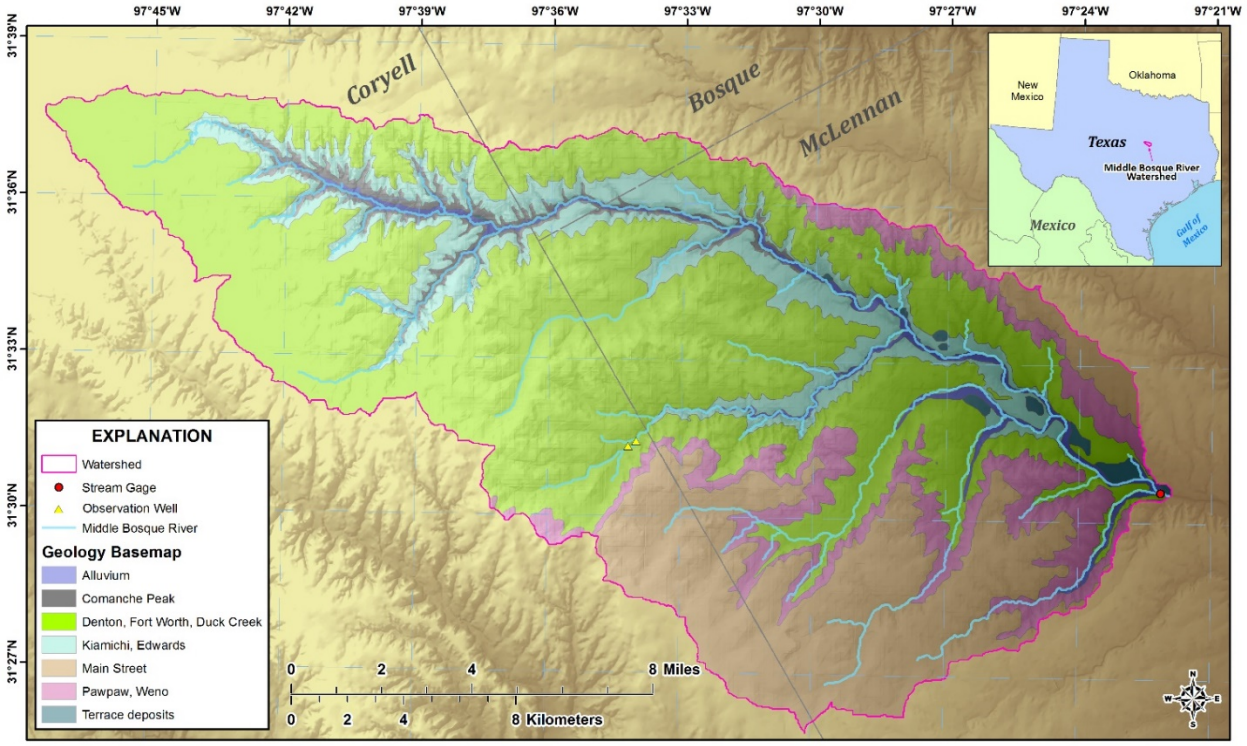

Figure 3.1. Location map showing the position of the study area within McLennan, Bosque, and Coryell Counties, Texas. Physiographic map showing the provinces composing and surrounding the study area. These include the Washita Prairie and Lampasas Cut Plain.

The climate of the study area is characterized by semi-arid, with long hot summers and brief mild winters (Figure 3.2). The warmest month, August, has an average maximum temperature of 36.5 C^o while the coldest month, January, has an average minimum temperature of 2.8 C^o (U.S. Depth. of Commerce, Weather Bureau, 1980 -2012). The annual precipitation ranges from about 602 to 1560 mm/year. The wettest months of a normal year are May and October with average precipitation amounts of 118 and 110 mm respectively, while the driest months are July and December with average precipitation amounts of 54 and 48 mm respectively. Monthly twenty-two-year averages for temperature (max, mean, and min) and precipitation (mean) are shown in Figure 3.2.

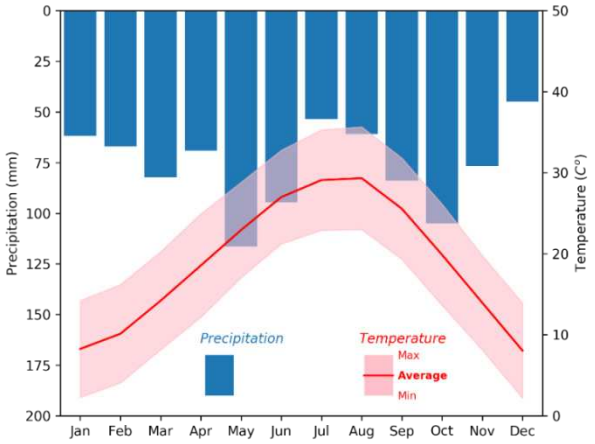

Figure 3.2. Monthly averages for precipitation and temperature (max, mean, and min) in the Middle Bosque River Watershed, 1980 – 2012.

3.2.2. Three-Dimensional Groundwater Model Development

The three-dimensional, finite-difference, groundwater flow modelling program MODFLOW-NWT, A Newton formulation for MODFLOW-2005 (Niswonger et al., 2011), was used to simulate the groundwater flow system of the MBRW during 1980–2012, incorporating time-varying recharge from SWAT and simulating groundwater-surface water interactions with the SWAT river network in the SWAT-MODFLOW model (see Section 3.2.4). Model construction includes designation of spatial and temporal discretization, assignment of boundary conditions and initial conditions, and delineation of aquifer properties. Hydraulic aquifer properties used to construct the model were initially based on published estimates but ultimately were varied to obtain better agreement between simulated and measured data. Geographic Information System (GIS) data containing the layer extent, layer top and base altitude values, geologic data, and other hydrologic, geologic, and geographic data were stored and manipulated using ArcGIS version 10.1. Input files for MODFLOW-NWT were generated from the GIS data with the graphical user interface ModelMuse (Winston, 2009).

The groundwater model encompasses the spatial extent of the MBRW with five geologic layers (Figure 3.3; Table 3.1). The model has 268 columns and 154 rows of square cells; each

cell measures 150 m by 150 m (22,500 m^2). The grid was generated in the USA Contiguous Albers equal area conic coordinate system (North American Datum of 1983, units: meter). The grid origin is located at the northwest corner of the model area (easting -169,236.1 m, northing 952,645.5 m). In general, grid cells were initially specified as active where a hydrological unit from the SWAT model is present and inactive where it is absent. Hydraulic properties of the hydrogeologic units were specified using the Upstream Weighting (UPW) Package of MODFLOW-NWT (Niswonger et al., 2011). In the UPW Package, each layer may be specified as either confined or convertible. Cells in layers specified as confined are assumed to have an unvarying saturated thickness, regardless of the calculated head, and do not become inactive if the calculated head is below the cell bottom. Cells in layers specified as convertible are simulated as having head-dependent saturated thickness when the calculated head is below the cell top, and these cells are deactivated if the head is below the cell bottom. Each of the layers except the Comanche limestone is unconfined in at least part of its extent (see Figure 3). The model layers representing a confining unit, which is composed primarily of fine-grained materials (Cannata, 1988) that are not expected to drain substantially as heads decline, were specified as confined.

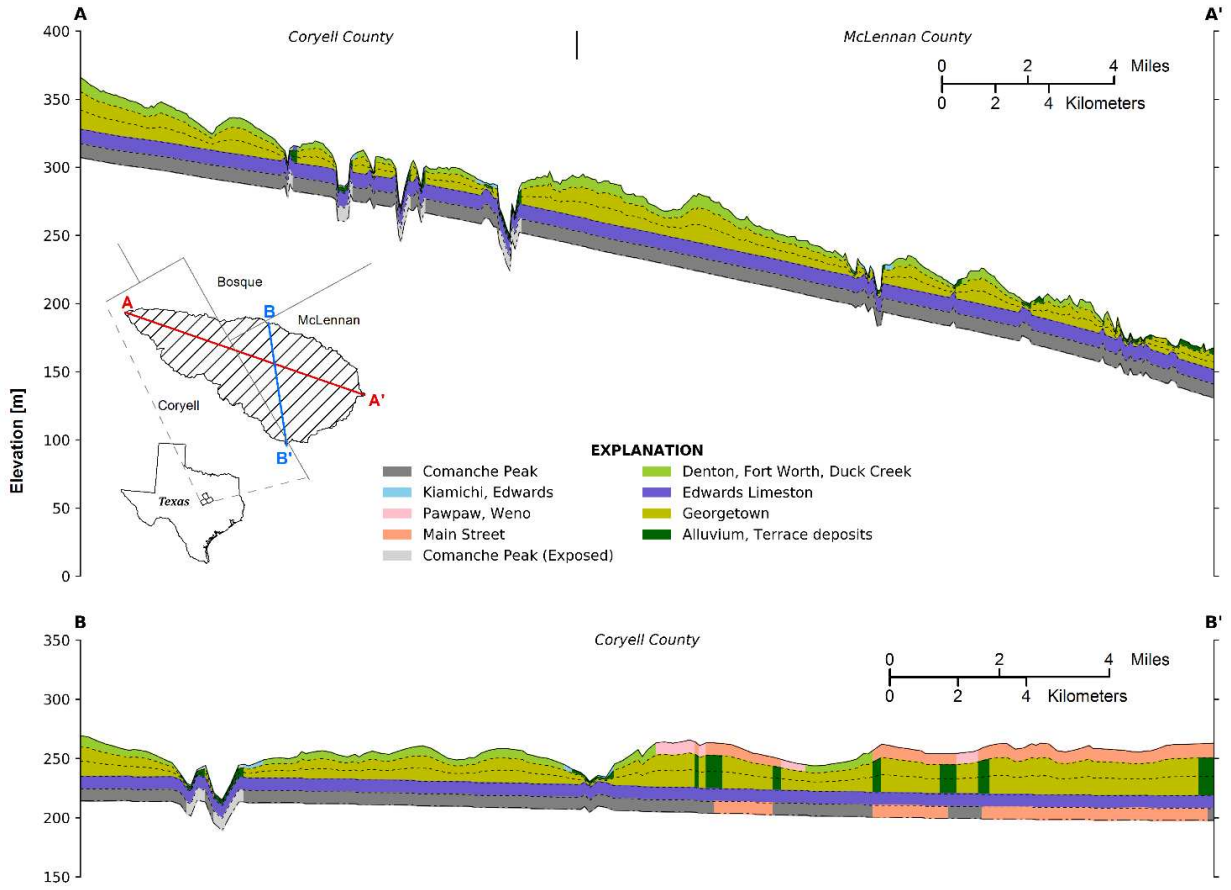

Figure 3.3. The Comanche peak limestone and the many shale units within the Georgetown formation form receding zones beneath the harder limestone units overlying them. A softer portion within the Edwards Limestone many times also forms receding zone.

Simulated time periods in MODFLOW-NWT (Niswonger et al., 2011) are subdivided into "model stress periods". Stress periods are further subdivided into "time steps" during the MODFLOW simulation to facilitate numerical calculations. For the MBRW model, a single stress period is used to represent the time period from January 1, 1980 through 2012 using a daily time step for linkage with SWAT. Before linkage with SWAT, a steady-state model is calibrated using interpolated water level elevation data for January 1, 1980 (see Section 3.2.2.1) to provide the SWAT-MODFLOW model with initial aquifer parameter values.

3.2.2.1. Initial Head Interpolation for Groundwater model

Groundwater level data from 28 observations wells and a geostatistical method which is based on Regionalized Variable theory (RVT) (Matheron, 1963) were used to interpolate initial groundwater head elevation in the study area The concept of the theory is that interpolation from points in space should not be based on smooth continuous object, but based on a stochastic model that takes into consideration the various trend original set of points. The theory considers there are three types of relationships within any dataset and they are as follows:

- structural part (trend),
- correlated variation, and
- uncorrelated variation or noise.

The RVT is also based on random functions and the measurements are assumed to be a realization of a particular random function for a given position, some restrictions have to be made on the data. These restrictions are called stationarity hypothesis (Journel and Huigbregts, 1978). The order of the stationarity hypothesis will depend on the order of the statistical moments required to be stationary. Thus, when second order stationarity is required, at least the first and second order moments (mean, variance and covariance) must be stationary.

Therefore, to make proper use of Geostatistics, at least the intrinsic hypothesis must be fulfilled (Journel and Huigbregts, 1978). The intrinsic hypothesis requires that the mean and the semi-variance depend strictly on the separation distance between samples and not on the coordinate position of the data. When the intrinsic hypothesis cannot be satisfied it is because the data has some trend which must be removed before the data can be adequately analysed through Geostatistics (Vieira et al., 1983). One very simple way to remove a trend is by fitting a trend surface by least squares and subtracting it from the original data, generating a new variable

called residuals with the difference (Vieira et al., 1983 In 2-dimensional space, to remove a trend the following equation can be used,

$$Z^*(x,y) = C_0 + C_1X + C_2Y \quad (1)$$

where $Z^*(x, y)$ is the estimated trend surface, X and Y are the coordinate positions and C_0, C_1 and C_2 are the regression parameters estimated by the least square's method. This surface is then subtracted from the original datasets generating a new variable called "Residuals".

$$Z_{res}(x,y) = Z(x,y) - Z^*(x,y) \quad (2)$$

After detrending and obtaining the residuals for each point, we performed the geostatistical analysis following its normal way, with the residual variable, calculation of the variogram and a best fit model (spherical model).

$$r(h) = \begin{cases} C_0 + C_1\left[1.5\frac{\| h \|}{a} - 0.5\left(\frac{\| h \|}{a}\right)^3\right], if \ \| h \| \leq a \\ C_0 + C_1, otherwise \end{cases} \quad (3)$$

where C_0, C_1, h, and a represent the nugget effects, the structural variation (sill), the separation vector and the range, respectively. After validating the experimental variogram with the spherical model, the kriging estimations of the residual variable was performed then the kriged residuals were added back to the trend surface creating interpolated initial hydraulic heads.

3.2.2.2. Aquifer Properties

Hydraulic conductivity and storage properties of the aquifers and confining units are required inputs for the UPW Package of MODFLOW-NWT (Niswonger et al., 2011). The input defines horizontal, vertical hydraulic conductivity and specific storage for all model layers. For the convertible layers, specific yield of the aquifer material also is required. The conceptualization and parameterization of horizontal hydraulic conductivity for the hydrogeologic units were

summarized in Table 1. Note that the conceptualization schemes described in the table incorporate simplifying assumptions. The Washita Prairie Edwards aquifer is an unconfined aquifer with the water table commonly less than 20 feet below the surface (Cannata, 1988). The aquifer is contained in the Edwards and Georgetown Limestones with the Comanche Peak Limestone forming the lower confining unit (Fig. 3.1 and 3.3). Where major streams completely dissect the Edwards Limestone, additional boundaries are formed where large amounts of water are lost through groundwater discharge to streams.

Parameterization of the hydraulic conductivity distributions for the Georgetown Limestone, Edwards Limestone, and Comanche Peak Limestone (Cannata, 1988) used the zoned parameterization approach as shown in Fig. 1 and 3. Georgetown Limestone is divided into various Rock Units: Kc (Comanche Peak), Kdfdc (Denton, Fort Worth, and Duck Creek), Kked (Kiamichi, Edwards), Kms (Mainstreet), Kpw (Pawpaw, Weno), Qal (Alluvium), and Qt (Terrace deposits) (Cannata, 1988; Pearson, 2013) (Table 1). The Texas geologic map shapefile (Pearson, 2013) and published estimates (Cannata, 1988) were used to assign a parameter distribution to the five layers. Hydrogeologic units represented as confined were assigned values of specific storage; units represented as convertible from confined to unconfined conditions were assigned values of both specific storage and specific yield. A specific-storage value of the confining unit was determined from published estimates in model input and specific-yield values were estimated by PEST using the SWAT-MODFLOW and their spatial distribution were determined for each hydrogeologic unit zone.

Table 3.1. Hydraulic-conductivity conceptualization and parameterization

Hydrogeologic unit	Parameter names and definitions	Hydraulic-conductivity conceptualization
Georgetown Limestone	**Kms** – Hydraulic conductivity of Main Street Limestone	Assumptions: (1) Hydraulic conductivity of Kms is attributable to materials with grain size reported as medium grained and chalky; (2) some 6-8-foot interbeds of calcareous shale, thin bedded to massive, distinctly bedded to wavy bedded and nodular; weathers light gray to white; thickness 25-35 feet.
	Kpw – Hydraulic conductivity of Pawpaw Formation Weno Limestone undivided	Assumptions: (1) Hydraulic conductivity of Kpw is attributable to materials with grain size reported as Pawpaw Formation and calcareous marl; (2) near middle soft ledge-forming limestone bed, unit as a whole recessive; thickness up to 10 feet, thins southward. Weno Limestone, some very thin marl interbeds thin to medium bedded, white to grayish yellow.
	Kdfdc – Hydraulic conductivity of Denton Clay, Fort Worth Limestone, and Duck Creek Limestone	Assumptions: (1) Hydraulic conductivity of Kdfdc is attributable to materials with grain size reported as limestone, chalky, medium grained, fairly hard ; (2) Denton Clay, calcareous, argillaceous limestone in upper part with, abundant Gryphaea, brownish grayish yellow; thickness 3-11 feet.
	Kked – Hydraulic conductivity of Kiamichi Clay and Edwards Limestone	Assumptions: (1) Hydraulic conductivity of Kked is attributable to materials with grain size reported as clay, shale, and limestone; clay and shale, calcareous, silty, yellowish brown limestone, marly, (2) thin nodular to wavy beds; thickness up to 17 feet at north edge of sheet, outcrop discontinuous south of Galesville.
	Qal – Hydraulic conductivity of Alluvium	Assumptions: (1) Hydraulic conductivity of Kked is attributable to materials with grain size reported as gravel, sand, silt, silty clay, and organic matter; (2) Flood-plain deposits, includes indistinct low terrace deposits.
	Qt – Hydraulic conductivity of Fluviatile terrace deposits	Assumption: Hydraulic conductivity of Kked is attributable to materials with grain size reported as gravel, sand, silt and clay
Edwards Limestone	**Ked** – Hydraulic conductivity of Edwards Limestone	Assumption: Hydraulic conductivity within Ked zone is homogeneous and isotropic in the lateral dimensions. Parameters represent hydraulic conductivity of entire unit thickness or vertical anisotropy.
Comanche Peak Limestone	**Kc** – Hydraulic conductivity of Comanche Peak Limestone	Assumptions: (1) Hydraulic conductivity of Kc is attributable to materials with grain size reported as Limestone and fairly hard; (2) numerous shale partings and filled burrows, nodular, gray to white, marine megafossils, forms mid-slope beneath scarp slope of Edwards Limestone; thickness 50-100 feet.

3.2.3. SWAT model construction

SWAT (Soil and Water Assessment Tool, Arnold et al., 1998) simulates water flow, nutrient mass transport and sediment mass transport at the watershed scale. It is a continuous, basin scale, distributed-parameter watershed model emphasizing land surface hydrologic and nutrient processes, dividing the watershed into subbasins which are then further divided into multiple

unique combinations (Hydrologic Response Units HRUs) of land use, soil type and topographic slope for which detailed water, nutrient and sediment mass balance calculations are performed. The SWAT model can also quantify hydrological components of water resources, e.g. surface runoff and deep aquifer recharge (blue water), soil water (green water) and actual evapotranspiration (green water).

A pre-calibrated SWAT model for the MBRW was used for the SWAT-MODFLOW simulation. In the SWAT model, a total of 69 subbasins were delineated based on a Digital Elevation Model (DEM). No thresholds were set for the HRU definition, resulting in 1,693 HRUs. Seven different land covers (Agricultural Land-generic, Forest-deciduous, Forest-mixed, Pasture, Residential-Low Density, Water, and Wetlands-forested) were included.

3.2.4. SWAT-MODFLOW Model

A SWAT-MODFLOW was created using the constructed MODFLOW and SWAT models. The process of linking SWAT HRUs and subbasins with MODFLOW grid cells and River cells is described in Bailey et al. (2016). The linkage process creates text files containing the information necessary to convert model output from HRUs to geographically located disaggregated Hydrologic Response Units (DHRUs), from DHRs to MODFLOW grid cells, and from SWAT sub-basin rivers to MODFLOW River cells. With the linkage files, the SWAT model can pass HRU-calculated soil deep percolation as recharge to the grid cells of MODFLOW, and then the MODFLOW model passes MODFLOW-calculated groundwater–surface water interaction fluxes (either groundwater discharge or stream seepage to the subbasin stream channels of SWAT. With this approach, SWAT calculates the volume of overland flow and soil lateral flow to streams, MODFLOW calculates the volume of groundwater discharge to streams, and SWAT routes the water through the stream network of the watershed.

Groundwater–surface water interaction is simulated using the River package of MODFLOW, with Darcy's law used to calculate the volumetric flow of water Q_{leak} $[L^3/T]$ through the cross-sectional flow area between the aquifer and the stream channel

$$Q_{leak} = K_{bed}(L_{str} \times P_{str}) \times \left(\frac{h_{str} - h_{gw}}{Z_{bed}} \right) \quad (4)$$

where K_{bed} is river bed hydraulic conductivity [L/T], L_{str} is the length of the stream [L], P_{str} is the wetted perimeter of the stream [L], h_{str} is river stage [L], h_{gw} is the hydraulic head of groundwater [L], and z_{bed} is the thickness of the river bed [L]. Q_{leak} is negative if groundwater flows to the river (i.e. groundwater hydraulic head h_{gw} is above the river stage h_{str}), and positive if river water seeps into the aquifer. These calculations are performed for any grid cell through which a stream passes, with cells identified initially through spatial intersection of the SWAT stream network with MODFLOW grid cells.

SWAT-MODFLOW is a single compileable FORTRAN code, in which MODFLOW is called by the main SWAT code, thereby replacing the original SWAT groundwater module. Upon reading input data for both the SWAT and MODFLOW models, the simulation runs through the repeated daily process of SWAT HRU calculations, passing data to MODFLOW, running MODFLOW, passing data to SWAT and routing water through the watershed's stream network, through the end of the simulation.

3.2.5. Parameter estimation for the coupled SWAT-MODFLOW model

Parameter estimation for hydrologic models can be accomplished using a variety of methods. SWAT-CUP (SWAT Calibration Uncertainty Procedures) has been used extensively for SWAT model calibration and uncertainty analysis and includes Generalized Likelihood Uncertainty Estimation (GLUE) (Beven and Binley, 1992), Parameter Solution (ParaSol) (van Griensven and Meixner, 2006), and Sequential Uncertainty FItting (SUFI-2) (Abbaspour, et al., 2007). Many

graphical user interfaces for groundwater models support PEST (Parameter EStimation Tool) (Doherty, 2006) & UCODE (Universal Computer code) (Poeter et al., 1998), model-independent calibration software. For this study, Parallel PEST (Doherty, 2006) is used to estimate values for both land surface (SWAT) and aquifer (MODFLOW) properties. PEST adjusts selected parameters in sequential simulation runs to minimize the objective function, which is the sum of the squared weighted residuals between the observed and simulated values:

$$\Phi = \sum_{i}^{n} w_i (o_i - s_i)^2 \tag{5}$$

where Φ is the objective function, n is the number of target variables, w_i is the weight assigned to the ith target variable, and o_i and s_i are the observed and simulated values of the ith target variable, respectively. The value of w_i for each target variable is calculated as the product of an uncertainty weight and a unit discrepancy weight. The uncertainty weight was calculated as the inverse of an estimated coefficient of variation (CV) reflective of the relative uncertainty in the observations of the target variable. The unit discrepancy weight was determined by unifying the sum of the square of each observed variable value. To calibrate surface parameters (SWAT domain) and subsurface parameters (MODFLOW domain) simultaneously, a Python script was implemented in batch mode containing all necessary executables and files.

Land surface parameters from SWAT [available water capacity of the soil layer (SOL_AWC), runoff curve number (CN2), soil evaporation compensation factor (ESCO)] and groundwater parameters from MODFLOW [hydraulic conductivity (K), specific yield (S_y), river bed conductance] were assigned as field parameters. Nine zones were used for K and S_y, and three values were used for river bed conductance, resulting in a total of 24 parameters. The objective function was composed of observed streamflow from 1993-2012, and groundwater levels from two observation wells during 1985-1986. Comparison statistics such as the Nash-Sutcliffe model

efficiency factor (NSE), R^2, and PBIAS are used to quantify model results. Parameter estimation was performed for the data through 2005, with 2005-2012 used for model testing.

3.2.6. Estimating Water Resource Availability

The monthly water resource availability in the MBRW was estimated using the global water balance data ("output.std" file) as output by SWAT-MODFLOW. The file for the SWAT-MODFLOW simulations has the same general format as the original SWAT model, but with several key additions that provide more information regarding groundwater and groundwater-surface water interactions. These additions are presented in Table 2 and include surface runoff, lateral flow, groundwater flow to streams, deep percolation to groundwater, soil water, seepage from streams to the aquifer, and groundwater volume. These results are used to estimate water resource availability for surface and groundwater during the 2000-2012 time period and to quantify the response of water storage and hydrologic fluxes to the decadal climate patterns.

Table 3.2 Variables in SWAT-MODFLOW simulations

Variable name	Definition	
	SWAT	SWAT-MODFLOW
PREC	Average amount of precipitation (mm)	
SURQGEN	Amount of surface runoff contribution from streamflow from HRU during simulation (mm)	
LATQ	Lateral flow contribution to streamflow (mm)	
GWQ	Groundwater contribution to streams (mm)	
	using original SWAT groundwater module	as calculated by the River package in MODFLOW
PERCO LATE	Water percolation past bottom of soil profile(mm)	
TILE Q	Drainage tile flow contribution to stream (mm)	
SW	Amount of water stored in soil profile (mm)	
ET	Actual evapotranspiration (mm)	
SWGW	x	Seepage from streams to the aquifer (mm) as calculated by the River package in MODFLOW
GW	x	Amount of groundwater stored in the watershed (mm)
WATER YIELD	Total water added to streams	
	SURQ + LATQ + GWQ + TILE Q	SURQ + LATQ + GWQ – SWGW + TILE Q

3.2.7. Quantifying Hydrological Responses to Climate Events

The calibrated and tested SWAT-MODFLOW model is then used to quantify the impact of short-term extreme climate events on water resource availability and hydrologic fluxes. The

impact of a severe year-long drought and thunderstorm, each of varying intensity for a suite of scenarios, are assessed.

During the simulation period, the 1999 climate year was used for analysis of drought impact (see Fig. 4). This drought was the cause of many deaths in the central Texas area, and the Dallas airport reported 26 consecutive days of 100^{o}F. Only 602 mm fell during the entire year (compared to an annual average of 950 mm), with the months of August-September with little rainfall (23mm). To determine the impact of varying intensity of drought on watershed hydrology, 6 different scenarios were simulated by multiplying the original precipitation rates of 1999 by a factor of 0.25, 0.5, 0.75, 1.25, 1.5, 1.75, respectively. The monthly precipitation depths (mm) for the 6 drought scenario simulations are shown in Figure 3.5a, in comparison with the original monthly rainfall depths of 1999.The storm event uses rainfall depths based on intense thunderstorm (in terms of rainfall depth per day) in recorded hydrologic history in central Texas. On September 9, 1921, a thunderstorm produced 480 mm (19 inches) of rain in Austin, Texas (Bishop, 1977), leading to strong flooding in the region. The short-term and long-term effect of such a storm on watershed water storage and hydrologic fluxes is investigated in this study by imposing a similar storm on the 2000-2013 simulation period, during 2004 (see Figure 3.4). The storm event scenario uses two pre-conditions, i.e., wet and dry, since antecedent conditions likely effect the hydrologic response of the storm event. Similar to the drought event, storms of varying intensity are simulated, with daily rainfall depths set to 5, 10, 15, and 20 inches. The storm event scenario uses two pre-conditions, wet and dry, since antecedent soil moisture and shallow groundwater tables likely effect the hydrologic response of the storm event, making a total of 8 storm simulations (Figure 3.5).

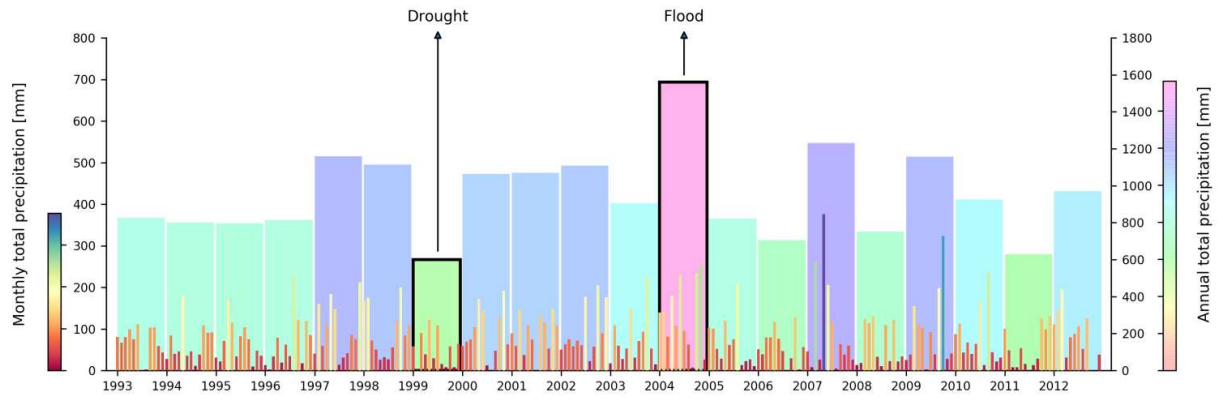

Figure 3.4. Monthly and annual total precipitation during the model corroboration period with a drought year of 1999 and a flood year of 2004.

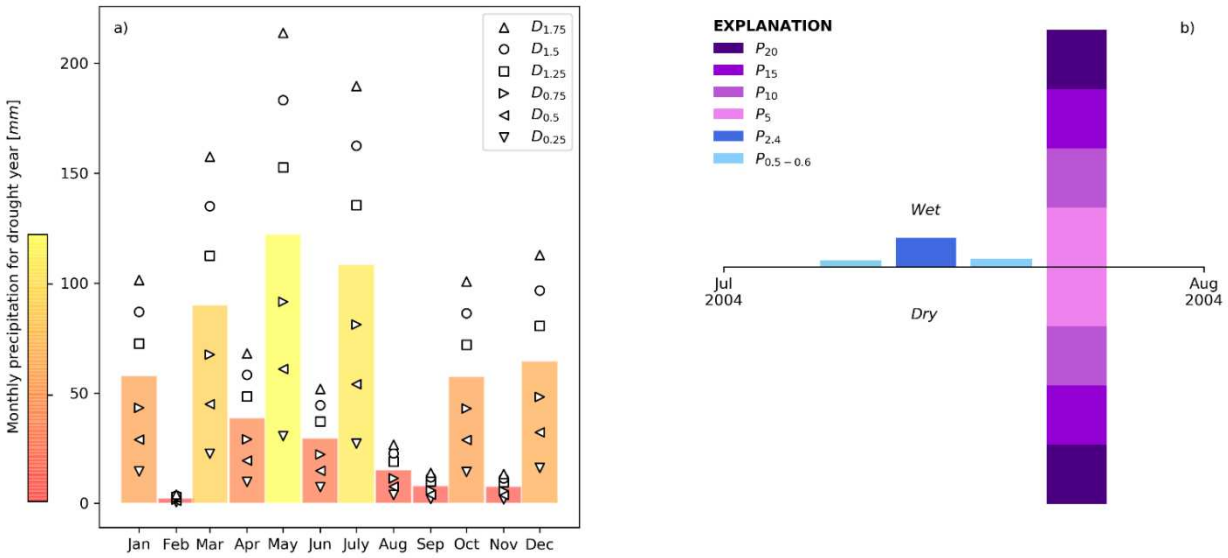

Figure 3.5. Different rainfall patterns in a) drought scenario with 6 different ratios (0.25, 0.5, 0.75, 1.25, 1.5, 1.75) multiplying by the original precipitation rates in 1999 and in b) flood scenarios using two pre-conditions, i.e., wet with the original precipitation data and dry with the deletion of 3-day rainfall events before the storm condition scenarios (5, 10, 15, and 20 inches).

3.3. Results and Discussion

3.3.1. Initial head interpolation

As shown in Fig. 3.6a, the behavior of the variogram from the 28 observed water level data is similar to a linear variogram model, suggesting a trend that can be considered as non-stationary. After detrending the original observed water level data with the trend surface function (e.q.1), the experimental variogram showed a clear sill at the variance value resulting in

following the intrinsic hypothesis after the trend removal (Fig. 7.6b). The kriging estimation of the residuals with the values of sill and range fitting to the spherical model were performed and then the kriged residuals were added to the trend surface, creating the initial interpolated hydraulic head as shown in Fig. 3.7, ranging from 170 to 342 m above MSL.

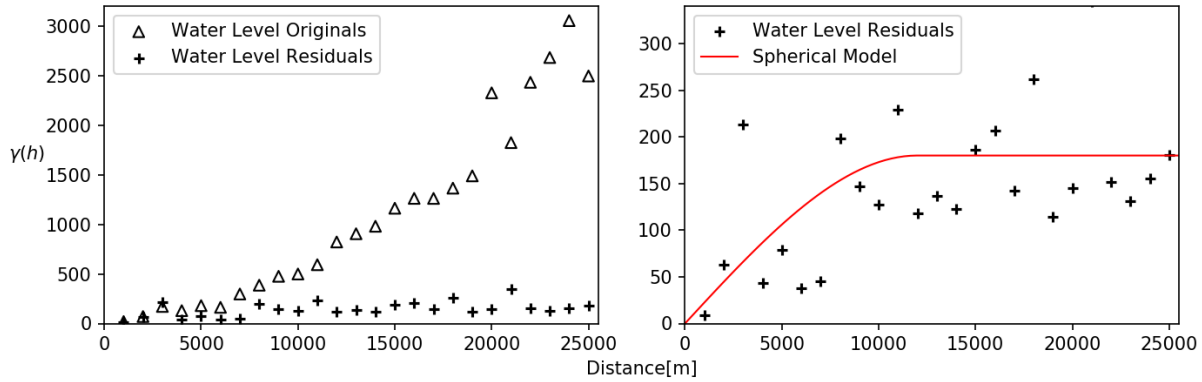

Figure 3.6 Variograms for the 28 observed water levels: a) original values with residuals; b) residuals with model fitted.

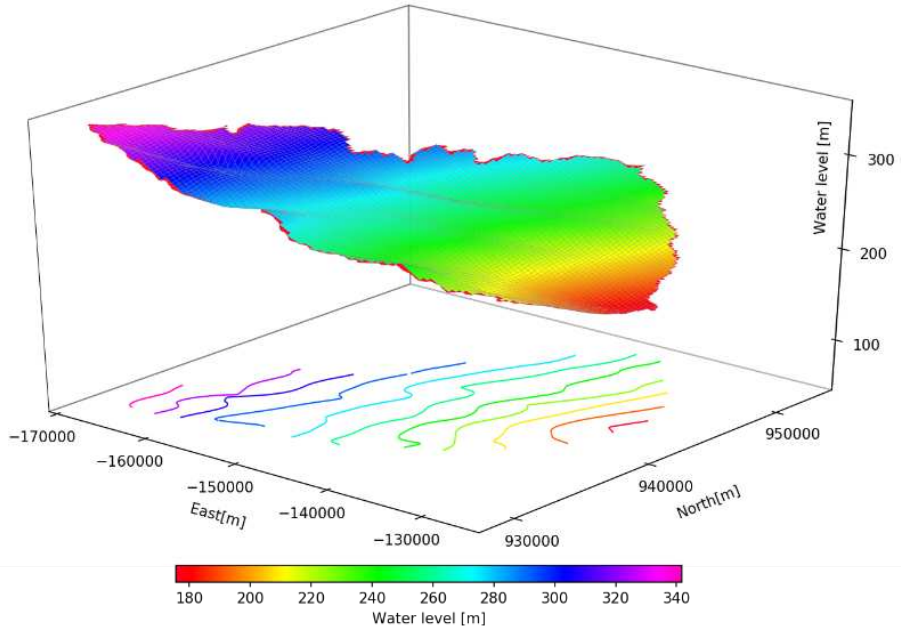

Figure 3.7. Interpolated initial hydraulic head with the de-trended 28 observed water level data using the ordinary kriging method and the spherical model.

3.3.2. Model corroboration

PEST stopped after 288 simulations through 7 iterations, the parameter estimation process stopped. The distribution of calibrated hydraulic conductivities and specific yields for the SWAT-MODFLOW model are presented in in Table 3.3. The highest hydraulic conductivity value is estimated to be 990 m/day, within the alluvium zone in the first layer, and the lowest hydraulic conductivity value is 0.10 m/day, at exposed-Comanche Peak Limestone in the first layer. The range of specific yield values varies from 0.05 to 0.35.

Table 3.3 Initial ranges and calibrated values for the selected parameters during streamflow discharge and hydraulic head calibration.

Parameter	Description	Initial range (relative change)	Calibrated value
CN2	Initial SCS runoff number for moisture condition II	(-0.40 – 0.10)	(-0.11)
SOL_AWC	Available water capacity of the soil layer (mm H2O mm soil^{-1})	0.10 – 0.90	0.85
ESCO	Soil evaporation compensation factor	0.10 – 0.90	0.74
cond_1	Riverbed hydraulic conductance (m/day) - upper	0.1 – 100	3.65
cond_2	Riverbed hydraulic conductance (m/day) - middle	0.1 – 100	3.18
cond_3	Riverbed hydraulic conductance (m/day) - lower	0.1 – 100	6.18
Kdfdc	Hydraulic conductivity of Denton Clay, Fort Worth Limestone, and Duck Creek Limestone	5.00E-03 - 100	1.03
Qal	Hydraulic conductivity of Alluvium	50 - 3000	989.57
Kc	Hydraulic conductivity of Comanche Peak Limestone (exposed)	2.00E-02 – 50	9.91E-02
Kked	Hydraulic conductivity of Kiamichi Clay and Edwards Limestone	2.00E-02 – 50	3.33
Kms	Hydraulic conductivity of Main Street Limestone	1.00E-03 – 10	10.00
Kpw	Hydraulic conductivity of Pawpaw Formation Weno Limestone undivided	2.00E-02 – 50	0.34
Qt	Hydraulic conductivity of Fluviatile terrace deposits	50 - 3000	984.52
George	Hydraulic conductivity of Georgetown Limestone	0.5 - 50	17.27
Edward	Hydraulic conductivity of Edwards Limestone	1 - 100	10.37
Ed_sy	Specific yield of Edwards Limestone	0.05 – 0.35	0.35
gg_sy	Specific yield of Georgetown Limestone	0.05 – 0.35	5.66E-02
Kc_sy	Specific yield of Comanche Peak Limestone (exposed)	0.05 – 0.35	0.35
Kd_sy	Specific yield of Denton Clay, Fort Worth Limestone, and Duck Creek Limestone	0.05 – 0.35	5.21E-02
Kk_sy	Specific yield of Kiamichi Clay and Edwards Limestone	0.05 – 0.35	5.00E-02
Km_sy	Specific yield of Main Street Limestone	0.05 – 0.35	0.35
Qal_sy	Specific yield of Alluvium	0.05 – 0.35	5.00E-02
Qt_sy	Specific yield of Fluviatile terrace deposits	0.05 – 0.35	0.29
Kpw_sy	Specific yield of Pawpaw Formation Weno Limestone undivided	0.05 – 0.35	5.00E-02

Observed and simulated streamflow discharges for the gauge site on the Middle Bosque river (see Figure 3.1 for location) is shown in Figure 3.8 resulting in good similarity of the SWAT-

MODFLOW simulation with the observed data. The monthly NSE values of streamflow discharge for calibration and validation were calculated to be 0.45 and 0.66, respectively, and for whole simulation was 0.55, which are considered acceptable for monthly stream discharge (≥ 0.5) (Moriasi et al., 2007) (Table 3.4). The monthly R^2 for validation also shows a better result than its calibration. The PBIAS value for calibration reveals a small percent under-prediction (2.62), but a large percent over-prediction (-16.79) for validation probably due to the slightly different behavior in the periods of low stream flow.

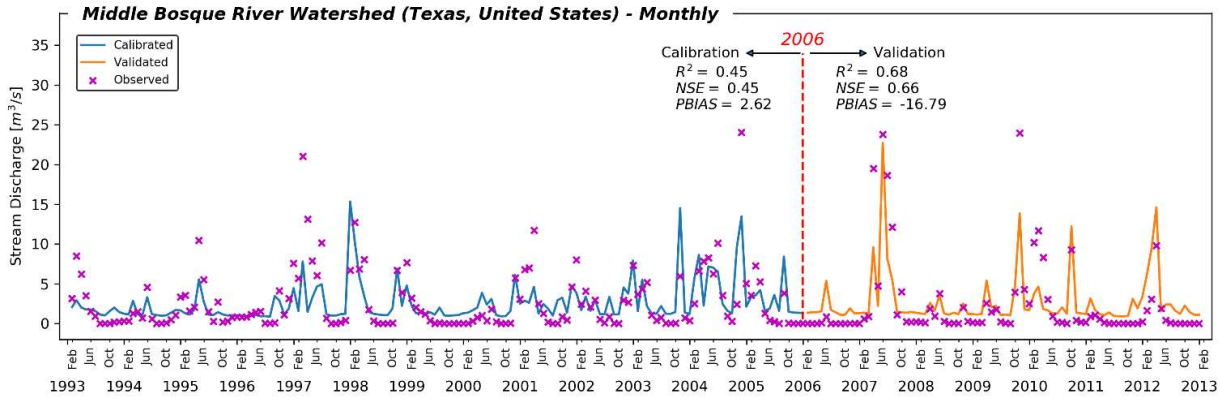

Figure 3.8. Observed and SWAT-MODFLOW simulated time series of stream discharge (m^3/s), and the statistics (R^2, NSE, PBIAS) for calibration (1993 – 2005) and validation (2006 – 2012) periods for the outlet of the Middle Bosque River watershed

Table 3.4 Comparison statistics (NSE; R^2; PBIAS) between the observed and simulated hydrograph at the stream gauge near the confluence of the Sycan and Sprague Rivers (Fig. 3.1) for calibration (1993 – 2005), validation (2005 – 2012), and whole simulation of the SWAT-MODFLOW model

Statistical Comparison	Calibration	Validation	Total
NSE	0.45	0.66	0.55
R^2	0.45	0.68	0.56
PBIAS	2.62	-16.79	-3.65

Figure 3.9 shows the hydrographs of measured and simulated hydraulic head for the observation wells (CO1L from 10/21/1985 – 3/7/1986 and CO2D from 11/30/1985 – 2/1/1986) (see Figure3.1 for location). Although the patterns of the hydrographs of simulated hydraulic

heads for both locations are similar to their observed data, the daily R^2 values for two observation wells are considered low because the simulated hydraulic head from CO1L shows less fluctuation compared to its observed value and from CO2D about 1 meter lower than the observed value. Although there are limited transient groundwater level data, field work in the watershed indicates an extremely shallow water table (< 20 ft), particularly in low areas along drainage tributaries, such as for CO1L and CO2D (see Figure 3.1), and that historically most groundwater rises dramatically after rainfall events (see Figure 3.9b) (Easterling et al., 2001).

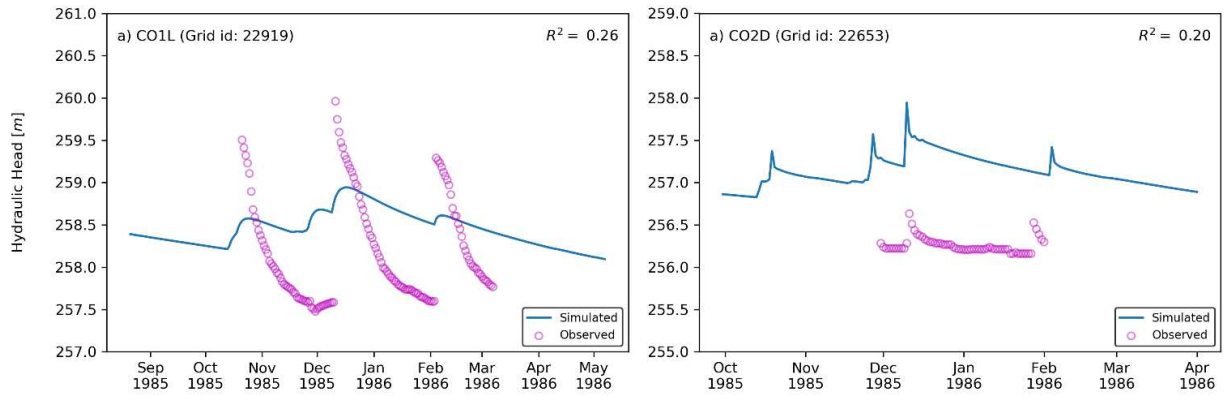

Figure 3.9. Hydrographs of measured and simulated hydraulic head for CO1L and CO2D wells in the Middle Bosque River watershed.

3.3.3. Spatio-Temporal Variation of Hydrologic Fluxes

Simulated cell-wise annual average hydraulic head (m) is shown in Figure 3.10a, ranging from 178 to 328 m above MSL. The spatial variation of annual average hydraulic head is similar to the ground surface elevation, with highest water table elevation occurring in the high surface elevation regions of the MBRW and lowest water table occurring along the main corridor of the Middle Bosque river. Average annual recharge (mm/year) is shown in Figure3.10b, with the highest recharge rates (~ 221mm/year) along the stream network and low recharge rates (2 mm/year) in the regions far from the stream network suggesting a high spatial variability in simulated recharge rates. It's because in the SWAT-MODFLOW simulation, the SWAT model

passed a soil deep percolation calculated by the combination (HRU) of different slope, land use and soil types as recharge to the grid cells of the MODFLOW.

The changes in the hydraulic head during the simulation period is shown in the maps of Figure 3.10, displayed as a departure from the annual average hydraulic head for the months of March, June, September and December. Except the southern region (latitude: 31^0 30N longitude: 97^0 35W) and north-east edge (latitude: 31^0 35N longitude: 97^0 25W) of the MBRW (change in drawdown over 1 meters), slight increases occur for the months of March, June and December and slight decreases for September. In the southern region and north-east edge of the study area, the highest increase is estimated to be 7 meters for March and the highest decrease of drawdowns 6.7 meters for September.

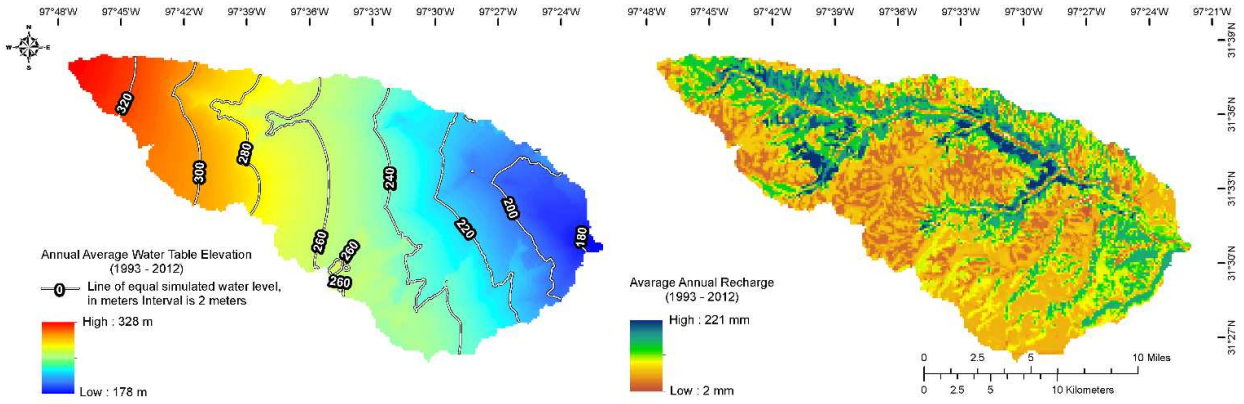

Figure 3.10. a) Simulated cell-wise annual average hydraulic head (m); b) Spatially-varying annual average recharge (mm) in the Middle Bosque watershed as simulated by the coupled SWAT-MODFLOW model

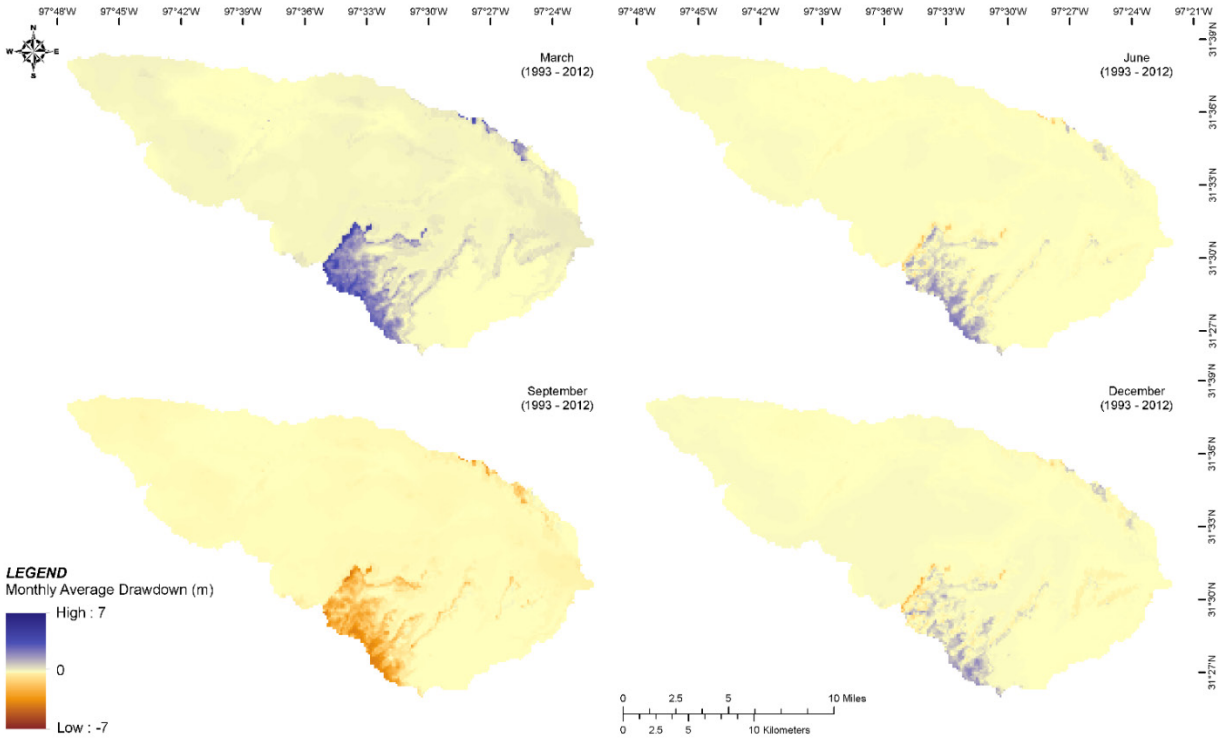

Figure 3.11. Changes from annual average hydraulic head (m) for the months of March, June, September and December over the 1993–2012 period

The spatio-temporal variation in water table elevation is mainly affected by recharge, calculated from the daily recharge values passed from SWAT to MODFLOW. Thus, the results from spatio-temporal drawdowns should be correlated to the results from spatio-temporal recharge. As seen in Figure 3.11, the highest decline of groundwater head occurs in September, due to the relatively low monthly recharge for September during the 1993 – 2012 period. The highest average annual recharge rate is estimated to be 25 mm for March and December, occurring along the main corridor of the Middle Bosque river in the same pattern of annual average recharge distribution (see Figure 3.10b and Figure 3.12).

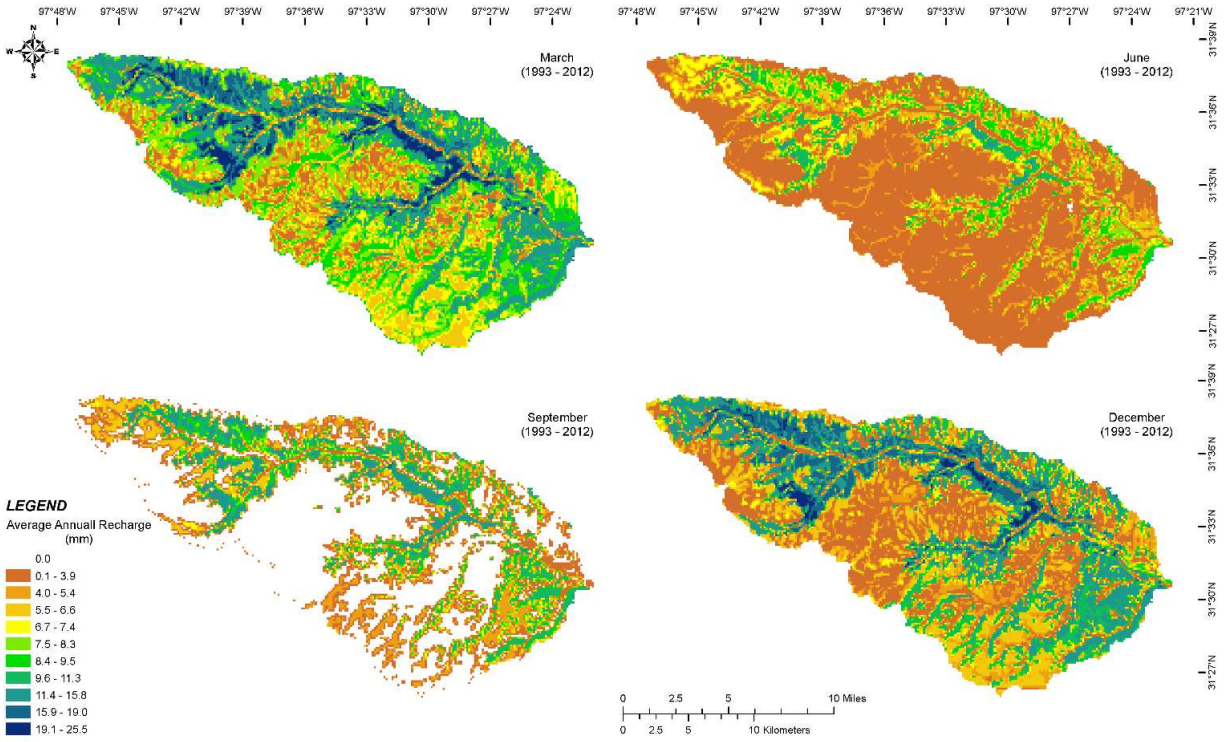

Figure 3. 12. Average annual recharge rates (mm) for the months of March, June, September and December over the 1970–2003 period

Figure 3.13 (centre chart) shows the annual average interaction rates (m^3/day) between groundwater and surface water for each MODFLOW River Cell. Positive values indicate groundwater discharge to the stream network, and negative values indicate stream seepage to the aquifer. The highest interaction rates occur in a section (easting: -130,236 m, northing: 938,678 based on UTM coordinate system) of the main corridor of the Middle Bosque river approximately 1 km from the watershed outlet. The majority of surface - subsurface interactions shows groundwater discharge to the stream, with a few locations where stream water seeps to the aquifer. This is in agreement with the field observations of Cannata (1988), that "where major streams completely dissect the Edwards Limestone, additional boundaries are formed where large amounts of water are lost through discharge to streams". This is also in agreement with the observations of Bishop (1977) for the overall Bosque basin that the presence of impermeable rock in the lower sections of the basin produces a large input of flood and runoff water. The

change in the spatial pattern of groundwater discharge during the year is shown in Figure 3.13, displayed as a departure from the average annual rates for the months of March (maximum groundwater discharge, Figure 3.13a) and September (minimum groundwater discharge, Figure 3.13d).

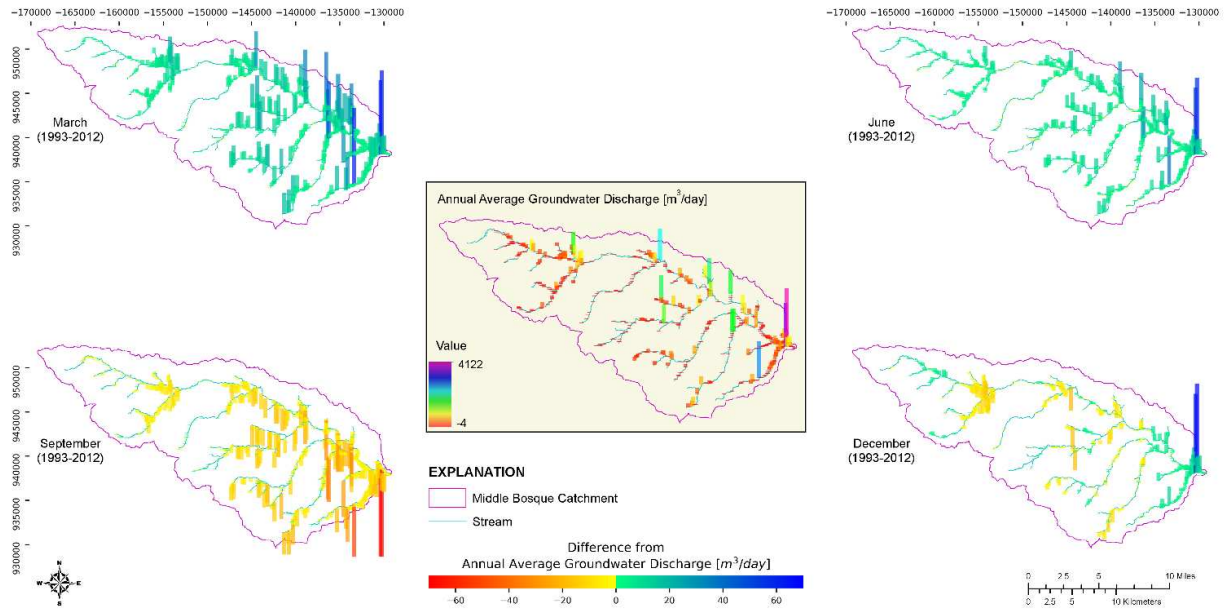

Figure 3.13. Departure from annual average groundwater discharge rates (m^3/day) for the months of March, June, September and December over the 1993–2012 period

Results demonstrate a high spatial-temporal variability in simulated hydraulic head, recharge rates and surface-subsurface water interaction rates, which can have a profound impact on watershed management. For instance, the spatio-temporal variation of recharge and groundwater discharge maps can help identify potential areas of nutrient loading from the aquifer to the stream network or of pollution infiltration from surface to the aquifer. In addition, this area could be used to support decisions about alternative management strategies in the areas of landuse change, climate change, water allocation, and pollution control.

3.3.4. Water resource availability

The monthly water resource availability in the MBRW is shown through a time series of water balance components in Figure 3.14. Components are based on depths (mm) for basin-wide values. The range of the amount of Soil Water (SW) is to be estimated to vary from 20.75 mm in August 2011, with the minimum amount of 0.14 mm for Lateral Flow (LATQ), to 243.83 mm in February 2005 during the 1993 – 2012 period. The amount of extractable groundwater (GW) stored in the watershed ranges from 6370 mm (result not shown in Figure 3.14) to 6765 mm, with about 400 mm difference. The amount of Surface Runoff (SURQ) is estimated to vary from 0 (several events) to 119 mm (May 2007). Regarding surface-subsurface water exchange, GWQ and SWGW can be used for verifying the results of the spatio-temporal patterns of groundwater–surface water interaction. The minimum values of GWQ and SWGW are estimated to be 5.2 (February 1996, result not shown in Figure 3.14) and 0 mm (several events), and the maximum values 9.8 (March 2005) and 0.06 mm (May 2007), respectively, demonstrating the high groundwater contribution to the stream for most of the study area. For water percolation to aquifer (PERCO), the highest PERCO (88.99 mm) occurs in November 2004 and no PERCO in several events.

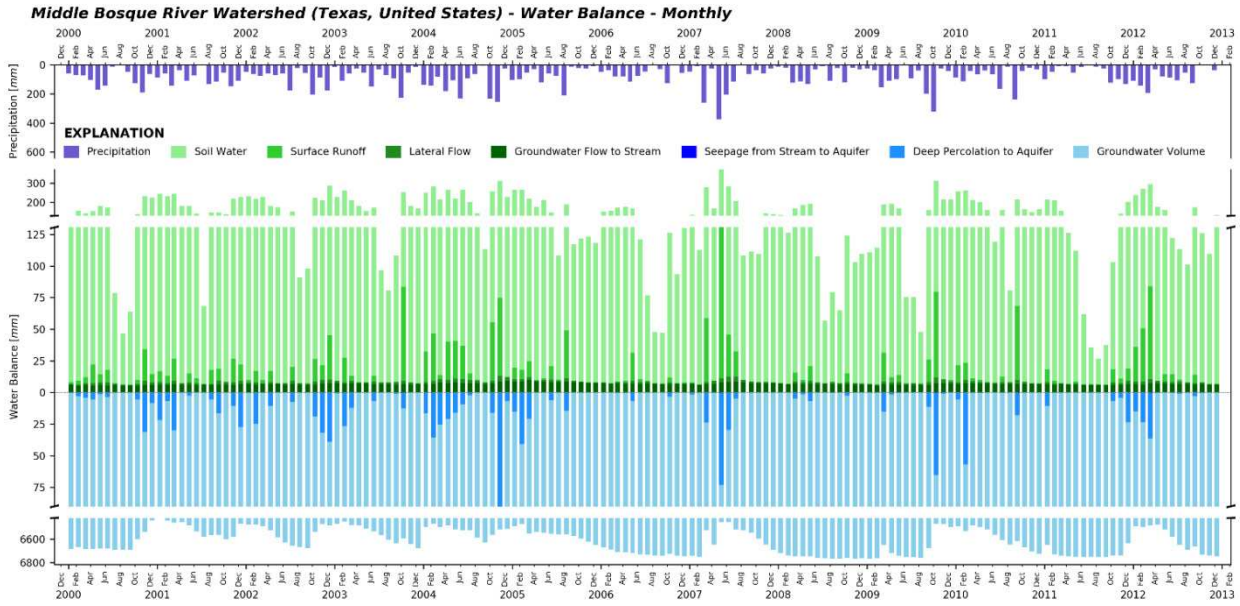

Figure 3. 14. Time series of monthly water resource availability in the Middle Bosque River watershed

3.3.5. Hydrological responses to climate events

Results from the 6 drought simulations are shown in Figures 3.15-3.17. In Scenario $D_{0.25}$, the monthly average streamflow discharge decreased ranging from -52 to -5 % in the control year (1999) and from -22 to -0.5 % in the post-control year (2000) compared to the calibrated model. With $D_{1.75}$, the highest increased percentage is estimated to be about 400 % in May 1999 and the lowest increased 12 % in February 1999 during the control year. In terms of hydraulic head elevations in the two observed locations, both the response times to the drought scenarios are quite slower with smaller scale changes and longer effects than the streamflow discharge. Similar to the results from the streamflow discharge, decrease in precipitation results in smaller scale changes than its increase.

For the water balance results from the drought scenarios, decreases in precipitation result in a relatively significant changes in total soil water (SW) and lateral flow to stream (LATQ) among the other elements of the water balance. SW and groundwater flow to streams (GWQ) are considered to have longer effects from the changes in precipitation. The surface runoff (SURQ)

shows high sensitivity and instantaneous response to the increased precipitation with larger scale changes compared to the other elements. Noteworthily, the total groundwater contained in the watershed (GW) results in a slight decrease (~ -3%) in its volume with the highest increased precipitation scenario ($D_{1.75}$). In addition, the amount of seepage from streams to the aquifer in the MBRW is too small to be influenced by the drought scenarios conditions.

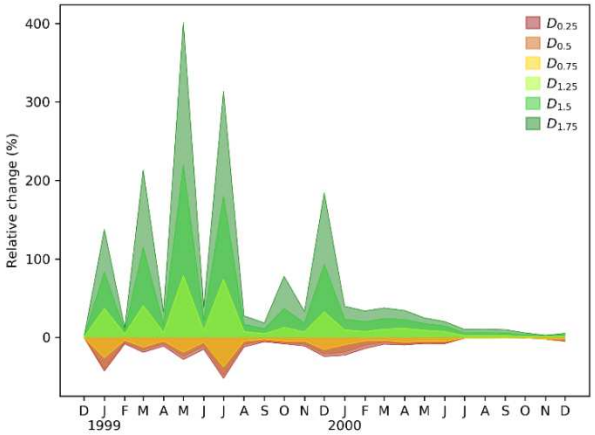

Figure 3.15. Streamflow discharges with 6 different ratios (0.25, 0.5, 0.75, 1.25, 1.5, 1.75) multiplying by the original precipitation rates in the controlling year of 1999 / to post-controlling year of 2000 for the drought scenarios.

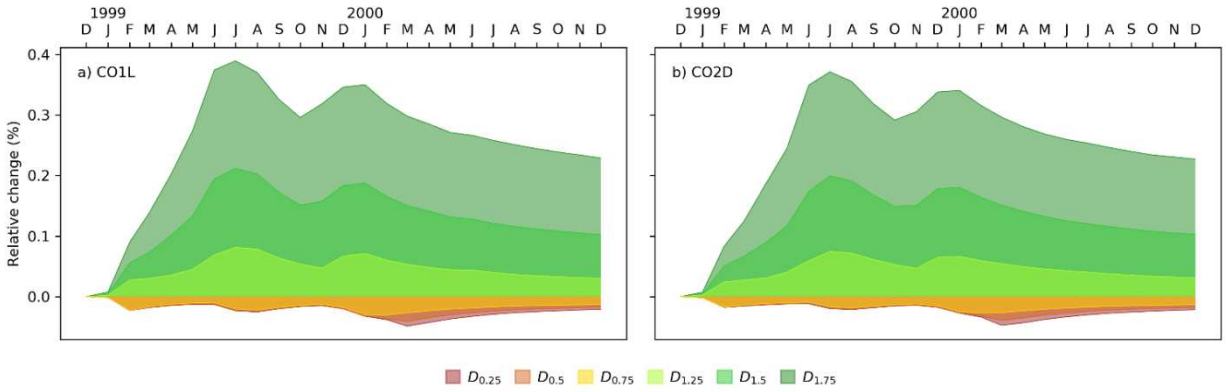

Figure 3.16. Hydraulic head elevations with 6 different ratios (0.25, 0.5, 0.75, 1.25, 1.5, 1.75) multiplying by the original precipitation rates in 1999 for the drought scenarios

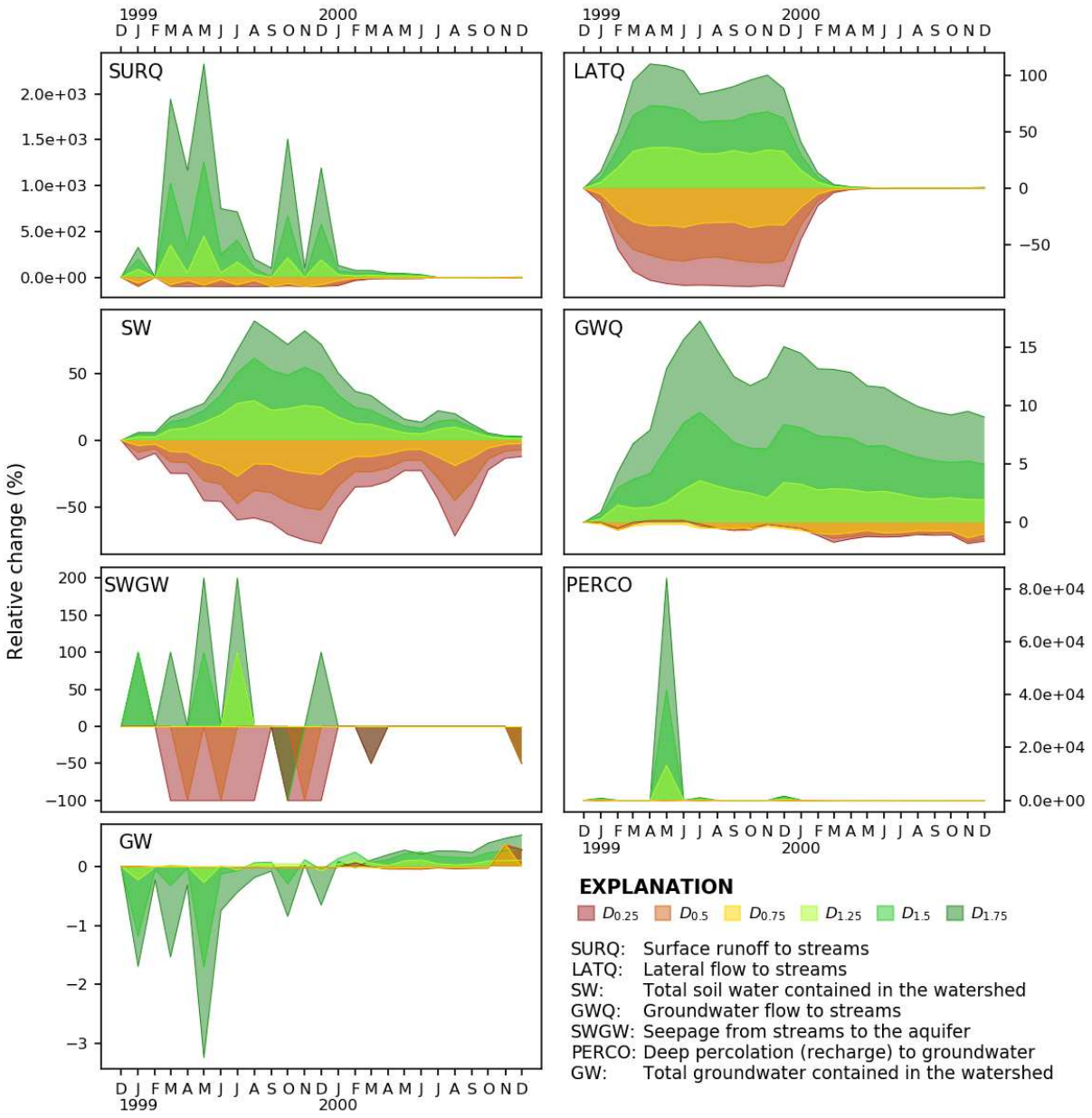

Figure 3.17. Relative changes in each element of water balance with 6 different ratios (0.25, 0.5, 0.75, 1.25, 1.5, 1.75) multiplying by the original precipitation rates in 1999 for the drought scenarios

The results of the 8 storm event scenarios are shown in Figures 3.18-3.20. For the streamflow discharge, the difference between a wet and dry pre-conditions can generate from 250 to 500 % relative changes. For instance, a rainfall of 5 inches after dry periods shows a relative change of 134 % and after wet periods with the same rainfall value the relative change is estimated to be 405 %. The differences of relative changes between the pre-conditions get larger with the higher

rates of the rainfall. In contrast, the differences of the hydraulic head elevations between the pre-conditions get smaller with the higher rates of the rainfall. Like the drought scenarios, the response times of the hydraulic heads to the storm events are slower with smaller scales and longer effects than the streamflow discharge.

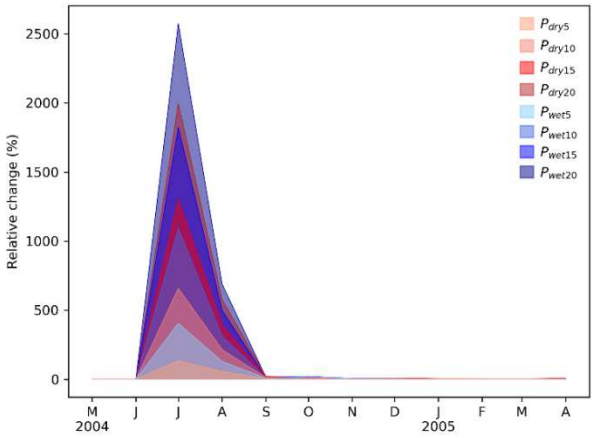

Figure 3.18. Streamflow discharge relative changes with different storm events (5, 10, 15, 20 inches) after a wet or dry pre-condition

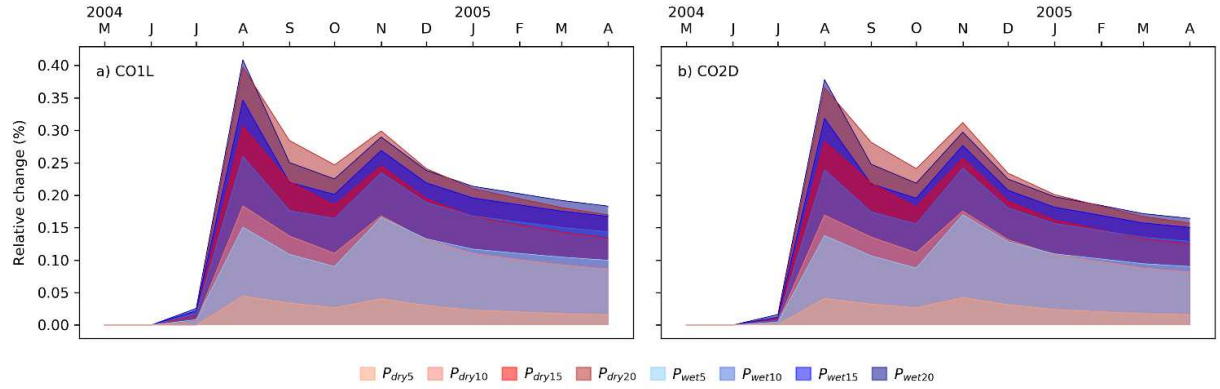

Figure 3.19. Hydraulic head elevations with different storm events (5, 10, 15, 20 inches) after a wet or dry pre-condition

For the water balance results from the storm event scenarios, an increase in the intensity of a storm event shows highly relative changes (higher than 500 %) in surface runoff to streams (SURQ), seepage from streams to the aquifer (SWGW) and deep percolation to groundwater (PERCO). SURQ and PERCO show short-term influence and instantaneous responses to the

storm events. For LATQ, GWQ and PERCO the dry pre-condition before the storm events causes high relative changes compared to the wet pre-condition because an unsaturated soil condition driven by the long-dried periods sucks more water from the storm events and sends it to the streams (LATQ) and induces more recharge (PERCO) that goes to groundwater. In addition, the lowered river stage because of the long-dried periods causes more groundwater flow to the streams (GWQ) after the storm events in the dry pre-condition than the wet pre-condition.

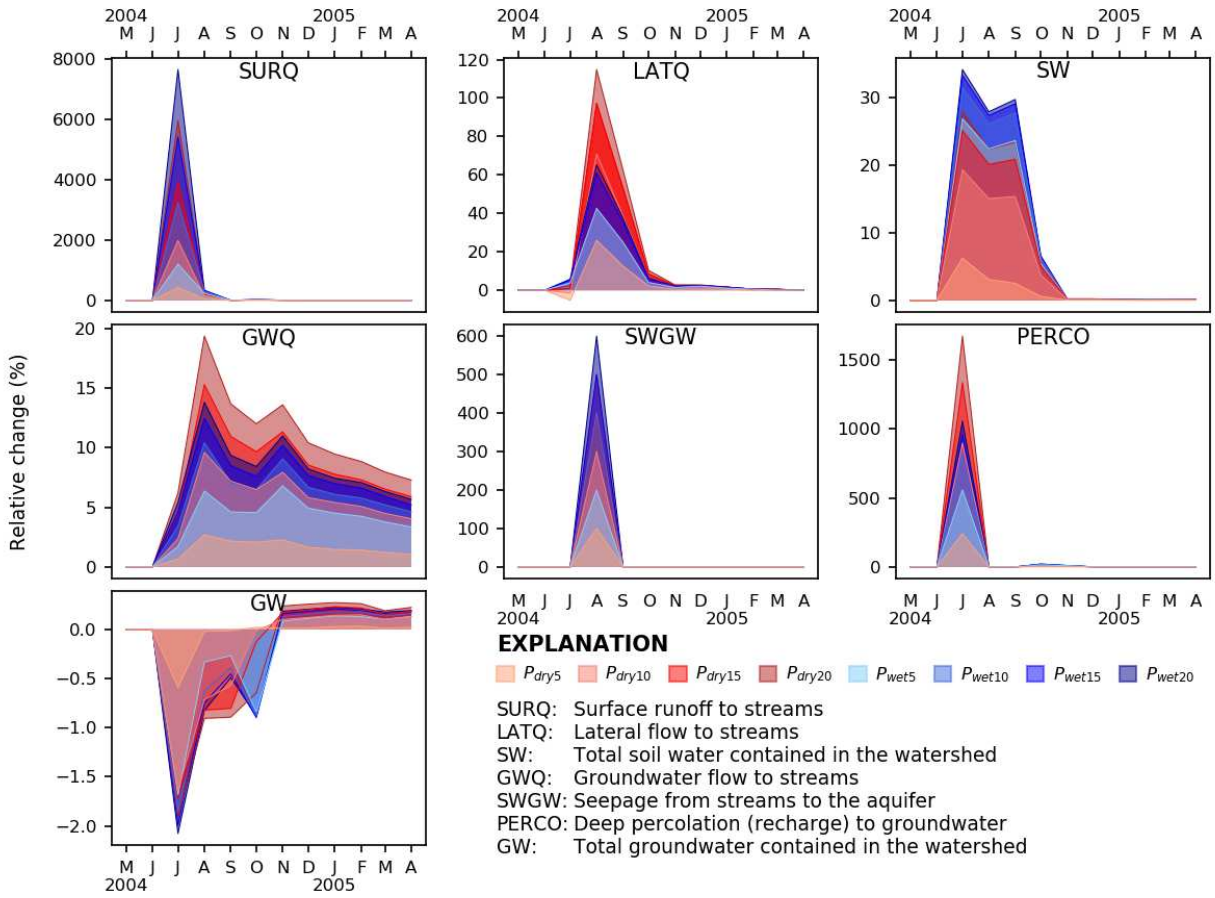

Figure 3.20. Relative changes in each element of water balance with different storm events (5, 10, 15, 20 inches) after a wet or dry pre-condition

These results show climate events such as drought, multi-year drought, and extreme flooding events have a significant impact on surface water storage, groundwater storage, and watershed

fluxes (recharge, groundwater-surface water interaction, lateral flow, surface runoff). Besides, the results show that even the same intensity and length of a stress or even its pre-conditions on different hydrologic response variables can result in their response time, scales and durations in a very different way. For instance, response times for sub-surface related-hydrologic responses such as water table and GWQ are slower than surface related-hydrologic responses such as streamflow discharge, SURQ, SW, and PERCO. Their response durations also quite different which sub-surface related-hydrologic responses are longer than surface related-hydrologic responses.

3.4. Summary and conclusions

This study investigates the water resource availability in the Middle Bosque River watershed (471 km^2) in the Texas-Gulf region of central Texas during the 1993 – 2012 period. The three-dimensional, finite-difference, groundwater flow modelling program MODFLOW-NWT was used to construct the Middle Bosque River Watershed sub-surface system during 1980–2012, and it incorporates time-varying recharge from the pre-calibrated SWAT model. The linked SWAT-MODFLOW model of the Middle River Watershed is tested and calibrated against streamflow and groundwater level using the auto-calibration process by the PEST tool with the post-processing in the batch mode. Model output includes cell-wise hydraulic head, recharge, and surface-subsurface water interaction, demonstrating a high spatio-temporal variability and correlations between the results. Regarding the water resource availability, the SWAT-MODFLOW model can simulate the water balance from surface and sub-surface domains simultaneously based on time series analysis and the results show the high temporal variation of the elements in the water balance. Using the calibrated model, the impact of precipitation on the streamflow discharge, hydraulic head elevation, and water resource availability was assessed

under different rainfall scenarios. The results show that their response time, scales and durations not only vary but also can influenced by their pre-conditions.

This study helps enhance understanding regarding the spatio-temporal patterns of hydraulic head elevation, recharge, surface-subsurface water interaction and the water resource availability and the hydrological responses with different rainfall patterns that support decisions about alternative management strategies in the areas of landuse change, climate change, water allocation, pollution control and groundwater development scenarios.

REFERENCES

Abbaspour, K.C., Rouholahnejad, E., Vaghefi, S., Srinivasan, R., Yang, H. and Klove, B. (2015) 'A continental-scale hydrology and water quality model for Europe: Calibration and uncertainty of a high-resolution large-scale SWAT model', Journal of Hydrology, 524, 733-752, available: http://dx.doi.org/10.1016/j.jhydrol.2015.03.027.

Alcamo, J., Doll, P., Henrichs, T., Kaspar, F., Lehner, B., Rosch, T. and Siebert, S. (2003) 'Development and testing of the WaterGAP 2 global model of water use and availability', Hydrological Sciences Journal-Journal Des Sciences Hydrologiques, 48(3), 317-337, available: http://dx.doi.org/10.1623/hysj.48.3.317.45290.

Alcamo, J., Döll, P., Kaspar, F. and Siebert, S., 1997. Global change and global scenarios of water use and availability: an application of WaterGAP 1.0. Center for Environmental Systems Research (CESR), University of Kassel, Germany, 1720.

Ali, R., McFarlane, D., Varma, S., Dawes, W., Emelyanova, I., Hodgson, G. and Charles, S. (2012) 'Potential climate change impacts on groundwater resources of south-western Australia', Journal of Hydrology, 475, 456-472, available: http://dx.doi.org/10.1016/j.jhydrol.2012.04.043.

Arnold, J.G., Srinivasan, R., Muttiah, R.S. and Williams, J.R. (1998) 'Large area hydrologic modeling and assessment - Part 1: Model development', Journal of the American Water Resources Association, 34(1), 73-89, available: http://dx.doi.org/10.1111/j.1752-1688.1998.tb05961.x.

Bailey, R.T., Wible, T.C., Arabi, M., Records, R.M. and Ditty, J. (2016) 'Assessing regional-scale spatio-temporal patterns of groundwater-surface water interactions using a coupled

SWAT-MODFLOW model', Hydrological Processes, 30(23), 4420-4433, available: http://dx.doi.org/10.1002/hyp.10933.

Beven, K. and Binley, A. (1992) 'THE FUTURE OF DISTRIBUTED MODELS - MODEL CALIBRATION AND UNCERTAINTY PREDICTION', Hydrological Processes, 6(3), 279-298, available: http://dx.doi.org/10.1002/hyp.3360060305.

Bishop, A.L., 1977. Flood potential of the Bosque Basin. Baylor University, Department of Geology.

Brown, S.C., Versace, V.L., Lester, R.E. and Walter, M.T. (2015) 'Assessing the impact of drought and forestry on streamflows in south-eastern Australia using a physically based hydrological model', Environmental Earth Sciences, 74(7), 6047-6063, available: http://dx.doi.org/10.1007/s12665-015-4628-8.

Camporese, M., Paniconi, C., Putti, M. and Salandin, P. (2009) 'Ensemble Kalman filter data assimilation for a process-based catchment scale model of surface and subsurface flow', Water Resources Research, 45, available: http://dx.doi.org/10.1029/2008wr007031.

Cannata, S.L., 1988. Hydrogeology of a portion of the Washita Prairie Edwards aquifer: central Texas (Doctoral dissertation, Baylor University).

Cosgrove, B. and Rijsberman, F., 2000. World water vision. J HYDRAUL RES, 38(4), p.57.

Cosgrove, D.M. and Johnson, G.S. (2005) 'Aquifer management zones, based on simulated surface-water response functions', Journal of Water Resources Planning and Management-Asce, 131(2), 89-100, available: http://dx.doi.org/10.1061/(asce)0733-9496(2005)131:2(89).

Dams, J., Salvadore, E., Van Daele, T., Ntegeka, V., Willems, P. and Batelaan, O. (2012) 'Spatio-temporal impact of climate change on the groundwater system', Hydrology and Earth System Sciences, 16(5), 1517-1531, available: http://dx.doi.org/10.5194/hess-16-1517-2012.

de Graaf, G., Bartley, D., Jorgensen, J. and Marmulla, G. (2015) 'The scale of inland fisheries, can we do better? Alternative approaches for assessment', Fisheries Management and Ecology, 22(1), 64-70, available: http://dx.doi.org/10.1111/j.1365-2400.2011.00844.x.

de Graaf, I.E.M., van Beek, R., Gleeson, T., Moosdorf, N., Schmitz, O., Sutanudjaja, E.H. and Bierkens, M.F.P. (2017) 'A global-scale two-layer transient groundwater model: Development and application to groundwater depletion', Advances in Water Resources, 102, 53-67, available: http://dx.doi.org/10.1016/j.advwatres.2017.01.011.

De Wrachien, D. and Fasso, C.A. (2002) 'Conjunctive use of surface and groundwater: Overview and perspective', Irrigation and Drainage, 51(1), 1-15, available: http://dx.doi.org/10.1002/ird.43.

Doherty, J., 2006. PEST Model-Independent Parameter Estimation, V10. 1, Papadopulos. SS, Inc., Bethesda, MA

Doll, P., Kaspar, F. and Lehner, B. (2003) 'A global hydrological model for deriving water availability indicators: model tuning and validation', Journal of Hydrology, 270(1-2), 105-134, available: http://dx.doi.org/10.1016/s0022-1694(02)00283-4.

Famiglietti, J.S., Lo, M., Ho, S.L., Bethune, J., Anderson, K.J., Syed, T.H., Swenson, S.C., de Linage, C.R. and Rodell, M. (2011) 'Satellites measure recent rates of groundwater depletion in California's Central Valley', Geophysical Research Letters, 38, available: http://dx.doi.org/10.1029/2010gl046442.

Faramarzi, M., Abbaspour, K.C., Vaghefi, S.A., Farzaneh, M.R., Zehnder, A.J.B., Srinivasan, R. and Yang, H. (2013) 'Modeling impacts of climate change on freshwater availability in Africa', Journal of Hydrology, 480, 85-101, available: http://dx.doi.org/10.1016/j.jhydrol.2012.12.016.

Feng, W., Zhong, M., Lemoine, J.M., Biancale, R., Hsu, H.T. and Xia, J. (2013) 'Evaluation of groundwater depletion in North China using the Gravity Recovery and Climate Experiment (GRACE) data and ground-based measurements', Water Resources Research, 49(4), 2110-2118, available: http://dx.doi.org/10.1002/wrcr.20192.

Ficklin, D.L., Luo, Y., Luedeling, E. and Zhang, M. (2009) 'Climate change sensitivity assessment of a highly agricultural watershed using SWAT', Journal of Hydrology, 374(1-2), 16-29, available: http://dx.doi.org/10.1016/j.jhydrol.2009.05.016.

Gauthier, M.J., Camporese, M., Rivard, C., Paniconi, C. and Larocque, M. (2009) 'A modeling study of heterogeneity and surface water-groundwater interactions in the Thomas Brook catchment, Annapolis Valley (Nova Scotia, Canada)', Hydrology and Earth System Sciences, 13(9), 1583-1596, available: http://dx.doi.org/10.5194/hess-13-1583-2009.

Goderniaux, P., Brouyere, S., Fowler, H.J., Blenkinsop, S., Therrien, R., Orban, P. and Dassargues, A. (2009) 'Large scale surface-subsurface hydrological model to assess climate change impacts on groundwater reserves', Journal of Hydrology, 373(1-2), 122-138, available: http://dx.doi.org/10.1016/j.jhydrol.2009.04.017.

Haddeland, I., Heinke, J., Voss, F., Eisner, S., Chen, C., Hagemann, S. and Ludwig, F. (2012) 'Effects of climate model radiation, humidity and wind estimates on hydrological simulations', Hydrology and Earth System Sciences, 16(2), 305-318, available: http://dx.doi.org/10.5194/hess-16-305-2012.

Hassan, S.M.T., Lubczynski, M.W., Niswonger, R.G. and Su, Z. (2014) 'Surface-groundwater interactions in hard rocks in Sardon Catchment of western Spain: An integrated modeling approach', Journal of Hydrology, 517, 390-410, available: http://dx.doi.org/10.1016/j.jhydrol.2014.05.026.

Journel, A.G. and Huijbregts, C.J., 1978. Mining geostatistics. Academic press.

Jyrkama, M.I. and Sykes, J.F. (2007) 'The impact of climate change on spatially varying groundwater recharge in the grand river watershed (Ontario)', Journal of Hydrology, 338(3-4), 237-250, available: http://dx.doi.org/10.1016/j.jhydrol.2007.02.036.

Kollet, S.J. and Maxwell, R.M. (2006) 'Integrated surface-groundwater flow modeling: A free-surface overland flow boundary condition in a parallel groundwater flow model', Advances in Water Resources, 29(7), 945-958, available: http://dx.doi.org/10.1016/j.advwatres.2005.08.006.

Liu, J.G., Zang, C.F., Tian, S.Y., Yang, H., Jia, S.F., You, L.Z., Liu, B. and Zhang, M. (2013) 'Water conservancy projects in China: Achievements, challenges and way forward', Global Environmental Change-Human and Policy Dimensions, 23(3), 633-643, available: http://dx.doi.org/10.1016/j.gloenvcha.2013.02.002.

Longuevergne, L., Scanlon, B.R. and Wilson, C.R. (2010) 'GRACE Hydrological estimates for small basins: Evaluating processing approaches on the High Plains Aquifer, USA', Water Resources Research, 46, available: http://dx.doi.org/10.1029/2009wr008564.

Markstrom, S.L., Niswonger, R.G., Regan, R.S., Prudic, D.E. and Barlow, P.M., 2008. GSFLOW-Coupled Ground-water and Surface-water FLOW model based on the integration of the Precipitation-Runoff Modeling System (PRMS) and the Modular Ground-Water Flow Model (MODFLOW-2005). US Geological Survey techniques and methods, 6, p.240.

Mateus, C., Tullos, D.D. and Surfleet, C.G. (2015) 'HYDROLOGIC SENSITIVITY TO CLIMATE AND LAND USE CHANGES IN THE SANTIAM RIVER BASIN, OREGON', Journal of the American Water Resources Association, 51(2), 400-420, available: http://dx.doi.org/10.1111/jawr.12256.

Matheron, G., 1963. Principles of geostatistics. Economic geology, 58(8), pp.1246-1266

Maxwell, S. (2005) '2005 update on water industry consolidation trends', Journal American Water Works Association, 97(10), 34-36.

Meixner, T., Manning, A.H., Stonestrom, D.A., Allen, D.M., Ajami, H., Blasch, K.W., Brookfield, A.E., Castro, C.L., Clark, J.F., Gochis, D.J., Flints, A.L., Neff, K.L., Niraula, R., Rodell, M., Scanlon, B.R., Singha, K. and Walvoord, M.A. (2016) 'Implications of projected climate change for groundwater recharge in the western United States', Journal of Hydrology, 534, 124-138, available: http://dx.doi.org/10.1016/j.jhydrol.2015.12.027.

Murray, C.J.L., Rosenfeld, L.C., Lim, S.S., Andrews, K.G., Foreman, K.J., Haring, D., Fullman, N., Naghavi, M., Lozano, R. and Lopez, A.D. (2012) 'Global malaria mortality between 1980 and 2010: a systematic analysis', Lancet, 379(9814), 413-431.

Niswonger, R.G., Panday, S. and Ibaraki, M., 2011. MODFLOW-NWT, a Newton formulation for MODFLOW-2005. US Geological Survey Techniques and Methods, 6(A37), p.44.

Oki, T. and Kanae, S. (2006) 'Global hydrological cycles and world water resources', Science, 313(5790), 1068-1072, available: http://dx.doi.org/10.1126/science.1128845.

Pearson, D.K., 2013. Geologic database of Texas: Project summary, Database contents, and user's guide: Document prepared by the US Geological Survey for the Texas Water Development Board, Austin, 22 p.

Perrin, J., Ferrant, S., Massuel, S., Dewandel, B., Marechal, J.C., Aulong, S. and Ahmed, S. (2012) 'Assessing water availability in a semi-arid watershed of southern India using a semi-distributed model', Journal of Hydrology, 460, 143-155, available: http://dx.doi.org/10.1016/j.jhydrol.2012.07.002.

Postel, S.L., Daily, G.C. and Ehrlich, P.R. (1996) 'Human appropriation of renewable fresh water', Science, 271(5250), 785-788, available: http://dx.doi.org/10.1126/science.271.5250.785.

Rodell, M., Chen, J.L., Kato, H., Famiglietti, J.S., Nigro, J. and Wilson, C.R. (2007) 'Estimating groundwater storage changes in the Mississippi River basin (USA) using GRACE', Hydrogeology Journal, 15(1), 159-166, available: http://dx.doi.org/10.1007/s10040-006-0103-7.

Schuol, J., Abbaspour, K.C., Srinivasan, R. and Yang, H. (2008) 'Estimation of freshwater availability in the West African sub-continent using the SWAT hydrologic model', Journal of Hydrology, 352(1-2), 30-49, available: http://dx.doi.org/10.1016/j.jhydrol.2007.12.025.

Scibek, J. and Allen, D.M. (2006) 'Modeled impacts of predicted climate change on recharge and groundwater levels', Water Resources Research, 42(11), available: http://dx.doi.org/10.1029/2005wr004742.

Scibek, J., Allen, D.M., Cannon, A.J. and Whitfield, P.H. (2007) 'Groundwater-surface water interaction under scenarios of climate change using a high-resolution transient groundwater model', Journal of Hydrology, 333(2-4), 165-181, available: http://dx.doi.org/10.1016/j.jhydrol.2006.08.005.

Tian, Y., Zheng, Y., Wu, B., Wu, X., Liu, J. and Zheng, C. (2015) 'Modeling surface water-groundwater interaction in arid and semi-arid regions with intensive agriculture', Environmental Modelling & Software, 63, 170-184, available: http://dx.doi.org/10.1016/j.envsoft.2014.10.011.

Tweed, S., Leblanc, M. and Cartwright, I. (2009) 'Groundwater-surface water interaction and the impact of a multi-year drought on lakes conditions in South-East Australia', Journal of Hydrology, 379(1-2), 41-53, available: http://dx.doi.org/10.1016/j.jhydrol.2009.09.043.

Vaghefi, S.A., Mousavi, S.J., Abbaspour, K.C., Srinivasan, R. and Arnold, J.R. (2015) 'Integration of hydrologic and water allocation models in basin-scale water resources management considering crop pattern and climate change: Karkheh River Basin in Iran', Regional Environmental Change, 15(3), 475-484, available: http://dx.doi.org/10.1007/s10113-013-0573-9.

van Griensven, A., Meixner, T., Grunwald, S., Bishop, T., Diluzio, A. and Srinivasan, R. (2006) 'A global sensitivity analysis tool for the parameters of multi-variable catchment models', Journal of Hydrology, 324(1-4), 10-23, available: http://dx.doi.org/10.1016/j.jhydrol.2005.09.008.

Vieira, S.R., Hatfield, J.L., Nielsen, D.R. and Biggar, J.W. (1983) 'GEOSTATISTICAL THEORY AND APPLICATION TO VARIABILITY OF SOME AGRONOMICAL PROPERTIES', Hilgardia, 51(3), 1-75.

VIEIRA, S.R., MILLETE, J., Topp, G.C. and Reynolds, W.D., 2002. Handbook for geostatistical analysis of variability in soil and climate data. Tópicos em ciência do solo, 2, pp.1-citation_lastpage.

Vorosmarty, C.J., Green, P., Salisbury, J. and Lammers, R.B. (2000) 'Global water resources: Vulnerability from climate change and population growth', Science, 289(5477), 284-288, available: http://dx.doi.org/10.1126/science.289.5477.284.

Voss, K.A., Famiglietti, J.S., Lo, M.H., de Linage, C., Rodell, M. and Swenson, S.C. (2013) 'Groundwater depletion in the Middle East from GRACE with implications for transboundary

water management in the Tigris-Euphrates-Western Iran region', Water Resources Research, 49(2), 904-914, available: http://dx.doi.org/10.1002/wrcr.20078.

Wada, Y., van Beek, L.P.H., van Kempen, C.M., Reckman, J., Vasak, S. and Bierkens, M.F.P. (2010) 'Global depletion of groundwater resources', Geophysical Research Letters, 37, available: http://dx.doi.org/10.1029/2010gl044571.

Wilson, D.J., Western, A.W., Grayson, R.B., Berg, A.A., Lear, M.S., Rodell, M., Famiglietti, J.S., Woods, R.A. and McMahon, T.A. (2003) 'Spatial distribution of soil moisture over 6 and 30 cm depth, Mahurangi river catchment, New Zealand', Journal of Hydrology, 276(1-4), 254-274, available: http://dx.doi.org/10.1016/s0022-1694(03)00060-x.

Winston, R.B., 2009. ModelMuse: a graphical user interface for MODFLOW-2005 and PHAST (p. 52). Reston, VA: US Geological Survey.

Woldeamlak, S.T., Batelaan, O. and De Smedt, F. (2007) 'Effects of climate change on the groundwater system in the Grote-Nete catchment, Belgium', Hydrogeology Journal, 15(5), 891-901, available: http://dx.doi.org/10.1007/s10040-006-0145-x.

CHAPTER 4

A FRAMEWORK FOR QUANTIFYING UNCERTAINTY, SENSITIVITY, AND ESTIMATING PARAMETERS FOR INTEGRATED SURFACE WATER - GROUNDWATER MODELS

Highlights

Hydrologic models often are used as aids in the water resources and environment planning and management in watersheds and river basins. These models, however, are fraught with uncertainty due to inaccurate model structures, indefinite magnitude of system stresses, and uncertain values of system parameters. This study proposed a general framework for performing sensitivity analysis, parameter estimation, and uncertainty analysis for integrated surface water-groundwater models, using the SWAT-MODFLOW modelling code as an example. The PEST software tool is used to jointly estimate the values and sensitivity of both land surface (SWAT) and subsurface (MODFLOW) parameters in a single automated calibration method. The monthly NSE values of streamflow discharge for calibration and validation were calculated to be 0.45 and 0.66, respectively, and for whole simulation was 0.55, which are considered acceptable for monthly stream discharge (≥ 0.5). Sensitivity analysis shows that land surface parameters have a strong control on streamflow and groundwater levels, followed by hydraulic conductivity and specific yield of the near-surface geologic units. Predictive uncertainty is demonstrated via an aquifer-storage-recovery groundwater development scenario, with water for injection diverted from the Middle Bosque River. Results are provided with uncertainty bands, and show that injecting water results in larger changes in water table level (increase of 2.1 m) than extracting

water (decrease of 1.2 m) from the aquifer, suggesting that response time, scales and durations are influenced by pre-conditions (i.e. soil moisture, water table). Effect of the scenario on streamflow was negligible. The proposed modelling work-flow can assist in implementing and applying integrated surface water-groundwater models for estimating watershed water resource and analysing the effect of changes in land use, population, and climate. This framework, particularly if used with SWAT-MODFLOW, can facilitate the use of integrated models worldwide to assist with finding technical solutions to water issues.

4.1. Introduction

Distributed hydrological models have been used extensively over the past three decades (Beven, 2010) to aid in decision making for water resources planning and management and environmental management within watershed systems (Mulet and Nicklow, 2005; Gallagher and Doherty, 2007; Cloke and Pappenberger, 2009; Park et al., 2013; Abbaspour et al., 2015), often through evaluating alternative watershed management strategies. In addition, as population growth, land use change, and climate change intensify current and future stresses on freshwater (Postel et al., 1996; Cosgrove and Rijsberman, 2000; Vorosmarty et al., 2000; Doll et al., 2003; Oki and Kanae, 2006; Murray et al, 2012), combined use of surface water and groundwater resources often becomes essential in many river basins to provide reliable water supply (Wrachien and Fasso, 2002; Cosgrove and Johnson, 2005; Liu et al., 2013; Singh et al., 2015).

Hydrologic models, however, include substantial uncertainties with respect to input data, forcing data, initial and boundary conditions, model structure, and parameter non-uniqueness due to a lack of data and poor knowledge of hydrological response mechanisms (Ye et al., 2008; Doherty and Welter, 2010; Shi and Zhou, 2010; Zhang et al., 2011; Gupta et al., 2012; Foglia et

al., 2013). These uncertainties have negative effects on the model accuracy, thereby inducing uncertainties in the simulated results. Therefore, if hydrologic models are to be used to as decision-making aids, the uncertainty associated with model calibration and model predictions must be assessed (Gallagher and Doherty, 2007). The general modelling approach requires a sequence of methods, including preliminary sensitivity analysis (SA) ("screening") to determine which parameters govern hydrologic responses in a given watershed; parameter estimation, to identify values of specified parameters; uncertainty analysis (UA), to determine the uncertainty in the model outputs that result from uncertainty in the model inputs/parameters; and final SA to evaluate how much each input/parameter contributes to the output uncertainty (Jakeman et al., 2006; Razavi et al., 2012; Wu and Liu, 2012; Nan et al., 2011; Song et al., 2011; Loosvelt et al., 2013). Ideally, SA and UA should be performed in tandem as both are essential parts of model development and quality assurance. UA can be applied to model results during the model calibration and testing phases, and also to the application of models for scenario analysis ("predictive uncertainty"), e.g. when investigating the effect of future management strategies, climate change, etc. on hydrologic responses and water resources of a watershed.

Conducting comprehensive SA and UA methods for watershed-scale hydrologic models often is performed using lumped, semi-distributed models such as the Soil and Water Assessment Tool (SWAT) (Arnold et al., 1998) or the Hydrological Simulation Program – FORTRAN (HSPF) (Bicknell et al., 2001). SWAT applications include Muleta and Nicklow (2005) to the Big Creek watershed, Illinois (133 km^2); Yang et al. (2007) to the Thur River basin, Switzerland; Li et al. (2010) to the Yingluoxia watershed in China (10,000 km^2); Shen et al. (2012) to the Daning River watershed in China (4,426 km^2); Wu and Liu (2012) to the Cedar River Basin in Iowa; and Abbaspour et al. (2015) to the European continent, with the latter

model providing information support to the European Water Framework Directive. HSPF applications include Gallagher and Doherty (2007) to the Contentnea Creek Basin, North Carolina (2,600 km^2) and Jia and Culver (2008) to a small watershed (90 km^2) in Virginia. These studies applied a variety of SA and UA methods, including the Generalized Likelihood Uncertainty Estimation (GLUE) (Beven and Binley, 1992) and Markov Chain Monte Carlo (MCMC). The majority of these studies applied UA only to parameter uncertainty during the model calibration and testing periods, and not to any predictive scenario analysis. For the model SWAT, these have been incorporated into the software tool SWAT-CUP (SWAT Calibration Uncertainty Procedures) (Abbaspour, 2011), which includes GLUE, Parameter Solution (ParaSol) (van Griensven and Meixner, 2006), and Sequential Uncertainty FItting (SUFI-2) (Abbaspour, et al., 2007).

There are, however, two principal drawbacks with the SA/UA studies using the SWAT and HSPF models, and any other lumped, moderately-distributed hydrologic model. First, applications of these models focus solely on stream discharge as the system response of concern. This is in part due to 1) a focus on surface water to satisfy river basin water needs, but also on 2) the simplistic treatment of groundwater flow and groundwater-surface water (GW-SW) interactions in the model structure. Second, due to simplistic treatment of groundwater flow and GW-SW, the models do not include all watershed variables that could affect the main hydrologic responses (surface runoff, infiltration, lateral flow, groundwater recharge, GW-SW, and streamflow), with governing watershed variables being input data, weather data, soil properties, and aquifer properties. The exclusion of physically-based, distributed groundwater flow modelling and GW-SW from hydrologic model applications likely simplifies the watershed

system beyond what is appropriate in many river basins, and thereby neglects the uncertainty associated with a combination of land surface and subsurface hydrologic parameters.

Several recent studies (Surfleet and Tullos, 2013; Wu et al., 2014) have attempted to include SA/UA methods for integrated surface water-groundwater models. Both used the GSFLOW model (Markstrom et al., 2008), which includes both land surface and subsurface hydrological processes a coupled PRMS (Leavesley et al., 1983) and MODFLOW (Harbaugh, 2005) approach. The study of Surfleet and Tullos (2013) applied GSFLOW to a 4,700 km^2 river basin in Oregon, assessing uncertainty associated with climate change predictions. Wu et al. (2014) provided a framework for applying UA to the 9,097 km^2 Zhangye Basin, China using GSFLOW, investigating the response of ET, soil moisture, infiltration, recharge, surface leakage, GW-SW exchange, groundwater level, and streamflow. Their methodology, however, uses manual calibration rather than automatic calibration, due to the computational burden, and also does not use the full GSFLOW model in UA, rather using a simplified, surrogate model (Wu et al., 2014). They state that "automatic calibration for such complex models is extremely challenging and deserves a separate study".

Overall, no systematic approach of model construction and use has been provided for the coupled surface-subsurface flow models, limiting their wide application. There is a need for a generalized approach to perform UA, quantify the influence of the vast array of model parameters and factors on watershed response (e.g. stream discharge, groundwater head) through SA, develop a systematic approach to parameter estimation for both land surface and hydrogeological parameters, thereby providing modelling results that assess both groundwater and surface water resources accurately in a watershed setting while relaying the degree of uncertainty to decision makers.

In this study, we present a framework to quantify sensitivity analysis, uncertainty analysis, and parameter estimation for coupled groundwater/surface water models, using the newly developed SWAT-MODFLOW code (Bailey et al., 2016) as an example modeling code. Thus, this paper serves as a guideline for applying integrated surface water-groundwater models generally, and for applying SWAT-MODFLOW models specifically, with several components of the framework requiring details specific to SWAT and MODFLOW. Application of the framework is demonstrated for a watershed in central Texas. Parameter estimation and uncertainty analysis is performed using PEST (Parameter ESTimation tool) (Doherty, 2006), with new pre-processing and post-processing algorithms developed to modify and assess jointly land surface hydrologic parameters (SWAT model) and hydrogeological parameters (MODFLOW). Sensitivity analysis is performed to determine controlling factors on hydrological responses. To demonstrate the implementation of uncertainty in scenario analysis, we include a groundwater development scenario (aquifer storage and recovery using river water and a set of pumping wells) that uses an ensemble of plausible model parameter sets. Uncertainty in both streamflow and groundwater levels are assessed.

4.2. Methodology

The general framework for quantifying uncertainty, sensitivity, and estimating parameters for the coupled surface water-groundwater model will be presented, with each phase of the process illustrated by application to a SWAT-MODFLOW model constructed for the Middle Bosque River Watershed in central Texas.

4.2.1. General Framework for Integrated SW-GW Models

The general framework for constructing, calibrating, and applying integrated surface water-groundwater models within a watershed system is shown by the flow chart in Figure 4.1. The

framework includes phases for quantifying uncertainty, sensitivity, and estimating parameters for the integrated models. The framework is divided into a) "Model construction" and b) "Framework for sensitivity, uncertainty analysis, parameter estimation". Whereas the details of a) are specific to SWAT-MODFLOW applications, b) is general to all integrated surface water-groundwater models. Details for each sub-section of a) and b) are provided in the remaining sub-sections of Section 2. Only a brief outline is presented here.

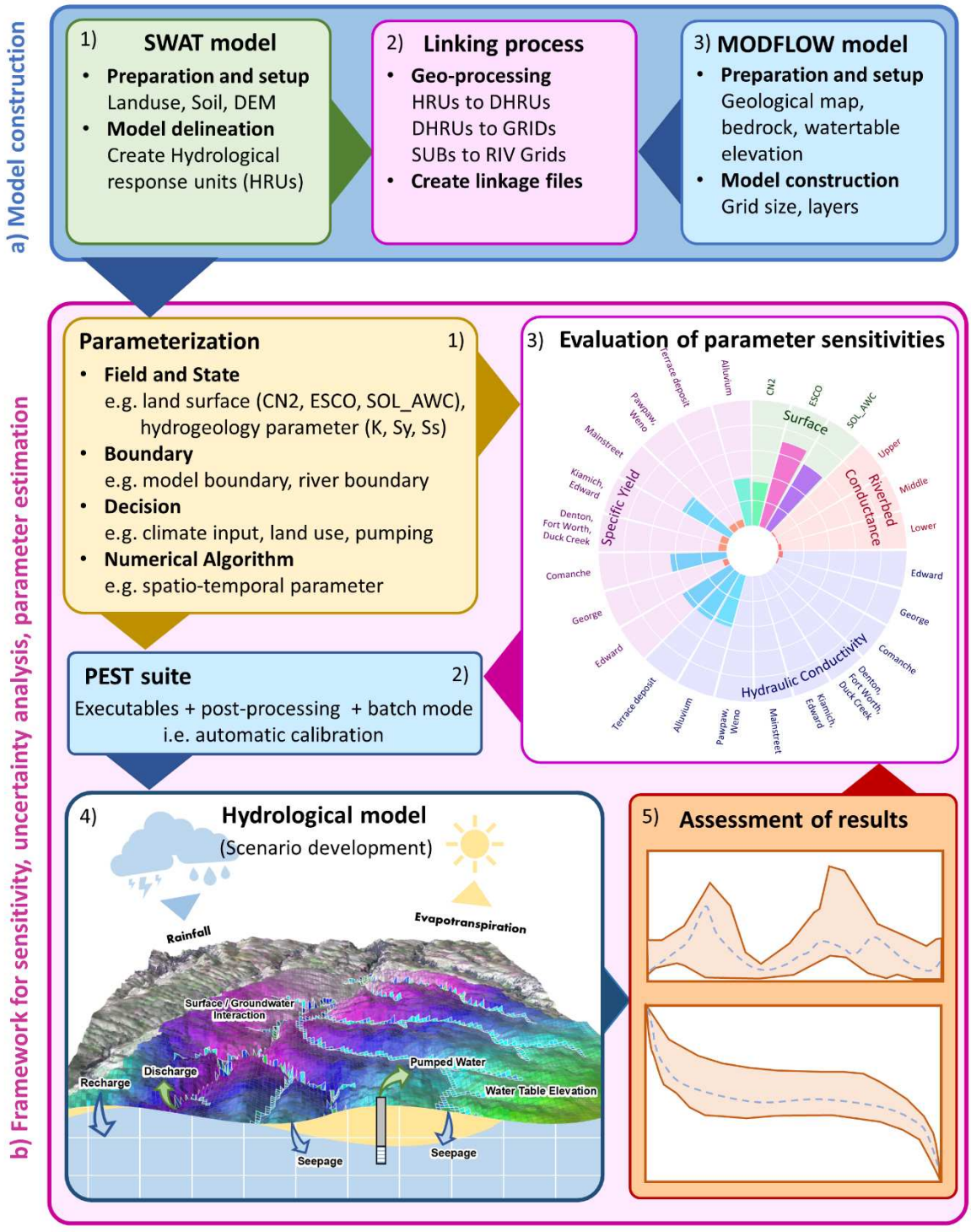

Figure 4.1. Framework for constructing, calibrating, and applying integrated surface water-groundwater models within a watershed system

For a), a SWAT model and MODFLOW model are constructed to utilize the SWAT-MODFLOW modelling code of Bailey et al. (2016). Details regarding these two models are

provided in Section 4.2.2 SWAT requires land use, soil, and digital elevation model (DEM) layers to delineate the watershed and create the set of hydrologic response units (HRUs), whereas MODFLOW requires aquifer unit layering, aquifer properties, aquifer stresses, and a finite difference grid. The two models are linked via geo-processing routines to create linkage files as inputs for the SWAT-MODFLOW model.

The b) segment consists of 1) model parameterization, 2) PEST, and 3) evaluation of parameter sensitivities, using 4) the Hydrological model and 5) assessment of model output. PEST is used since it is a model-independent program, capable of working with any hydrologic model executable. Using the interaction between PEST and the Hydrological model, both traditional parameter estimation, based on the use of only a few parameters, and highly-parameterized regularized inversion based on the use of hundreds of parameters, can be performed. PEST also has options for parallelizing simulation runs across multiple processors on the same machine, across machines, and across networks. The impacts of model inputs and parameters on hydrological responses (streamflow, groundwater levels, groundwater-surface water exchange rates) can be assessed with 3) sensitivity analysis, and the model can be used to assess future development scenarios as a part of a 5) predictive uncertainty analysis.

4.2.2. Model Construction and Setup

A SWAT-MODFLOW model is constructed for the Middle Bosque River Watershed (MBRW) (Figure 4.2) (471 km^2) in the Texas-Gulf region of central Texas. This watershed is selected due to the presence of both surface water and groundwater resources, with groundwater interacting strongly with stream water in the surficial geologic system. The model simulation time is 1980-2012. Complete details of the SWAT-MODFLOW model are provided in Park et al. (2018), with only major aspects described here.

The MBRW covers portions of McLennan, Bosque, and Coryell counties (Figure 4.2) with sedimentary rocks from the Washita and Fredericksburg Groups of early Cretaceous, and Comanchean age. The formation of the Washita Group is the Georgetown Limestone including Main Street, Pawpaw, Weno, Denton, Fort Worth, Duck Creek, and Kiamichi members (Cannata, 1988; Pearson, 2007). The two formations of the Fredericksburg Group, the Edwards Limestone and Comanche Peak Limestone, are used in the study area. The altitude of the study region varies from 367 m at the highest point on the north-western edge to 161 m on the eastern edge. The MBRW is predominantly comprised of pasture (65.4 % of area) and farms (20.3 % of area), with minor land covers of forests (8.5 % of area), and residential areas (3.2% of area) (USGS, 2007). The Middle Bosque River dissects the Edwards Limestone and has therefore produced major groundwater discharge and stream seepage areas (Cannata, 1988). The climate of the study area is characterized by semi-arid, with long hot summers and brief mild winters, ranging from an average of 36.5^{o}C in August to 2.8^{o}C in January (U.S. Depth. of Commerce, Weather Bureau, 1980 -2012). The annual precipitation ranges from about 602 to 1560 mm/year.

SWAT is a continuous, basin scale, distributed-parameter watershed model emphasizing land surface hydrologic processes, dividing the watershed into subbasins which are then further divided into multiple unique combinations (Hydrologic Response Units: HRUs) of land use, soil type and topographic slope for which detailed water mass balance calculations are performed. The SWAT model for MBRW has a total of 69 subbasins, delineated based on a Digital Elevation Model (DEM) of the region. No thresholds were set for the HRU definition, resulting in 1,693 HRUs. Seven different land covers (Agricultural Land-generic, Forest-deciduous, Forest-mixed, Pasture, Residential-Low Density, Water, and Wetlands-forested) were included.

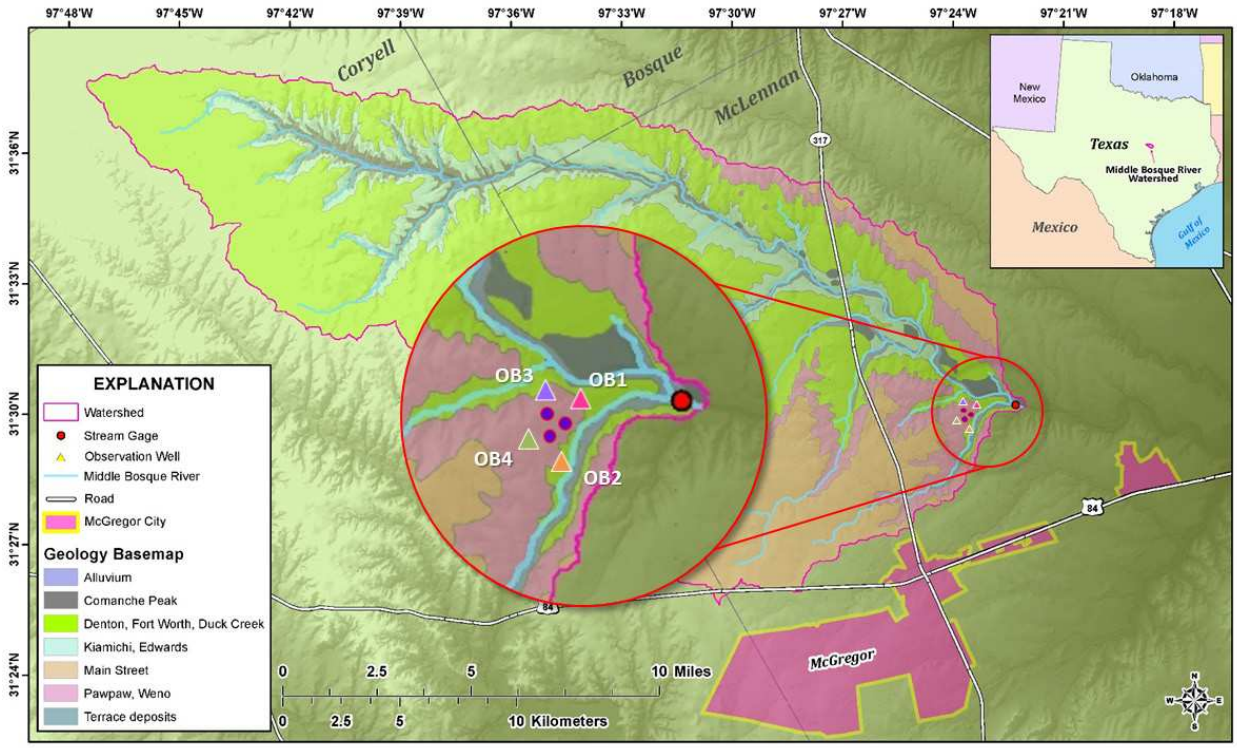

Figure 4.2. Location map showing the position of the study area within McLennan, Bosque, and Coryell Counties, Texas. Physiographic map showing the provinces composing and surrounding the study area. These include the Washita Prairie and Lampasas Cut Plain.

MODFLOW-NWT (Niswonger et al., 2011) is a three-dimensional, finite-difference, groundwater flow modelling program that is used to simulate groundwater head and groundwater-surface water interactions for the MBRW. The model grid has 268 columns and 154 rows of square cells; each cell measures 150 m by 150 m (22,500 m^2) with five layers including 10 different hydrogeologic zones (Park et al., 2018). The grid was generated in the USA Contiguous Albers equal area conic coordinate system (North American Datum of 1983, units: meter). Geologic layers represented as layers in the model are the Georgetown Limestone and the Edwards Limestone, with the Georgetown Limestone divided into the following units: Comanche Peak Denton; Fort Worth, and Duck Creek; Kiamichi, Edwards; Mainstreet; Pawpaw, Weno; Alluvium; and Terrace deposits (Cannata, 1988; Pearson, 2013). Initial hydraulic aquifer properties (hydraulic conductivity K, specific yield S_y, specific storage S_s) for the geologic layers

are based on published literature. Initial head for each grid cell is estimated using interpolated values from 28 observation wells in 1980.

SWAT-MODFLOW (Bailey et al., 2016) is a single FORTRAN code in which MODFLOW is called a subroutine by SWAT, with subroutines that pass data between the two modeling systems. For each day of the simulation period, the following process is performed:

1. SWAT performs land surface and soil water processes for each HRU;
2. SWAT maps HRU soil percolation MODFLOW's Recharge package and subbasin stream channel depths to MODFLOW's River package;
3. MODFLOW solves the groundwater flow equation for hydraulic head at each grid cell; secondary equations calculate volumetric exchange rates between groundwater and streams using the River package;
4. MODFLOW passes simulated hydraulic head to each HRU, and estimated SW-GW exchange rate to each subbasin stream;
5. SWAT routes all water yield (surface runoff, lateral flow, groundwater discharge) through the watershed stream network.

When MODFLOW is used, the original SWAT groundwater module is turned off. Linkage between SWAT HRUs and subbasins to the MODFLOW grid is performed using spatial pre-processing methods in a geographical information system (GIS) such as ArcMap or QGIS. Specific procedures include separating HRUs into geographically located disaggregated Hydrologic Response Units (DHRUs), intersecting DHRs and MODFLOW grid cells, and intersecting SWAT subbasins and MODFLOW River cells. Linkage data are summarized in four text files that are included with all SWAT and MODFLOW input files. Preparation of the linkage data can be performed using either a step-by-step tutorial or graphical user interface (GUI) tools.

For the latter, two tools have been created: SWATMOD-Prep (Bailey et al., 2017), a stand-alone python-based GUI that readers in SWAT GIS shape files and creates a single-layer MODFLOW model; or QSWATMOD (Park et al., 2018), a plugin for QGIS that can link SWAT with an existing MODFLOW model and display maps and simulations results in the QGIS canvas.

4.2.3. Estimation of SWAT and MODFLOW Parameters

PEST (Doherty, 2006) is used to perform automatic calibration for both land surface and hydrogeological parameters of the coupled SWAT-MODFLOW model. PEST was chosen for this framework due to its model-independent nature. PEST adjusts selected parameters in sequential simulation runs to minimize the objective function, which is the sum of the squared weighted residuals between the observed and simulated values:

$$\Phi = \sum_{i}^{n} w_i (o_i - s_i)^2 \quad (1)$$

where Φ is the objective function, n is the number of target variables, w_i is the weight assigned to the ith target variable, and o_i and s_i are the observed and simulated values of the ith target variable, respectively. The value of w_i for each target variable is calculated as the product of an uncertainty weight and a unit discrepancy weight. The uncertainty weight is calculated as the inverse of an estimated coefficient of variation (CV) reflective of the relative uncertainty in the observations of the target variable. The unit discrepancy weight is determined by unifying the sum of the square of each observed variable value.

PEST requires three types of input files. These are:

- Template files, one for each model input file in which parameters to be estimated are defined, containing placeholders for parameter values so that the PEST program can insert updated parameter values;

- Instruction files, one for each model output file on which model-generated observations exist; and
- Control file, supplying PEST with the names of all template and instruction files, the names of the corresponding model input and output files, the problem size, control variables, initial parameter values, measurement values and weights, etc.

The overall method of using PEST to estimate SWAT-MODFLOW land surface and hydrogeological parameters is summarized in Figure 4.3. The 4 main program executables used for the method are (1) *PEST.exe*; (2) *SWAT-MODFLOW.exe*; 3) *Swat_Edit.exe*; and 4) *exSimValue.py*. The programs are called sequentially in batch mode, according to the following steps:

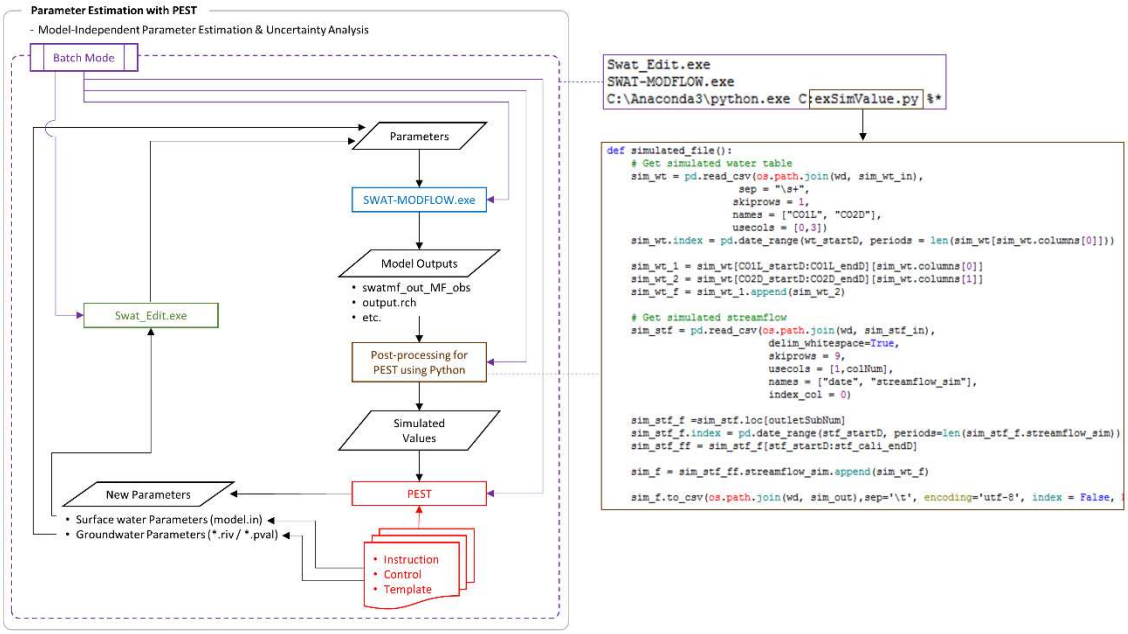

Figure 4.3. Schematic diagram for automatic calibration for both land surface and hydrogeological parameters

1. *SWAT-MODFLOW.exe* is called and runs to completion. For the MBRW model, it runs for 1980-2012, generating simulated streamflow, groundwater head, GW-SW exchange rates, and watershed water balance terms;

2. *exSimValue.py* is called: this Python script passes simulated values (streamflow, water table) from the SWAT-MODFLOW output files to PEST. Some of the code is shown in Figure 4.3. The script extracts all simulated outputs from the SWAT (output.rch for subbasin streamflow) and MODFLOW (swatmf_out_MF_obs for head at observation locations) output files and stores them in files that match the PEST instruction files. The "model.in" SWAT file and the parameter value file (PVAL) for MODFLOW are used for the template files to replace parameters defined in the files. If the PVAL package of MODFLOW is not used to list parameter values, other input files such as River (RIV), Upstream Weighting (UPW), and boundary condition packages in MODFLOW could be used for template files to designate parameters to be modified by PEST.
3. *PEST.exe* is called. It obtains simulated outputs and observation data from instruction files. Based on the objective function results of a simulation, PEST distributes new parameter values to the MODFLOW files which have companion template files.
4. *Swat_Edit.exe* is called. SWAT requires a set of files, containing information on soil properties, land management, surface water routing, nutrient ratios and concentrations, etc. for each subbasin and each HRU. Thus, changing a parameter for SWAT requires the editing of thousands of input files. *SWAT_Edit.exe*, part of the SWAT Editor program (Abbaspour et al., 2007), automates the editing of SWAT input files. When new parameter values are provided by PEST, *SWAT_Edit.exe* replaces parameters in the SWAT input files based on a setting in the "model.in" file.

In batch mode, PEST first calls the "*SWAT_Edit.exe*" program, replacing parameters in the SWAT input files by reading the "model.in" file, then runs SWAT-MODFLOW to start the iterative parameter estimation process. The simulation loop continues until a better fit between

model outcomes and corresponding observed data is not achieved or the number of iterations reaches a maximum number defined by the user.

For the MBRW study, we included the following land surface parameters from SWAT: available water capacity of the soil layer (SOL_AWC), runoff curve number (CN2), and soil evaporation compensation factor (ESCO) in the "model.in" file; and the following hydrogeological parameters from MODFLOW: hydraulic conductivity K and specific yield S_y in the "*.pval" file. We also included the River Package (RIV) as a template file to parameterize river bed conductance. Nine zones were used for K and S_y, and three values were used for river bed conductance, resulting in a total of 24 parameters. The objective function was composed of observed streamflow from 1993-2012 at the outlet of the MBRW and groundwater levels from two observation wells during 1985-1986. To evaluate the model, comparison statistics such as the Nash-Sutcliffe model efficiency factor (NSE), R^2, and PBIAS are used. Parameter estimation was performed for the data through 2005, with 2005-2012 used for model testing.

4.2.4. Sensitivity Analysis

The main purpose of model sensitivity analysis (SA) is to identify key parameters that affect modeled variables most (Saltelli et al., 2004; Schurz et al., 2018), supporting model parameterization, calibration, optimization, and uncertainty quantification (Xiomeng et al., 2015). To provide a more efficient SA approach for hydrological modeling, various SA methods have been introduced in recent years. For instance, global sensitivity analysis (GSA) assesses the sensitivity of a model output for the entire feasible range of model inputs (Gupta and Razavi, 2017; Pianosi et al., 2016). Due to its high computational cost, a substantial part of recent GSA literature focuses on the computational efficiency and robustness of GSA methods (e.g. Rakovec et al., 2014; Cuntz et al., 2015; Pianosi and Wagener, 2015; Razavi and Gupta, 2016a; Sarrazin

et al., 2016), but also on increasing the insight into modeled systems from certain number of model computations (e.g. Borgonovo et al., 2017; Dai et al., 2017; Guse et al., 2016a; Massmann et al., 2014; Razavi and Gupta, 2016a). Compared to GSA, the complexity and computational demand of a local sensitivity analysis (LSA) are low.

PEST provides a companion program called SENSAN, which adopts LSA that employs a one-at-a-time (OAT) approach. The OAT approach evaluates the impact of changing values of each parameter on modeled variables one at a time (Saltelli and Annoni, 2010; Baroni and Tarantola, 2014), i.e. model output responses are calculated through sequentially varying each of the model parameters and by fixing all other parameters to their nominal values, often taken from literatures. The combination of nominal values for all the model parameters under inspection can be called the "control" scenario (Saltelli et al., 2008). Sensitivity for a particular model output can be calculated as the difference between that model output and the pertinent model output "nominal" value, divided by the difference between the current parameter set and the parameter nominal values. If only a single parameter P differs from the nominal set, the sensitivity for a particular model output Φ is defined as:

$$\frac{\Phi - \Phi_0}{P - P_0} \tag{2}$$

where Φ_0 and P_0 are model output and parameter nominal values and Φ and P is the model output and parameter values pertaining to a particular model run. The normalized sensitivity coefficient (or sensitivity index) is calculated by:

$$NSC = \frac{|\Phi - \Phi_0|}{|P - P_0|} \times \frac{|P_0|}{|\Phi_0|} \tag{3}$$

where the NSC is a dimensionless positive number, whose value indicates the relative importance of parameter *P* on the model output Φ, i.e. the relative sensitivity of the particular model output Φ with respect to the changing of the particular model parameter *P*.

As a by-product of the results from the parameter estimation process by PEST, the "composite parameter sensitivity" can be provided (Tang et al., 2007; Doherty 2015). Based on the contents of the Jacobian matrix, PEST calculates a figure related to the sensitivity with respect to each parameter of all observations (with the latter weighted as per user-assigned weights). Thus, the "composite sensitivity" of parameter *i* is defined as:

$$csp_i = \frac{\left[J^t Q J\right]_{ii}^{1/2}}{n} \tag{4}$$

where *J* is the Jacobian matrix and *Q* is the cofactor matrix which in most cases is a diagonal matrix whose elements are composed of squared weights for model outputs. The number of outputs, *n*, is the number of data records, which in the application to the MBRW are the data points from the time series of streamflow and water table elevation. Thus, csp_i is the normalized magnitude of the Jacobian matrix column with respect to parameter *i*.

Although LSA and composite parameter sensitivity are limited to a univariate analysis of parameter impacts on model outputs resulting in non-correlated input parameters, which is often not the case for hydrological models (Rosolem et al., 2012; Baroni and Tarantola, 2014; Schurz et al., 2018) due to their low computational demands and their easy accesses to the evaluation of individual parameter sensitivities on individual hydrological responses (water table, streamflow, surface-subsurface interaction, global water balance, etc.), LSA and composite parameter sensitivity are used in this study to investigate how land surface hydrologic parameters (SWAT model) and hydrogeological parameters (MODFLOW) affect hydrological responses. 10% relative change in each parameter was used for the OAT analysis with the nominal value. These

simulations are also used to provide an indication of uncertainty of model results during the simulation periods.

4.2.5. Uncertainty Analysis for Model Scenarios

Due to the fact that many sets of model parameters can represent watershed behavior reasonably well (the "Equifinality problem", Beven, 2006), parameter sets that provide acceptable model calibration should be considered when using the model in scenario analysis, i.e. investigate system response to changes in land use, climate, stresses, etc. For this study, one example is provided to demonstrate the procedure in the overall SA/UA modeling framework. Parameter sets from the OAT sensitivity analysis phase are used to run an ensemble of simulations to investigate the response of the MBRW system to an aquifer story and recovery (ASR) scenario for water supply using the SWAT-MODFLOW model. The ASR method injects river water into the aquifer during a high-rainfall year, and extracts (recovers) the groundwater from the aquifer during a drought year.

The town of McGregor, located just to the south of the MBRW, was selected as the user of the water. McGregor has approximately 5,000 residents, and assuming a per capita water use of 100 gal/day, injection rates of 1,000 gal/min for three wells were applied during the wet year of 2004 to provide storage of double the annual required water supply for the town. Injected water is assumed to be removed from the lower reaches of the Middle Bosque River, simulated by removing the corresponding daily water volume from a SWAT subbasin stream. This was performed through a minor change to the SWAT-MODFLOW executable. The groundwater is then pumped from the three wells during the following drought year of 2005. The same volume injected during 2004 is removed during 2005.

Simulated streamflow, groundwater level, and SW-GW exchange rates are analyzed to determine the short-term and long-term effects of the ASR scenario on watershed response. Using the ensemble of parameter sets, the corresponding ensemble of hydrologic responses incorporates uncertainty in model parameters and yields a band of results that can assist in water management decisions.

4.3. Results and Discussion

4.3.1. Parameter Estimation

PEST stopped after 288 simulations through 7 iterations. The highest hydraulic conductivity value is estimated to be 990 m/day, within the alluvium zone in the first layer, and the lowest hydraulic conductivity value is 0.10 m/day, at exposed-Comanche Peak Limestone in the first layer. The range of specific yield values varies from 0.05 to 0.35.

Observed streamflow (m^3/s) and simulated streamflow at the MBRW outlet is shown in Figure 4.4, with the simulated results provided by the ensemble of parameter sets used in the 24 OAT simulations. ensemble of parameter sets. The best simulated parameter set shows good similarity between the SWAT-MODFLOW simulation and the observed data: the monthly NSE values of streamflow discharge for the calibration and testing periods were calculated to be 0.45 and 0.66, respectively, 0.55 for the entire simulation, considered to be "acceptable" (≥ 0.5) for monthly stream discharge (Moriasi et al., 2007). The monthly R^2 for the testing period also shows a better result than for the calibration period. The PBIAS value for the calibration period reveals a small percent under-prediction (2.62), but a large percent over-prediction (-16.79) for the testing period, probably due to the slightly different behavior in the periods of low stream flow between the two period.

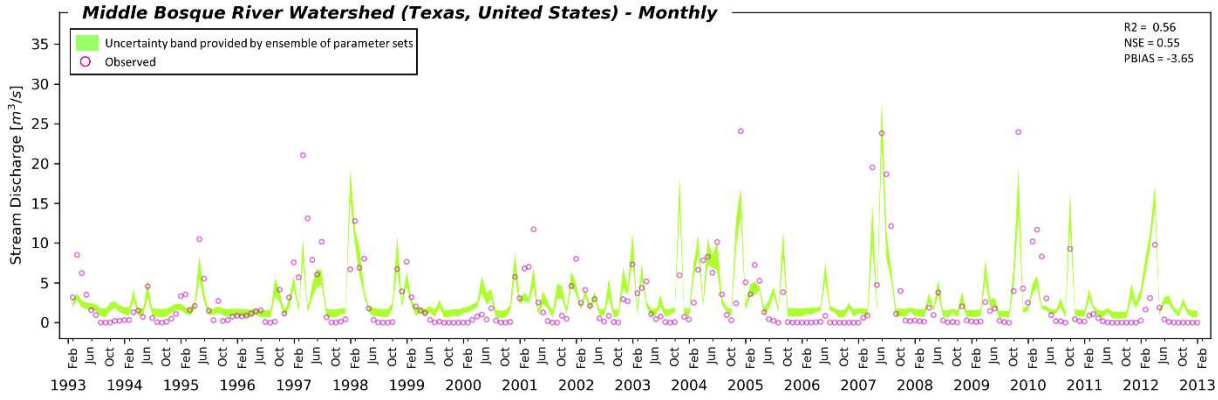

Figure 4.4. Observed and simulated results provided by the ensemble of parameter sets time series of stream discharge (m^3/s), and the statistics (R^2, NSE, PBIAS) for calibration period (1993 – 2012) for the outlet of the Middle Bosque River watershed

Figure 4.5 shows the hydrographs of measured and simulated hydraulic head for the observation wells (CO1L from 10/21/1985 – 3/7/1986 and CO2D from 11/30/1985 – 2/1/1986) (see Figure 4.2 for location), with simulated results provided by the ensemble of parameter sets of the 24 OAT simulations. Although the patterns of the hydrographs of simulated hydraulic heads for both locations are similar to the observed data, the daily R^2 values for two observation wells are considered low because the simulated hydraulic head from CO1L shows less fluctuation compared to its observed value and the simulated head from CO2D is about 1 meter lower than the observed value. Although there are limited transient groundwater level data, field work in the watershed indicates an extremely shallow water table (< 6 m), particularly in low areas along drainage tributaries, such as for CO1L and CO2D (see Figure 4.2), and that historically most groundwater rises dramatically after rainfall events (Easterling et al., 2001).

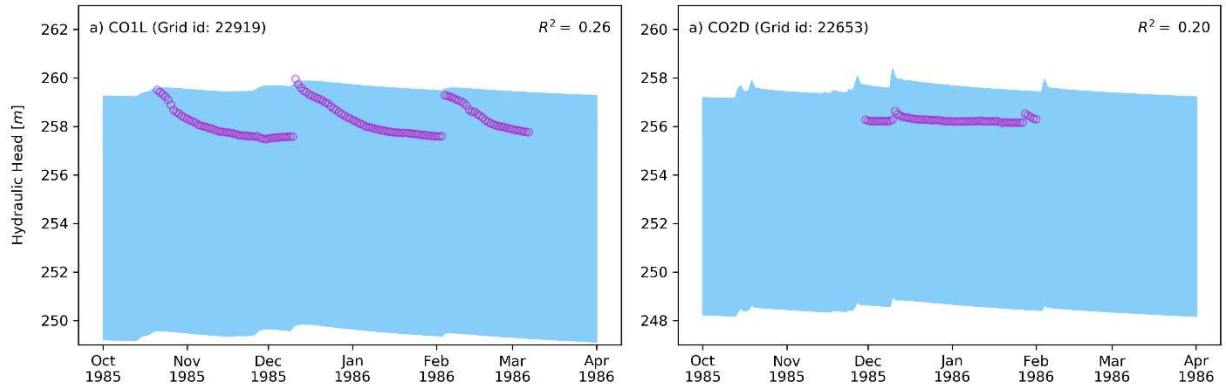

Figure 4.5. the hydrographs of measured and simulated hydraulic head for the observation wells (CO1L from 10/21/1985 – 3/7/1986 and CO2D from 11/30/1985 – 2/1/1986)

4.3.2. Sensitivity Analysis

The composite sensitivities (CSP) were calculated by PEST for the three land surface parameters, three river bed conductance values, 9 hydraulic conductivity zones, and 9 specific yield zones on simulated model results (streamflow at the MBRW outlet, groundwater levels at the two observation wells), and shown in Figure 4.2. The CSP values show in general the significance of the land surfaces parameters (CN2, ESCO, SOL_AWC) for the simulation of streamflow and groundwater level. The CSP values range from 0.24 to 0.38 for the land surface parameters. The CSP of CN2 was the highest, whereas the CSP of the river bed conductance were negligible (Figure 4.6). The CSP for the K and S_y zones are also low. This likely is due to the high weight attributed to streamflow, with the land surface parameters governing streamflow more than hydrogeological parameters. Also, the locations of the two groundwater observation points are close to one of the tributaries of the Middle Bosque River, so that the water table is continuously high in the shallow subsurface.

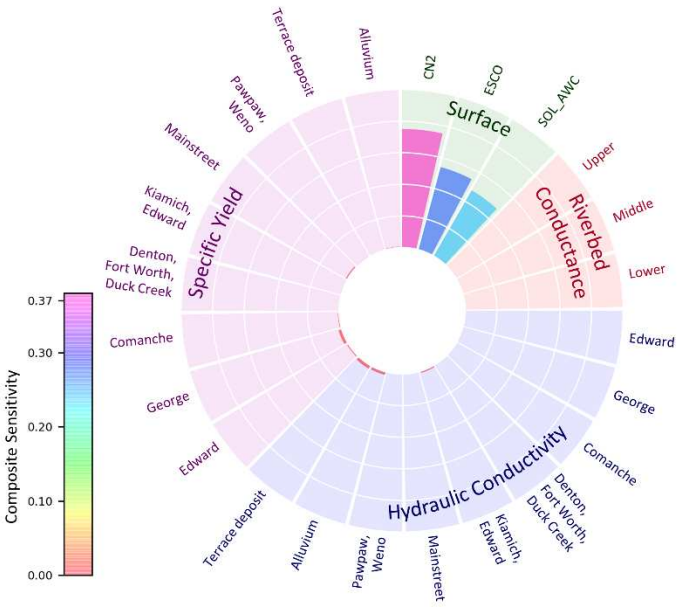

Figure 4.6. Model input composite sensitivities (CSP) for signature measures of streamflow discharge and two water table elevations in the Middle Bosque watershed. Circle plot shows the set of CSP calculated for model inputs. The CSP indices are illustrated in coloured groups showing in clockwise order the sensitivities of selected land surface parameters in green, of river bed conductance in red, of 9 hydraulic conductivity zones, and of 9 specific yield zones.

For the model used in this study, the LSA (OAT) approach is better suited for investigating the control of each parameter on streamflow and groundwater hydraulic head. Figure 4.7 shows results of the OAT approach, with Figure 4.7a showing the Normalized Sensitivity Coefficient (NSC) for streamflow and groundwater head, and Figure 4.7b showing the NSC for streamflow only. Similar to the CSP, the NSC of the land surface parameters is higher than for the hydrogeological properties; however, the aquifer properties (K, S_y) do exhibit a moderate influence particularly for alluvium and terrace deposits, which are near-surface geologic units and thus have a control and land surface processes and associated surface runoff and streamflow in the MBRW watershed system. When analyzing influence solely on streamflow (Figure 4.7b), the relative effect of the parameters is the same as when analyzing jointly streamflow and groundwater head. Riverbed conductance does not show a strong control in either analysis

(results shown in Figure 4.7a or 4.7b), likely because exchange rates between surface water and groundwater are not of sufficient magnitude to change streamflow significantly.

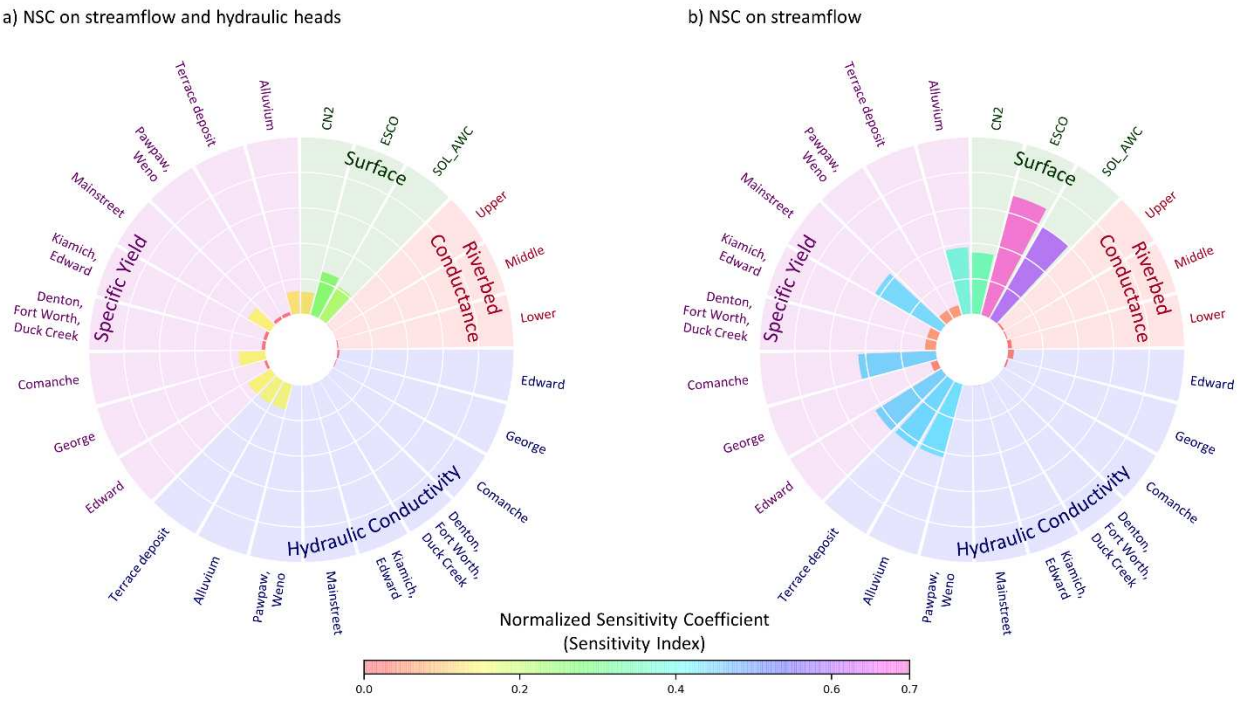

Figure 4.7. Model input Normalized Sensitivity Coefficient (NSC) for signature measures of a) streamflow discharge and two water table elevations and b) streamflow discharge only. Circle plot shows the set of NSC calculated for model inputs. The NSC indices are illustrated in coloured groups showing in clockwise order the sensitivities of selected land surface parameters in green, of river bed conductance in red, of 9 hydraulic conductivity zones, and of 9 specific yield zones.

4.3.3. Simulation Uncertainties for Groundwater Development Scenario

The effect of the aquifer storage and recovery scenarios on groundwater levels is shown in Figure 4.8. The results from OB1 shows the maximum increase in water table is 2.1 meters in Dec. For OB2 the maximum increase is 2.1 meters in Jul. 2004 and decrease is 1.2 m in Dec. 2005. OB3 shows that the maximum increase is 2.4 meters in Nov. 2004 and decrease is 1.4 m in Dec. 2005.OB5 results in the highest water table increase (5.3m) in Dec. 2004 and smallest (1.1m) in Dec. 2005. In general, injecting water results in higher changes in water table than extracting water from the aquifer (similar to scale change of hydrological responses and water balance). The results show that their response time, scales and durations not only vary but also

are influenced by pre-conditions (i.e. soil moisture, water table), their distances to pumping wells.

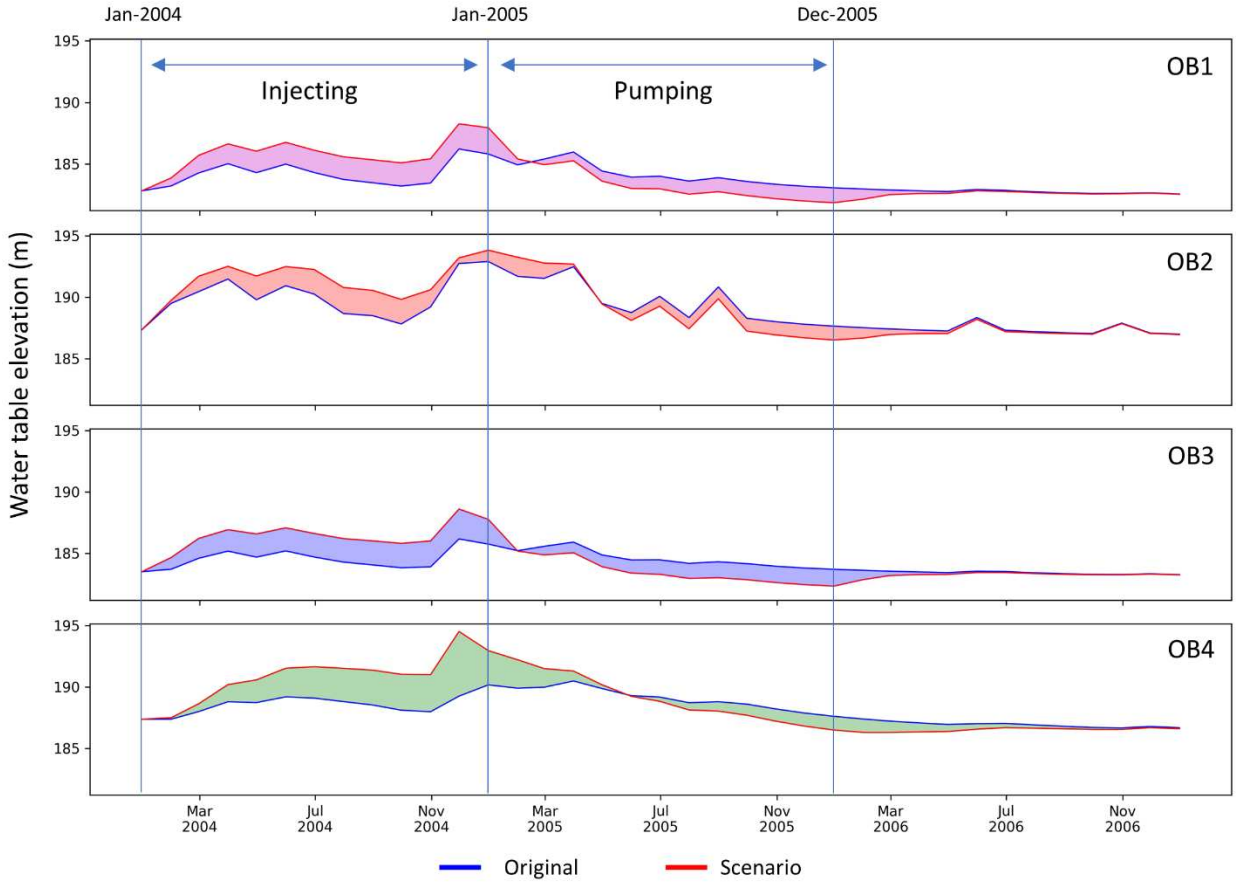

Figure 4.8. Effect of the aquifer storage and recovery scenarios on groundwater levels

These results can be used by regional water managers and planners to determine long-term effects of aquifer storage and recovery on the stream system and the aquifer system.

The Normalized Sensitivity Coefficient (NSC) on water balance from the calibrated model and with groundwater development scenario is shown in Figure 4.9. For the calibrated model, NSC on water balance ranges from 0 to 10.3 (PERCO). The aquifer properties (K, S_y) exhibit a moderate influence particularly for alluvium and terrace deposits, which are near-surface geologic units and thus have a control and land surface processes and associated surface runoff and streamflow in the MBRW watershed system. The lateral flow (LATQ) and groundwater deep percolation (PERCO) components of the water balance show moderate influences by all 9

hydrogeologic zones with respect to their specific yields suggesting parameters related to porosities resulting in higher sensitivities. The results from NSC in groundwater development scenario show decreases in 9 S_y sensitivities on hydrologic responses (water components) suggesting the addition of a decision parameter (pumping or injecting) can reduce the sensitivities of the hydrogeologic parameters.

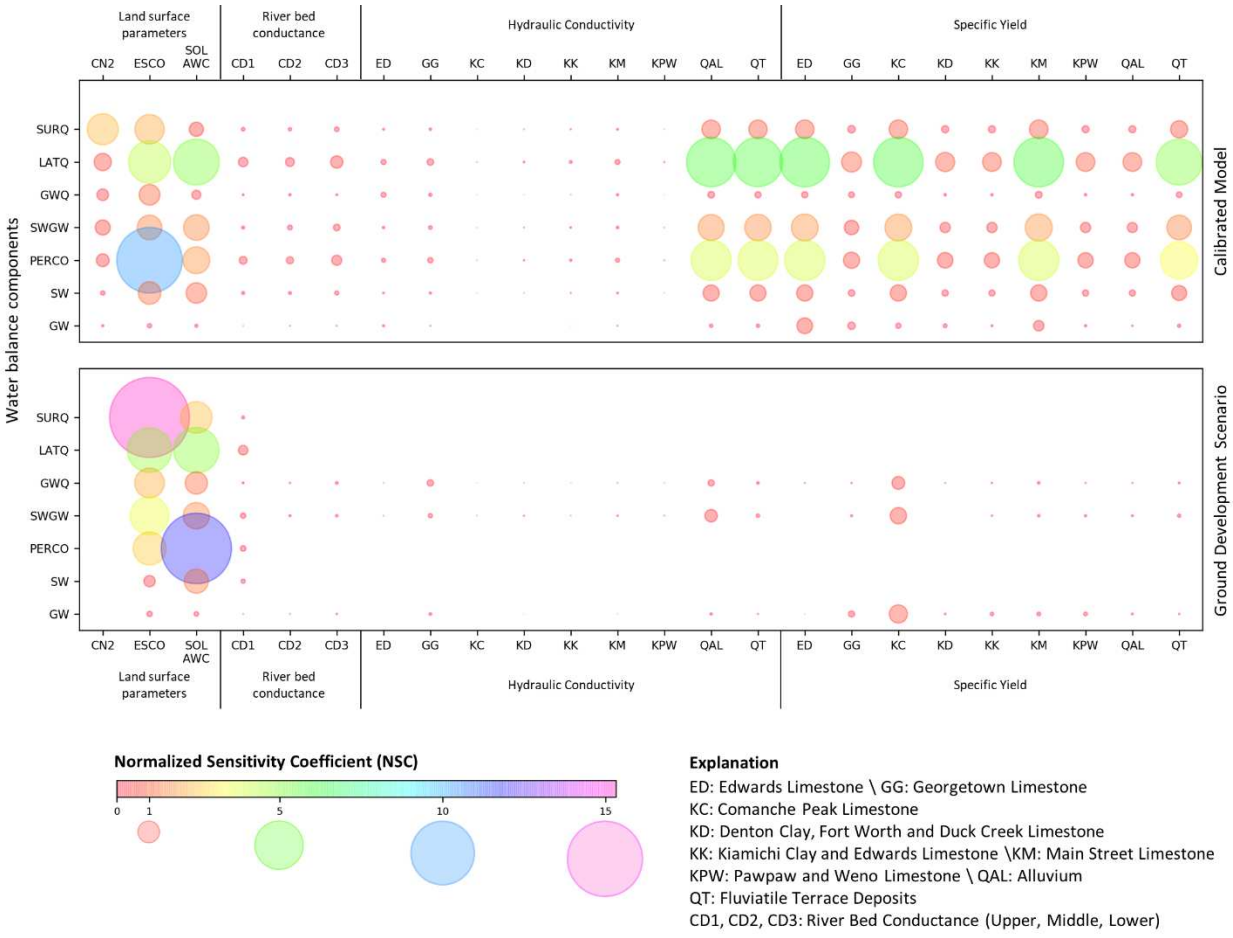

Figure 4.9. Normalized Sensitivity Coefficient (NSC) on water balance in (upper) calibrated model and (lower) with groundwater development scenario

4.4. Summary and Conclusions

This paper introduces a general framework for quantifying sensitivity, uncertainty, and parameter values for integrated surface water-groundwater models. Using the SWAT-MODFLOW modelling code as an example integrated model, the framework outlines the phases

of model construction, parameter estimation and sensitivity analysis, uncertainty analysis, and model application to scenario analysis. PEST is used as the software tool for parameter estimation and sensitivity analysis, with an accompanying Local Sensitivity Analysis (LSA) used to provide uncertainty around the best-calibrated parameter set. A methodology is developed for PEST in which both SWAT (land surface, stream, soil) parameters and MODFLOW (hydrogeological) parameters can be estimated jointly during the PEST iterations. Uncertainty in model predictions, i.e. scenario analysis is provided using the simulations used in the LSA.

The framework is applied to the Middle Bosque River watershed (471 km^2), located in central Texas. The SWAT-MODFLOW model for the watershed is calibrated by estimating the values of 24 parameters (land surface parameters, hydraulic conductivity for geologic units, specific yield for geologic units, riverbed conductance) and comparing model output with streamflow at the watershed outlet and groundwater levels at two observation wells. The land surface parameters (available water capacity of the soil layer, runoff curve number, soil evaporation compensation factor) had the strongest control on streamflow and groundwater head, followed by specific yield and hydraulic conductivity of the alluvium material and near-surface terrace deposits. The model was then applied to an aquifer storage and recovery scenario to store water during wet years and extract groundwater during drought years. Results show the influence of this groundwater development scenario on hydrologic response (streamflow, water table elevation, GW-SW interactions) and overall watershed water balance, with uncertainty bands of simulation results provided to provide decision makers with possible ranges of responses.

The proposed modelling framework can assist in implementing and applying integrated surface water-groundwater models for estimating watershed water resource and analysing the effect of changes in land use, population, and climate. Keys to the framework are the ability to

jointly estimate land surface and hydrogeological parameters and quantify their impact on hydrologic responses (streamflow, water table elevation, GW-SW interactions). This framework, particularly if used with SWAT-MODFLOW, can facilitate the use of integrated models worldwide to assist with finding technical solutions to water issues.

REFERENCES

Abbaspour, K.C., Vejdani, M., Haghighat, S. and Yang, J., 2007, December. SWAT-CUP calibration and uncertainty programs for SWAT. In *MODSIM 2007 International Congress on Modelling and Simulation, Modelling and Simulation Society of Australia and New Zealand* (pp. 1596-1602).

Abbaspour, K.C., 2011. Swat-Cup2: SWAT Calibration and Uncertainty Programs Manual Version 2, Department of Systems Analysis, Integrated Assessment and Modelling (SIAM), Eawag. Swiss Federal Institute of Aquatic Science and Technology, Duebendorf, Switzerland. 106 p.

Abbaspour, K.C., Rouholahnejad, E., Vaghefi, S., Srinivasan, R., Yang, H., and B. Klove (2015), A continental-scale hydrology and water quality model for Europe: Calibration and uncertainty of a high-resolution large-scale SWAT model. Journal of Hydrology 524, 733-752.

Bailey, R.T., Wible, T.C., Arabi, M., Records, R.M., and J. Ditty (2016), Assessing regional-scale spatio-temporal patterns of groundwater-surface water interactions using a coupled SWAT-MODFLOW model. Hydrological Processes 30, 4420-4433.

Bailey, R., Rathjens, H., Bieger, K., Chaubey, I., and J. Arnold (2017), SWATMOD-Prep: Graphical user interface for preparing coupled SWAT-MODFLOW simulations. J American Water Resources Association 53(2), 400-410.

Beven, K. (2006). A manifesto for the equifinality thesis. Journal of Hydrology, 320(1-2), 18-36.

Bicknell, B.R., J.C. Imhoff, J.L. Kittle, Jr., T.H. Jobes, and A.S. Donigian, Jr., 2001. Hydrological Simulation Program –FORTRAN (HSPF), User's Manual for Version 12.0. USEPA, Athens, Georgia.

Gallagher, M., and J. Doherty (2007), Parameter estimation and uncertainty analysis for a watershed model. Environmental Modelling & Software 22, 1000-1020.

Li, Z., Shao, Q., Xu, Z., and X. Cai (2010), Analysis of parameter uncertainty in semi-distributed hydrologic models using bootstrap method: A case study of SWAT model applied to Yingluoxia watershed in northwest China. Journal of Hydrology 385, 76-83.

Muleta, M.K. and J.W. Nicklow (2005), Sensitivity and uncertainty analysis coupled with automatic calibration for a distributed watershed model. Journal of Hydrology 306, 127-145.

Park, S., Nielsen, A., Bailey, R.T., Trolle, D., and K. Bieger (2018), A QGIS-based graphical user interface for application and evaluation of SWAT-MODFLOW models. Environmental Modelling & Software, *in Second Review*.

Poeter, Eileen P., Mary C. Hill, Dan Lu, Claire R. Tiedeman, and Steffen Mehl, 2014, UCODE_2014, with new capabilities to define parameters unique to predictions, calculate weights using simulated values, estimate parameters with SVD, evaluate uncertainty with MCMC, and more: Integrated Groundwater Modeling Center Report Number GWMI 2014-02.

Shen, Z.Y., Chen, L., and T. Chen (2012), Analysis of parameter uncertainty in hydrological and sediment modeling using GLUE method: a cast study of SWAT model applied to Three Gorges Reservoir Region, China. Hydrol. Earth Syst. Sci. 16, 121-132.

Surfleet, C.G., and D. Tullos (2013), Uncertainty in hydrologic modelling for estimating hydrologic response due to climate change (Santiam River, Oregon), Hydrological Processes 27, 3560-3576.

Wu, B., Zheng, Y., Tian, Y., Wu, X., Yao, Y., Han, F., Liu, J., and Chunmiao Zheng (2014), Systematic assessment of the uncertainty in integrated surface water-groundwater modeling

based on the probabilistic collocation method. Water Resources Research, doi: 10.1002/2014WR015366.

Wu, Y., and S. Liu (2012), Automating calibration, sensitivity and uncertainty analysis of complex models using the R package Flexible Modeling Environment (FME): SWAT as an example. Environmental Modelling & Software 31, 99-109.

Yang, J., Reichert, P., and K.C. Abbaspour (2007), Bayesian uncertainty analysis in distributed hydrologic modelling: A case study in the Thur River basin (Switzerland). Water Resources Research 43, doi:10.1029/2006WR005497.

CHAPTER 5

CONCLUSIONS AND FUTURE WORK

The research presented in this dissertation summarizes efforts providing a general framework for implementation and use of integrated surface water-groundwater hydrologic models. The efforts included developing an easy-to-use workflow (QSWATMOD) for model construction, configuring simulation settings, and visualizing and interpreting results and a general framework for performing sensitivity analysis, parameter estimation, and uncertainty analysis for integrated surface water-groundwater models, using the SWAT-MODFLOW modelling code as an example. The model also was applied to a central Texas watershed to investigate the influence of drought and high-intensity storm events on water resources and watershed water balance components.

5.1. A QGIS-based graphical user interface for application and evaluation of SWAT-MODFLOW models

- Conclusions:
  - A new graphical user interface (QSWATMOD) is introduced to facilitate the linkage of SWAT and MODFLOW models.
  - QSWATMOD is created as a QGIS plug-in tool, which allows maps of SWAT and MODFLOW domains and variables to be easily viewed on the QGIS map canvas.
  - QSWATMOD requires an existing SWAT model and can link with an existing MODFLOW model or a single-layer MODFLOW model created within the QGIS environment.

- QSWATMOD runs a SWAT-MODFLOW simulation and allows for viewing of system responses such as stream discharge, groundwater head, groundwater recharge, and groundwater-surface interactions.
- QSWATMOD can compare model results with observed stream discharge and groundwater level data.
- QSWATMOD can be a valuable tool in assisting users to create and manage SWAT-MODFLOW projects, allowing coupled surface water/groundwater models to become more accessible to a broader hydrologic modelling community.

- Future work:
  - Introduction of dynamic plots for streamflow discharge and water table elevation
  - Implementation of help option including beginner's guide and tutorial
  - Implementation of RT3D option creating input files to help users simulate solute transports
  - Migration to a new version of QGIS (QGIS3)
  - Introduction of parameter estimation providing basic input files for PEST

5.2. Quantifying effect of decadal and extreme climate events on watershed water resources and fluxes using SWAT-MODFLOW

- Conclusions:
  - Model outputs: cell-wise hydraulic head, recharge, and surface-subsurface water interaction, demonstrate a high spatio-temporal variability and correlations between the results.

- Water balance from surface and sub-surface domains was simulated simultaneously based on time series analysis and the results show high temporal variation of water balance components.
- Using the calibrated model, the impact of precipitation on streamflow discharge, hydraulic head elevation, and water resource availability was assessed under different rainfall scenarios. The results show that their response time, scales and durations not only vary but also are influenced by pre-conditions (i.e. soil moisture).
- This study helps enhance understanding regarding the spatio-temporal patterns of hydraulic head elevation, recharge, surface-subsurface water interaction and the water resource availability and the hydrological responses with different rainfall patterns that support decisions about alternative management strategies in the areas of land use change, climate change, water allocation, pollution control and groundwater development scenarios.

- Future work:
  - Optimize the SWAT-MODFLOW model of the MBRW by finding the optimal spatio-temporal discretization (e.g. grid cell size, time step size); report general guidelines regarding adoption of grid cells size and time step size for integrated surface water-groundwater models.
  - Perform analysis of effect on baseflow in the study area
    - Setting up boundary conditions for MODFLOW model
    - Check streamflow and water table for each subbasin
    - Check groundwater discharge for each subbasin

- Perform comprehensive simulation of solute transport in this study area (coupled surface-subsurface hydrologic systems) using the linked SWAT-MODFLOW-RT3D model.

5.3. A framework for quantifying uncertainty, sensitivity, and estimating parameters for integrated surface water - groundwater models

- Conclusions:
  - A methodology is developed for automatic parameter estimation in which SWAT (land surface, stream, soil) parameters and MODFLOW (hydrogeological) parameters can be estimated jointly using the PEST software program.
  - Uncertainty in model predictions, i.e. scenario analysis is provided using the simulations used in a Local Sensitivity Analysis method.
  - The proposed modelling framework can assist in implementing and applying integrated surface water-groundwater models for estimating watershed water resource and analysing the effect of changes in land use, population, and climate.
  - This framework, particularly if used with SWAT-MODFLOW, can facilitate the use of integrated models worldwide to assist with finding technical solutions to water issues.
- Future work:
  - Introduction of methods for Global sensitivity analysis (GSA) application and the visual analysis of uncertainties for integrated surface water – groundwater models
  - Introduction of methods for future change and development scenarios with global climate models (GCM) and land use change.

5.4. General Conclusions

The presented modelling methodology with SWAT-MODFLOW can facilitate model use worldwide to find technical solutions to water issues. These issues include water supply, the impact of groundwater development on groundwater supply and surface water depletion, the movement and remediation of contaminants (nutrients, trace elements) in the watershed system, the mobilization and presence of salt ions and their effect on water quality and crop yield, and transboundary groundwater conflicts.

APPENDIX A

Supplementary Material for (CHAPTER 2)

A QGIS-based graphical user interface for application and evaluation of SWAT-MODFLOW models

Seonggyu Park[1, *], Anders Nielsen[2], Ryan T. Bailey[1], Dennis Trolle [2], Katrin Bieger[3]

[1]Dept. of Civil and Environmental Engineering, Colorado State University, Fort Collins, CO, USA
[2]Aarhus University, Department of Bioscience, Vejlsøvej, Silkeborg, Denmark
[3]Blackland Research & Extension Center, Texas A&M AgriLife, Temple, TX, United States

[*]*Correspondence to*: Seonggyu Park (seonggyu.park@colostate.edu); Tel: 970-889-9081, Fax: 970-491-7727

Environmental Modelling & Software

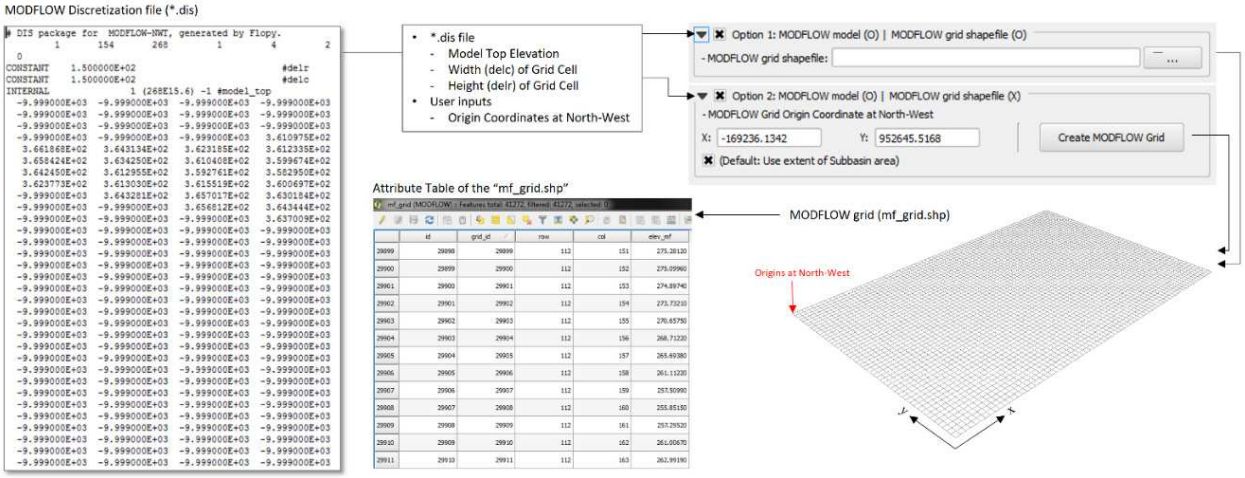

Figure 2A.1. QSWATMOD interface for MODFLOW options.

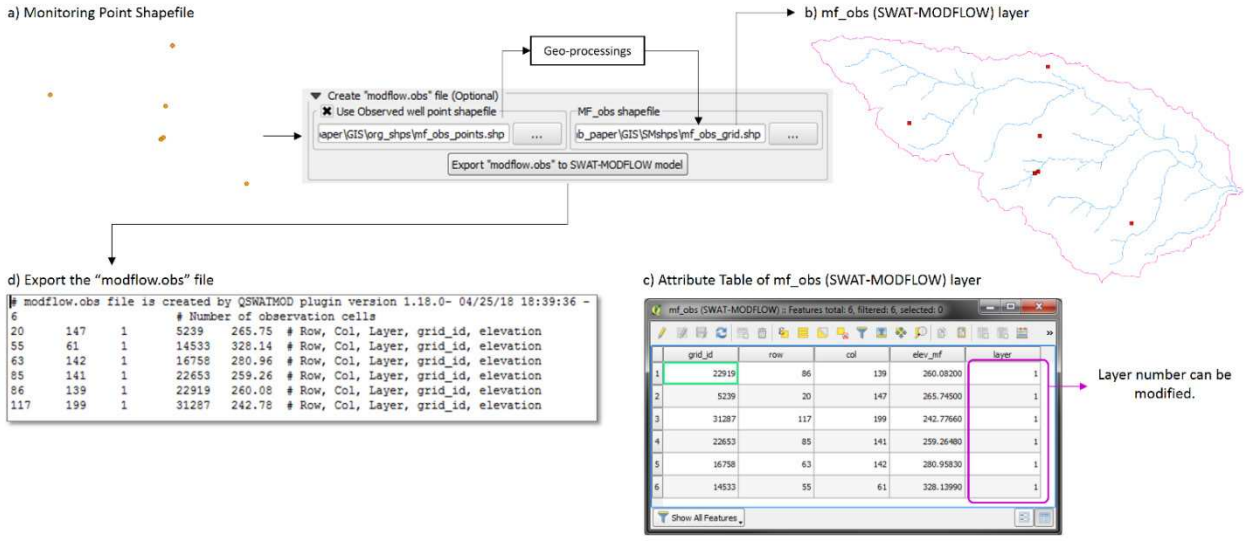

Figure 2A.2. Creating "modflow.obs" file using either a) Monitoring point; or b) "mf_grid.shp" shapefile.

a) “streamflow.obd” file

Date	sub_58	sub_56	sub_1	sub_3
2/1/1993	5.88		1.93	5.88
2/2/1993	5.31		3.5	5.31
2/3/1993	11.3		3.2	11.3
2/4/1993	41.56		2.64	41.56
2/5/1993	14.79		2.64	14.79
2/6/1993	9.44		2.3	9.44
2/7/1993	6.97		2.22	6.97
2/8/1993	6.03		2.22	
2/9/1993	5.31		2.15	
2/10/1993	12.7		2.07	
2/11/1993	8.04		2.07	
2/12/1993	5.31		2	
2/13/1993	4.78		3.1	
2/14/1993	4.53		2.73	
2/15/1993	18.75		2.3	
2/16/1993	11.3		2.22	
2/17/1993	6.49		1.93	
2/18/1993	5.74		1.79	
2/19/1993	5.45		1.79	
2/20/1993	5.18		1.79	
2/21/1993	4.78		1.79	
2/22/1993	4.17		16.42	
2/23/1993	3.5		10.6	
2/24/1993	3.4		6.64	
2/25/1993	16.42		5.88	
2/26/1993	4.78		5.31	
2/27/1993	3		11.3	
2/28/1993	3.1		41.56	
3/1/1993	9.9		14.79	
3/2/1993	6.49	2.07	9.44	
3/3/1993	3.83	2.15	6.97	
3/4/1993	3.1	2.15	6.03	
3/5/1993	2.64	2.22	5.31	
3/6/1993	2.55	3.83	12.7	
3/7/1993	2.47	1.79	8.04	
3/8/1993	2.15	1.86	5.31	
3/9/1993	2.07	1.93	4.78	
3/10/1993	1.93	3.5		
3/11/1993	2.3	3.2		
3/12/1993	24.1	2.64		
3/13/1993	5.04	2.64		
3/14/1993	3.72	2.3		
3/15/1993	3.61	2.22		
3/16/1993	4.29	2.22		
3/17/1993	3.1	2.15		
3/18/1993	2.73	2.07		
3/19/1993	11.3	2.07		
3/20/1993	25.03	2		
3/21/1993	6.64	3.1		
3/22/1993	23.87	2.73		

b) “modflow.obd” file

Date	C01L_22919_wt	C02D_22653_wt	C01L_22919	C02D_22653
10/21/1985	259.503644		-0.85344	
10/22/1985	259.412204		-0.94488	
10/23/1985	259.320764		-1.03632	
10/24/1985	259.229324		-1.12776	
10/25/1985	259.107404		-1.24968	
10/26/1985	258.894044		-1.46304	
10/27/1985	258.680684		-1.6764	
10/28/1985	258.589244		-1.76784	
10/29/1985	258.528284		-1.8288	
10/30/1985	258.436844		-1.92024	
10/31/1985	258.375884		-1.9812	
11/1/1985	258.314924		-2.04216	
11/2/1985	258.253964		-2.10312	
11/3/1985	258.208244		-2.14884	
11/4/1985	258.162524		-2.19456	
11/5/1985	258.071084		-2.286	
11/6/1985	258.040604		-2.31648	
11/7/1985	258.010124		-2.34696	
11/8/1985	257.979644		-2.37744	
11/9/1985	257.933924		-2.42316	
11/10/1985	257.918684		-2.4384	
11/11/1985	257.872964		-2.48412	
11/12/1985	257.827244		-2.52984	
11/13/1985	257.796764		-2.56032	
11/14/1985	257.781524		-2.57556	
11/15/1985	257.766284		-2.5908	
11/16/1985	257.751044		-2.60604	
11/17/1985	257.735804		-2.62128	
11/18/1985	257.705324		-2.65176	
11/19/1985	257.690084		-2.667	
11/20/1985	257.644364		-2.71272	
11/21/1985	257.629124		-2.72796	
11/22/1985	257.623028		-2.734056	
11/23/1985	257.613884		-2.7432	
11/24/1985	257.598644		-2.75844	
11/25/1985	257.598644		-2.75844	
11/26/1985	257.583404		-2.77368	
11/27/1985	257.598644		-2.75844	
11/28/1985	257.522444		-2.83464	
11/29/1985	257.507204		-2.84988	
11/30/1985	257.476724	256.282096	-2.88036	-0.77724
12/1/1985	257.507204	256.236376	-2.84988	-0.82296
12/2/1985	257.522444	256.221136	-2.83464	-0.8382
12/3/1985	257.537684	256.221136	-2.8194	-0.8382
12/4/1985	257.54378	256.221136	-2.813304	-0.8382
12/5/1985	257.552924	256.221136	-2.80416	-0.8382
12/6/1985	257.562068	256.221136	-2.795016	-0.8382
12/7/1985	257.568164	256.221136	-2.78892	-0.8382
12/8/1985	257.57426	256.221136	-2.782824	-0.8382
12/9/1985	257.583404	256.221136	-2.77368	-0.8382

Figure 2A.3. Observation file formats (Tab delimited) for a) “streamflow.obd”; and b) “modflow.obd” files. These data will be compared to SWAT-MODFLOW output once the simulation has finished.

output.mp4 (Command Line)

Video 2A.4. Annual Average Surface and Groundwater Interactions from 1980 – 2011 for the Middle Bosque River Watershed.

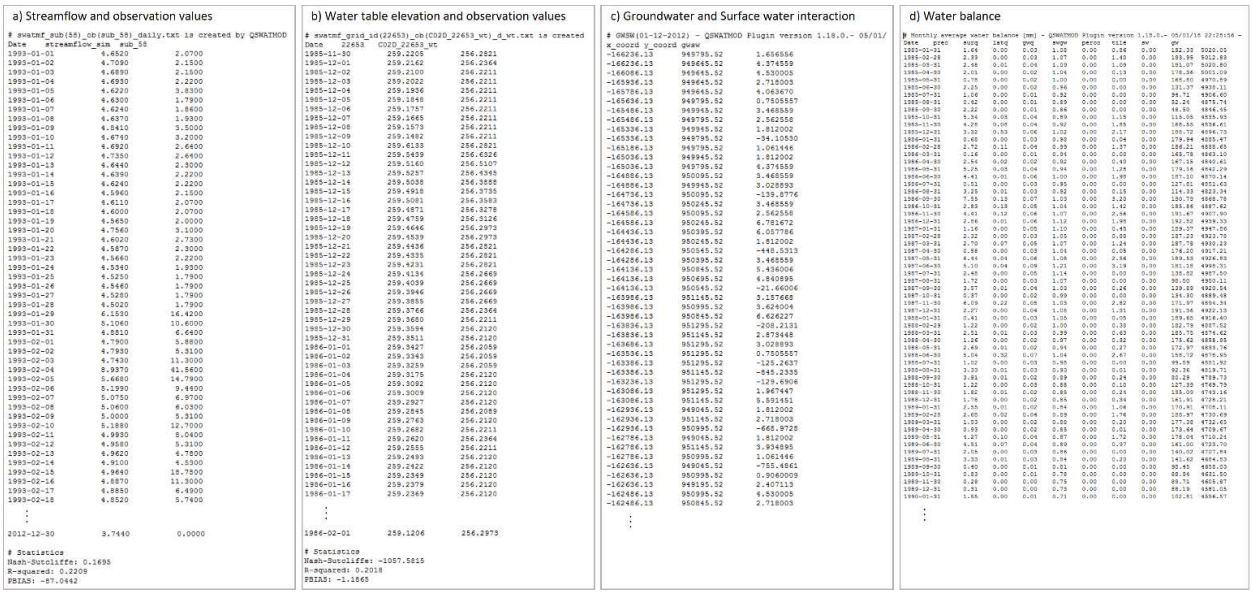

Figure 2A.5. Exported files for a) streamflow and observation values; b) water table elevation and observation values; c) groundwater and surface water interaction for a specific date; and d) water balance for the period of a simulation.

APPENDIX B

QSWATMOD (a part of source code)

```
# -*- coding: utf-8 -*-
"""
/***************************************************************************
 QSWATMOD / MODFLOW function
                          A QGIS plugin
 This plugin displays the result of SM simulation
                         -------------------
      begin            : 2017-08-02
      git sha          : $Format:%H$
      copyright          : (C) 2017 by Seonggyu and Dr. Anders
      email            : envpsg@colostate.edu
 ***************************************************************************/

/***************************************************************************
 *                                                                         *
 *   This program is free software; you can redistribute it and/or modify  *
 *   it under the terms of the GNU General Public License as published by  *
 *   the Free Software Foundation; either version 2 of the License, or     *
 *   (at your option) any later version.                                   *
 *                                                                         *
 ***************************************************************************/
"""
import os
import os.path
import posixpath
import ntpath
import shutil
import glob
import processing
from PyQt4.QtSql import QSqlDatabase, QSqlQuery, QSqlTableModel
from PyQt4.QtCore import *
from PyQt4.QtCore import QCoreApplication
from PyQt4.QtGui import *
from PyQt4 import QtGui, uic

import numpy as np
# import pandas as pd
from qgis.core import QgsProject
import distutils.dir_util
from datetime import datetime


# import modules related flopy
import flopy
import flopy.utils.binaryfile as bf
from osgeo import gdal

from QSWATMOD.QSWATMOD import *
from QSWATMOD.QSWATMOD_dialog import QSWATMODDialog
from QSWATMOD.pyfolder import modflow_functions
from QSWATMOD.pyfolder import writeMF
from QSWATMOD.pyfolder import db_functions
from QSWATMOD.pyfolder import linking_process

#
FORM_CLASS, _ = uic.loadUiType(os.path.join(os.path.dirname(__file__), 'ui/createMFmodel.ui'))
```

```
class createMFmodelDialog(QDialog, FORM_CLASS):
    def __init__(self, iface):
        QDialog.__init__(self)
        self.iface = iface
        self.setupUi(self)
    # def __init__(self, parent = None):
    #   super(createMFmodelDialog, self).__init__(parent)
    #   self.setupUi(self)


    #   self.pushButton_TxtInOut.clicked.connect(self.test)

    # def test(self):
    #   options = QtGui.QFileDialog.DontResolveSymlinks | QtGui.QFileDialog.ShowDirsOnly
    #   directory = QtGui.QFileDialog.getExistingDirectory(None,
    #       "QFileDialog.getExistingDirectory()",
    #       "self.dlg.Lakemodel_directory.text()", options)
    #   if directory:
    #       proj = QgsProject.instance()
    #       Project_Name = QFileInfo(proj.fileName()).baseName()

    #       Out_folder_temp = QgsProject.instance().readPath("./")
    #       Out_folder = os.path.normpath(Out_folder_temp + "/" + Project_Name + "/" + "existingModel" + "/" + "SWAT-MODFLOW")
    #       #distutils.dir_util.remove_tree(Out_folder)
    #       distutils.dir_util.copy_tree(directory, Out_folder)
    #       #self.dlg.Lakemodel_directory.setText(Out_folder)
    #       #self.DB_Update_Lakemodel_Directory()
    #       #time.sleep(1)

    #       # Check file extension
    #       file_check = os.path.abspath(os.path.join(Out_folder, "tr_041316.nam"))

    #       if os.path.isfile(file_check) is True:

    #           msgBox = QMessageBox()
    #           msgBox.setText("The MODLFOW folder was succesfully copied")
    #           msgBox.exec_()
    #           self.lineEdit_TxtInOut.setText(Out_folder)
    #       else:
    #           msgBox = QMessageBox()
    #           msgBox.setText("There was a problem copying the folder")
    #           msgBox.exec_()


        #-------------------------------------------------------------------------------------------
        self.checkBox_ratio.setCheckState(Qt.Checked)
        self.pushButton_createMFfolder.clicked.connect(self.createMFfolder)
        self.pushButton_loadDEM.clicked.connect(self.loadDEM)
        self.checkBox_use_sub.toggled.connect(self.use_sub_shapefile)
        self.pushButton_create_MF_shps.clicked.connect(self.create_MF_shps)

        # -------------------------------------------------------------------------------------------
        self.radioButton_aq_thic_single.toggled.connect(self.aqufierThickness_option)
        self.radioButton_aq_thic_uniform.toggled.connect(self.aqufierThickness_option)
        self.radioButton_aq_thic_raster.toggled.connect(self.aqufierThickness_option)
        self.pushButton_aq_thic_raster.clicked.connect(self.loadBotElev)

        self.radioButton_hk_single.toggled.connect(self.hk_option)
        self.radioButton_hk_raster.toggled.connect(self.hk_option)
        self.pushButton_hk_raster.clicked.connect(self.loadHK)

        self.comboBox_layerType.clear()
        self.comboBox_layerType.addItems([' - Confined - ', ' - Convertible - '])

        self.radioButton_ss_single.toggled.connect(self.ss_option)
        self.radioButton_ss_raster.toggled.connect(self.ss_option)
```

```
    self.pushButton_ss_raster.clicked.connect(self.loadSS)

    self.radioButton_sy_single.toggled.connect(self.sy_option)
    self.radioButton_sy_raster.toggled.connect(self.sy_option)
    self.pushButton_sy_raster.clicked.connect(self.loadSY)

    self.radioButton_initialH_single.toggled.connect(self.initialH_option)
    self.radioButton_initialH_uniform.toggled.connect(self.initialH_option)
    self.radioButton_initialH_raster.toggled.connect(self.initialH_option)
    self.pushButton_initialH_raster.clicked.connect(self.loadInitialH)

    self.pushButton_writeMF.clicked.connect(self.writeMF)
    self.DB_Pull_mf_inputs() # instant call
    self.pushButton_reset.clicked.connect(self.DB_resetTodefaultVal)
    self.pushButton_create_mf_riv_shapefile.clicked.connect(self.create_mf_riv)

    # Retrieve info
    self.retrieve_ProjHistory_mf()

    #-------------------------------------------------------------------------------------------
    QObject.connect(self.doubleSpinBox_delc, SIGNAL("valueChanged(double)"), self.esti_ngrids)
    QObject.connect(self.doubleSpinBox_delr, SIGNAL("valueChanged(double)"), self.esti_ngrids)
    QObject.connect(self.doubleSpinBox_delc, SIGNAL("valueChanged(double)"), self.set_delr)
    #-------------------------------------------------------------------------------------------

##### QUESTIONS!! Is this function should be here too? ######
def dirs_and_paths(self):
    global QSWATMOD_path_dict
    # project places
    Projectfolder = QgsProject.instance().readPath("./")
    proj = QgsProject.instance()
    Project_Name = QFileInfo(proj.fileName()).baseName()

    # definition of folders
    org_shps = os.path.normpath(Projectfolder + "/" + Project_Name + "/" + "GIS/org_shps")
    SMshps = os.path.normpath(Projectfolder + "/" + Project_Name + "/" + "GIS/SMshps")
    SMfolder = os.path.normpath(Projectfolder + "/" + Project_Name + "/" + "SWAT-MODFLOW")
    Table = os.path.normpath(Projectfolder + "/" + Project_Name + "/" + "GIS/Table")
    SM_exes = os.path.normpath(Projectfolder + "/" + Project_Name + "/" + "SM_exes")
    exported_files = os.path.normpath(Projectfolder + "/" + Project_Name + "/" + "exported_files")

    QSWATMOD_path_dict = {'org_shps': org_shps,
                          'SMshps': SMshps,
                          'SMfolder': SMfolder,
                          'Table': Table,
                          'SM_exes': SM_exes,
                          'exported_files': exported_files}

    return QSWATMOD_path_dict

# def dirs_and_paths(self):
#   # project places
#   Projectfolder = QgsProject.instance().readPath("./")
#   proj = QgsProject.instance()
#   Project_Name = QFileInfo(proj.fileName()).baseName()

#   # definition of folders
#   org_shps = os.path.normpath(Projectfolder + "/" + Project_Name + "/" + "GIS/org_shps")
#   SMshps = os.path.normpath(Projectfolder + "/" + Project_Name + "/" + "GIS/SMshps")
#   SMfolder = os.path.normpath(Projectfolder + "/" + Project_Name + "/" + "SWAT-MODFLOW")
#   Table = os.path.normpath(Projectfolder + "/" + Project_Name + "/" + "GIS/Table")
#   SM_exes = os.path.normpath(Projectfolder + "/" + Project_Name + "/" + "SM_exes")
#   return org_shps, SMshps, SMfolder, Table, SM_exes

def DB_Pull_mf_inputs(self):
    db = db_functions.db_variable(self)
```

```
    query = QtSql.QSqlQuery(db)
    query.exec_("SELECT user_val FROM mf_inputs WHERE parNames = 'ss' ")
    LK = str(query.first()) # What does LK do?
    self.lineEdit_ss_single.setText(str(query.value(0)))

# ...
def DB_push_mf_userVal(self):
    db = db_functions.db_variable(self)
    query = QtSql.QSqlQuery(db)
    query.prepare("UPDATE mf_inputs SET user_val = :UP1 WHERE parNames = 'ss'")
    query.bindValue (":UP1", self.lineEdit_ss_single.text())
    query.exec_()

def DB_resetTodefaultVal(self):
    msgBox = QMessageBox()
    msgBox.setWindowIcon(QtGui.QIcon(':/newPrefix/pics/logo.png'))
    response = msgBox.question(self, 'Set to default?',
        "Are you sure you want to reset the current aquifer property settings to the default values?",
        QMessageBox.Yes | QMessageBox.No, QMessageBox.No)

    if response == QMessageBox.Yes:
        db = db_functions.db_variable(self)
        query = QtSql.QSqlQuery(db)
        query.exec_("SELECT default_val FROM mf_inputs WHERE parNames = 'ss' ")
        LK = str(query.first())
        self.lineEdit_ss_single.setText(str(query.value(0)))
        self.DB_push_mf_userVal()

def retrieve_ProjHistory_mf(self):
    QSWATMOD_path_dict = self.dirs_and_paths()

    # Define folders and files
    SMfolder = QSWATMOD_path_dict['SMfolder']
    org_shps = QSWATMOD_path_dict['org_shps']
    SMshps = QSWATMOD_path_dict['SMshps']

    # retrieve DEM
    if os.path.isfile(os.path.join(org_shps, 'DEM.tif')):
        self.lineEdit_loadDEM.setText(os.path.join(org_shps, 'DEM.tif'))
    else:
        self.textEdit_mf_log.append("* Provide DEM raster file.")


def createMFfolder(self):
    settings = QSettings()
    if settings.contains('/QSWATMOD/LastInputPath'):
        path = unicode(settings.value('/QSWATMOD/LastInputPath'))
    else:
        path = ''
    options = QtGui.QFileDialog.DontResolveSymlinks | QtGui.QFileDialog.ShowDirsOnly
    title = "create MODFLOW folder"
    mffolder = QFileDialog.getExistingDirectory(None, title, path, options)
    mffolder_path = self.lineEdit_createMFfolder.setText(mffolder)
    return mffolder_path


# navigate to the DEM raster from SWAT
def loadDEM(self):
    QSWATMOD_path_dict = self.dirs_and_paths()
    settings = QSettings()
    if settings.contains('/QSWATMOD/LastInputPath'):
        path = unicode(settings.value('/QSWATMOD/LastInputPath'))
    else:
        path = ''
    title = "Choose DEM rasterfile"
    inFileName = QFileDialog.getOpenFileName(None, title, path, "Rasterfiles (*.tif);; All files (*.*)")
```

```
    if inFileName:
        settings.setValue('/QSWATMOD/LastInputPath', os.path.dirname(unicode(inFileName)))
        Out_folder = QSWATMOD_path_dict['org_shps']
        inInfo = QFileInfo(inFileName)
        inFile = inInfo.fileName()
        pattern = os.path.splitext(inFileName)[0] + '.*'
        baseName = inInfo.baseName()

        # inName = os.path.splitext(inFile)[0]
        inName = 'DEM'
        for f in glob.iglob(pattern):
            suffix = os.path.splitext(f)[1]
            if os.name == 'nt':
                outfile = ntpath.join(Out_folder, inName + suffix)
            else:
                outfile = posixpath.join(Out_folder, inName + suffix)
            shutil.copy(f, outfile)

        if os.name == 'nt':
            DEM = ntpath.join(Out_folder, inName + ".tif")
        else:
            DEM = posixpath.join(Out_folder, inName + ".tif")
        layer = QgsRasterLayer(DEM, '{0} ({1})'.format("DEM","SWAT"))
        # Put in the group
        root = QgsProject.instance().layerTreeRoot()
        swat_group = root.findGroup("SWAT")
        QgsMapLayerRegistry.instance().addMapLayer(layer, False)
        swat_group.insertChildNode(0, QgsLayerTreeLayer(layer))
        self.lineEdit_loadDEM.setText(DEM)
        return DEM


def loadHK(self):
    writeMF.loadHK(self)

def loadBotElev(self):
    writeMF.loadBotElev(self)

def loadSS(self):
    writeMF.loadSS(self)

def loadSY(self):
    writeMF.loadSY(self)

def loadInitialH(self):
    writeMF.loadInitialH(self)

def use_sub_shapefile(self):
    from PyQt4 import QtCore, QtGui, QtSql
    QSWATMOD_path_dict = self.dirs_and_paths()

    try:
        input1 = QgsMapLayerRegistry.instance().mapLayersByName("sub (SWAT)")[0]
        #provider = layer.dataProvider()
        if self.checkBox_use_sub.isChecked():
            name = "mf_boundary"
            name_ext = "mf_boundary.shp"
            output_dir = QSWATMOD_path_dict['org_shps']
            # output_file = os.path.normpath(output_dir + "/" + name)

            mf_boundary = os.path.join(output_dir, name_ext)
            processing.runalg("qgis:dissolve", input1, True, None, mf_boundary)

            # defining the outputfile to be loaded into the canvas
            layer = QgsVectorLayer(mf_boundary, '{0} ({1})'.format("mf_boundary","MODFLOW"), 'ogr')
```

```
            # Put in the group
            root = QgsProject.instance().layerTreeRoot()
            mf_group = root.findGroup("MODFLOW")
            QgsMapLayerRegistry.instance().addMapLayer(layer, False)
            mf_group.insertChildNode(0, QgsLayerTreeLayer(layer))
            #subpath = layer.source()
            self.lineEdit_boundary.setText(mf_boundary)

        except:
            msgBox = QMessageBox()
            msgBox.setWindowIcon(QtGui.QIcon(':/newPrefix/pics/logo.png'))
            msgBox.setWindowTitle("What the FXXXX!")
            msgBox.setText("There is no 'sub' shapefile!")
            msgBox.exec_()
            # self.dlg.checkBox_default_extent.setChecked(0)
        # return layer

    def create_MF_grid(self): # Create fishnet based on user inputs
        QSWATMOD_path_dict = self.dirs_and_paths()
        input1 = QgsMapLayerRegistry.instance().mapLayersByName("mf_boundary (MODFLOW)")[0]

        ext = input1.extent()
        xmin = ext.xMinimum()
        xmax = ext.xMaximum()
        ymin = ext.yMinimum()
        ymax = ext.yMaximum()

        delc = float(self.doubleSpinBox_delc.value())
        delr = float(self.doubleSpinBox_delr.value())

        nx = round((xmax - xmin) / delc)
        ny = round((ymax - ymin) / delr)
        ngrid = abs(int(nx*ny))

        MF_extent = "{a},{b},{c},{d}".format(a = xmin, b = xmax, c = ymin, d = ymax)

        #
        name = "mf_grid"
        name_ext = "mf_grid.shp"
        output_dir = QSWATMOD_path_dict['org_shps']
        output_file = os.path.normpath(output_dir + "/" + name)

        # running the acutal routine:
        processing.runalg("qgis:vectorgrid", MF_extent, delc,delr,0, output_file)

        # Define the outputfile to be loaded into the canvas
        mf_grid_shapefile =  os.path.join(output_dir, name_ext)
        layer = QgsVectorLayer(mf_grid_shapefile, '{0} ({1})'.format("mf_grid","MODFLOW"), 'ogr')

        # Put in the group
        root = QgsProject.instance().layerTreeRoot()
        mf_group = root.findGroup("MODFLOW")
        QgsMapLayerRegistry.instance().addMapLayer(layer, False)
        mf_group.insertChildNode(0, QgsLayerTreeLayer(layer))

    def create_grid_id_ii(self):
            self.layer = QgsMapLayerRegistry.instance().mapLayersByName("mf_grid (MODFLOW)")[0]
            provider = self.layer.dataProvider()

            if self.layer.dataProvider().fields().indexFromName("grid_id") == -1:
                field = QgsField("grid_id", QVariant.Int)
                provider.addAttributes([field])
                self.layer.updateFields()

                # I don't know
```

```
            grid_id = self.layer.dataProvider().fields().indexFromName("grid_id")
            feats = self.layer.getFeatures()
            self.layer.startEditing()
            for i, f in enumerate(feats):
               self.layer.changeAttributeValue(f.id(), grid_id, i+1)
            self.layer.commitChanges()
            time = datetime.now().strftime('[%m/%d/%y %H:%M:%S]')
            self.textEdit_mf_log.append(time+' -> ' + "'grid_id' has been created ...")
         else:
            time = datetime.now().strftime('[%m/%d/%y %H:%M:%S]')
            self.textEdit_mf_log.append(time+' -> ' + "'grid_id' already exists ...")

# for elev, not using *.dis file. instead using DEM
def create_row_col_elev_mf_ii (self):
   import math
   QSWATMOD_path_dict = self.dirs_and_paths()
   self.layer = QgsMapLayerRegistry.instance().mapLayersByName("mf_grid (MODFLOW)")[0]
   provider = self.layer.dataProvider()

   # from qgis.core import QgsField, QgsExpression, QgsFeature
   if self.layer.dataProvider().fields().indexFromName( "row" ) == -1:
      field = QgsField("row", QVariant.Int)
      provider.addAttributes([field])
      self.layer.updateFields()

   # Create Column field
   if self.layer.dataProvider().fields().indexFromName( "col" ) == -1:
      field = QgsField("col", QVariant.Int)
      provider.addAttributes([field])
      self.layer.updateFields()

   # Get the index numbers of the fields
   # elev_mean = self.layer.dataProvider().fields().indexFromName( "elev_mean" )
   row = provider.fields().fieldNameIndex("row")
   col = provider.fields().fieldNameIndex("col")

   # Change name
   for field in self.layer.pendingFields():
      if field.name() == 'elev_mean':
         self.layer.startEditing()
         idx = self.layer.fieldNameIndex(field.name())
         self.layer.renameAttribute(idx, "elev_mf")
         self.layer.commitChanges()

   # Get number of rows and of columns
   input1 = QgsMapLayerRegistry.instance().mapLayersByName("mf_boundary (MODFLOW)")[0]

   ext = input1.extent()
   xmin = ext.xMinimum()
   xmax = ext.xMaximum()
   ymin = ext.yMinimum()
   ymax = ext.yMaximum()

   delc = float(self.doubleSpinBox_delc.value())
   delr = float(self.doubleSpinBox_delr.value())

   nx = math.ceil(abs(abs(xmax) - abs(xmin)) / delc)
   ny = math.ceil(abs(abs(ymax) - abs(ymin)) / delr)

   # Get row and column lists
   iy = [] # row
   ix = [] # col
   for i in range(1, ny + 1):
      for j in range(1, nx + 1):
         ix.append(j)
         iy.append(i)
```

```
    # Get features (Find out a way to change attribute values using another field)
    feats = self.layer.getFeatures()
    self.layer.startEditing()

    # add row number
    for f, r, c in zip(feats, iy, ix):
        self.layer.changeAttributeValue(f.id(), row, r)
        self.layer.changeAttributeValue(f.id(), col, c)
        # self.layer.changeAttributeValue(f.id(), elev_mf, elev)
        # self.layer.changeAttributeValue(f[grid_id] - 1, row, r)
        # self.layer.changeAttributeValue(f[grid_id] - 1, col, c)
    self.layer.commitChanges()


#  ======= Update automatically when 1:1 ratio is checked
def set_delr(self, value):
    if self.checkBox_ratio.isChecked():
        self.doubleSpinBox_delr.setValue(value)

# ======= Estimate number of grid cells
def esti_ngrids(self):
    import math
    input1 = QgsMapLayerRegistry.instance().mapLayersByName("mf_boundary (MODFLOW)")[0]

    try:
        ext = input1.extent()
        xmin = ext.xMinimum()
        xmax = ext.xMaximum()
        ymin = ext.yMinimum()
        ymax = ext.yMaximum()

        delc = float(self.doubleSpinBox_delc.value())
        delr = float(self.doubleSpinBox_delr.value())
        if delc !=0 and delr !=0:
            nx = math.ceil(abs(abs(xmax) - abs(xmin)) / delc)
            ny = math.ceil(abs(abs(ymax) - abs(ymin)) / delr)
            ngrid = abs(int(nx*ny))
        else:
            ngrid = ' '
    except:
        ngrid = ' '
    self.lcdNumber_numberOfgrids.display(unicode(ngrid))

# ========== createMF_active
def create_mf_act_grid(self):
    from PyQt4 import QtCore, QtGui, QtSql
    QSWATMOD_path_dict = self.dirs_and_paths()
    input1 = QgsMapLayerRegistry.instance().mapLayersByName("mf_grid (MODFLOW)")[0]
    input2 = QgsMapLayerRegistry.instance().mapLayersByName("mf_boundary (MODFLOW)")[0]

    name = "mf_grid_active"
    name_ext = "mf_grid_active.shp"
    output_dir = QSWATMOD_path_dict['org_shps']

    # output_file = os.path.normpath(os.path.join(output_dir, name))
    # Select features by location
    processing.runalg('qgis:selectbylocation', input1, input2, ['intersects'], 0, 0)

    # Save just the selected features of the target layer
    mf_grid_act_shp = os.path.join(output_dir, name_ext)
    QgsVectorFileWriter.writeAsVectorFormat(input1, mf_grid_act_shp,
        "utf-8", input1.crs(), "ESRI Shapefile", 1)

    # Deselect the features
    processing.runalg('qgis:selectbylocation', input1, input2, ['intersects'], 0, 2)
```

```
    layer = QgsVectorLayer(mf_grid_act_shp, '{0} ({1})'.format("mf_act_grid","MODFLOW"), 'ogr')

    # Put in the group
    root = QgsProject.instance().layerTreeRoot()
    mf_group = root.findGroup("MODFLOW")
    QgsMapLayerRegistry.instance().addMapLayer(layer, False)
    mf_group.insertChildNode(0, QgsLayerTreeLayer(layer))


def create_MF_shps(self):
    self.progressBar_mf.setValue(0)
    self.create_MF_grid()
    time = datetime.now().strftime('[%m/%d/%y %H:%M:%S]')
    self.textEdit_mf_log.append(time+' -> ' + 'MODFLOW grid is created ...')
    self.progressBar_mf.setValue(30)
    QCoreApplication.processEvents() # it works as F5 !! Be careful to use this for long geoprocessing

    # Create grid_id
    self.create_grid_id_ii()
    time = datetime.now().strftime('[%m/%d/%y %H:%M:%S]')
    self.textEdit_mf_log.append(time+' -> ' + 'MODFLOW grid id is added ...')
    self.progressBar_mf.setValue(40)
    QCoreApplication.processEvents()

    # Extract elevation
    self.getElevfromDem()
    self.progressBar_mf.setValue(50)
    time = datetime.now().strftime('[%m/%d/%y %H:%M:%S]')
    self.textEdit_mf_log.append(time+' -> ' + 'Extrating elevation info from DEM is done ... ...')
    QCoreApplication.processEvents()

    # Extract elevation
    self.create_row_col_elev_mf_ii()
    self.progressBar_mf.setValue(60)
    time = datetime.now().strftime('[%m/%d/%y %H:%M:%S]')
    self.textEdit_mf_log.append(time+' -> ' + 'Writing row and col ... ...')
    QCoreApplication.processEvents()

    # Get active cells
    self.create_mf_act_grid()
    self.progressBar_mf.setValue(70)
    time = datetime.now().strftime('[%m/%d/%y %H:%M:%S]')
    self.textEdit_mf_log.append(time+' -> ' + 'MODLFOW active grid is created ...')
    QCoreApplication.processEvents()

    self.mf_act_grid_delete_NULL()
    QCoreApplication.processEvents()

    self.cvtElevToR()
    QCoreApplication.processEvents()

    time = datetime.now().strftime('[%m/%d/%y %H:%M:%S]')
    self.textEdit_mf_log.append(time+' -> ' + 'Done!')
    self.progressBar_mf.setValue(100)
    QCoreApplication.processEvents()

    msgBox = QMessageBox()
    msgBox.setWindowIcon(QtGui.QIcon(':/newPrefix/pics/logo.png'))
    msgBox.setWindowTitle("Created!")
    msgBox.setText("MODFLOW shapefiles were created!")
    msgBox.exec_()

# sp 03-20-18 : Change input1 mf_act_grid to mf_grid
def getElevfromDem(self):
    from qgis.analysis import QgsZonalStatistics
```

```
    input1 = QgsMapLayerRegistry.instance().mapLayersByName("mf_grid (MODFLOW)")[0]
    input2 = QgsMapLayerRegistry.instance().mapLayersByName("DEM (SWAT)")[0]
    provider = input2.dataProvider()
    rpath = provider.dataSourceUri()
    zoneStat = QgsZonalStatistics (input1, rpath, 'elev_', 1, QgsZonalStatistics.Mean)
    zoneStat.calculateStatistics(None)

  def cvtElevToR(self):
    QSWATMOD_path_dict = self.dirs_and_paths()

    delc = float(self.doubleSpinBox_delc.value())
    delr = float(self.doubleSpinBox_delr.value())

    extlayer = QgsMapLayerRegistry.instance().mapLayersByName("mf_grid (MODFLOW)")[0]
    input1 = QgsMapLayerRegistry.instance().mapLayersByName("mf_act_grid (MODFLOW)")[0]

    # get extent
    ext = extlayer.extent()
    xmin = ext.xMinimum()
    xmax = ext.xMaximum()
    ymin = ext.yMinimum()
    ymax = ext.yMaximum()
    extent = "{a},{b},{c},{d}".format(a = xmin, b = xmax, c = ymin, d = ymax)

    name = 'top_elev'
    name_ext = "top_elev.tif"
    output_dir = QSWATMOD_path_dict['org_shps']

    output_raster = os.path.join(output_dir, name_ext)
    processing.runalg("gdalogr:rasterize",
      input1,
      "elev_mf",1,delc,delr,
      extent,
      False,5,"-9999",0,75,6,1,False,0,"",
      output_raster)

    # fileInfo = QFileInfo(output_raster)
    # path = fileInfo.filePath()
    # baseName = fileInfo.baseName()

    # for raster no 'ogr'
    layer = QgsRasterLayer(output_raster, '{0} ({1})'.format("top_elev","MODFLOW"))

    # Put in the group
    root = QgsProject.instance().layerTreeRoot()
    mf_group = root.findGroup("MODFLOW")
    QgsMapLayerRegistry.instance().addMapLayer(layer, False)
    mf_group.insertChildNode(0, QgsLayerTreeLayer(layer))


  def mf_act_grid_delete_NULL(self):
    layer = QgsMapLayerRegistry.instance().mapLayersByName("mf_act_grid (MODFLOW)")[0]
    provider = layer.dataProvider()
    request =  QgsFeatureRequest().setFilterExpression('"elev_mf" IS NULL' )
    request.setSubsetOfAttributes([])
    request.setFlags(QgsFeatureRequest.NoGeometry)

    layer.startEditing()
    for f in layer.getFeatures(request):
      layer.deleteFeature(f.id())
    layer.commitChanges()

  def create_mf_riv(self):
    ### ========================================== why!!!!!!!!!!!!!!!!!!!!!!!!
    self.dlg = QSWATMODDialog()
    self.dlg.groupBox_river_cells.setEnabled(True) # not working
```

```
    self.dlg.radioButton_mf_riv2.setChecked(1) # not working
    ### ============================================
    modflow_functions.mf_riv2(self)
    linking_process.river_grid(self)
    linking_process.river_grid_delete_NULL(self)
    linking_process.rgrid_len(self)
    linking_process.delete_river_grid_with_threshold(self)
    modflow_functions.rivInfoTo_mf_riv2_ii(self)
    modflow_functions.riv_cond_delete_NULL(self)
    writeMF.create_layer_inRiv(self)
    QCoreApplication.processEvents()

#-------------------------------------------------------------------------------
def aqufierThickness_option(self):
    # Single
    if self.radioButton_aq_thic_single.isChecked():
        self.lineEdit_aq_thic_single.setEnabled(True)
        self.lineEdit_aq_thic_uniform.setEnabled(False)
        self.lineEdit_aq_thic_raster.setEnabled(False)
        self.pushButton_aq_thic_raster.setEnabled(False)

    # Uniform
    elif self.radioButton_aq_thic_uniform.isChecked():
        self.lineEdit_aq_thic_uniform.setEnabled(True)
        self.lineEdit_aq_thic_single.setEnabled(False)
        self.lineEdit_aq_thic_raster.setEnabled(False)
        self.pushButton_aq_thic_raster.setEnabled(False)

    # Raster
    elif self.radioButton_aq_thic_raster.isChecked():
        self.lineEdit_aq_thic_raster.setEnabled(True)
        self.pushButton_aq_thic_raster.setEnabled(True)
        self.lineEdit_aq_thic_single.setEnabled(False)
        self.lineEdit_aq_thic_uniform.setEnabled(False)

    # else:
    #   self.lineEdit_aq_thic_single.setEnabled(False)
    #   self.lineEdit_aq_thic_uniform.setEnabled(False)
    #   self.lineEdit_aq_thic_raster.setEnabled(False)
    #   self.pushButton_aq_thic_raster.setEnabled(False)

def hk_option(self):
    if self.radioButton_hk_single.isChecked():
        self.lineEdit_hk_single.setEnabled(True)
        self.lineEdit_vka.setEnabled(True)
        self.comboBox_layerType.setEnabled(True)
        self.lineEdit_hk_raster.setEnabled(False)
        self.pushButton_hk_raster.setEnabled(False)

    elif self.radioButton_hk_raster.isChecked():
        self.lineEdit_hk_raster.setEnabled(True)
        self.pushButton_hk_raster.setEnabled(True)
        self.lineEdit_vka.setEnabled(True)
        self.comboBox_layerType.setEnabled(True)
        self.lineEdit_hk_single.setEnabled(False)
    # else:
    #   self.lineEdit_hk_single.setEnabled(False)


def ss_option(self):
    if self.radioButton_ss_single.isChecked():
        self.lineEdit_ss_single.setEnabled(True)
        self.lineEdit_ss_raster.setEnabled(False)
        self.pushButton_ss_raster.setEnabled(False)

    elif self.radioButton_ss_raster.isChecked():
```

```
        self.lineEdit_ss_raster.setEnabled(True)
        self.pushButton_ss_raster.setEnabled(True)
        self.lineEdit_ss_single.setEnabled(False)


def sy_option(self):
    if self.radioButton_sy_single.isChecked():
        self.lineEdit_sy_single.setEnabled(True)
        self.lineEdit_sy_raster.setEnabled(False)
        self.pushButton_sy_raster.setEnabled(False)
    else:
        self.lineEdit_sy_raster.setEnabled(True)
        self.pushButton_sy_raster.setEnabled(True)
        self.lineEdit_sy_single.setEnabled(False)

def initialH_option(self):
    if self.radioButton_initialH_single.isChecked():
        self.lineEdit_initialH_single.setEnabled(True)
        self.lineEdit_initialH_uniform.setEnabled(False)
        self.lineEdit_initialH_raster.setEnabled(False)
        self.pushButton_initialH_raster.setEnabled(False)

    elif self.radioButton_initialH_uniform.isChecked():
        self.lineEdit_initialH_single.setEnabled(False)
        self.lineEdit_initialH_uniform.setEnabled(True)
        self.lineEdit_initialH_raster.setEnabled(False)
        self.pushButton_initialH_raster.setEnabled(False)

    else:
        self.lineEdit_initialH_single.setEnabled(False)
        self.lineEdit_initialH_uniform.setEnabled(False)
        self.lineEdit_initialH_raster.setEnabled(True)
        self.pushButton_initialH_raster.setEnabled(True)


def writeMF(self):
    self.DB_push_mf_userVal()

    from QSWATMOD.pyfolder.writeMF import extentlayer
    self.textEdit_mf_log.append(" ")
    self.textEdit_mf_log.append("- Exporting MODFLOW input files...")

    # '''
    self.checkBox_mfPrepared.setChecked(0)
    self.progressBar_mf.setValue(0)
    writeMF.createBotElev(self)
    self.progressBar_mf.setValue(10)
    QCoreApplication.processEvents()

    writeMF.cvtBotElevToR(self)
    self.progressBar_mf.setValue(20)
    QCoreApplication.processEvents()

    writeMF.createHK(self)
    self.progressBar_mf.setValue(30)
    QCoreApplication.processEvents()

    writeMF.cvtHKtoR(self)
    self.progressBar_mf.setValue(40)
    QCoreApplication.processEvents()

    writeMF.createSS(self)
    self.progressBar_mf.setValue(50)
    QCoreApplication.processEvents()

    writeMF.cvtSStoR(self)
```

```
self.progressBar_mf.setValue(60)
QCoreApplication.processEvents()

writeMF.createSY(self)
self.progressBar_mf.setValue(70)
QCoreApplication.processEvents()

writeMF.cvtSYtoR(self)
self.progressBar_mf.setValue(80)
QCoreApplication.processEvents()

writeMF.createInitialH(self)
self.progressBar_mf.setValue(90)
QCoreApplication.processEvents()

writeMF.cvtInitialHtoR(self)
self.progressBar_mf.setValue(95)
QCoreApplication.processEvents()
# '''
writeMF.writeMFmodel(self)
self.progressBar_mf.setValue(100)
self.checkBox_mfPrepared.setChecked(1)
```